

NONLINEAR PHENOMENA AND COMPLEX SYSTEMS

DEAN J. DRIEBE

*Fully Chaotic Maps
and Broken Time
Symmetry*

Springer-Science+Business Media, B.V.

Contents

Foreword	vii
Preface	ix
1 Chaos and Irreversibility	1
1.1 Irreversibility and Complexity	1
1.2 Densities in Chaotic Maps	3
1.3 Types of Behavior in Phase Space	5
2 Statistical Mechanics of Maps	11
2.1 Statistical Mechanics	11
2.2 Decay of Correlations and Resonances	14
3 The Bernoulli Map	19
3.1 The System	19
3.2 Exponential Correlation Decay	21
3.3 The Continuous Spectrum	23
3.4 The Generalized Spectral Decomposition	26
3.5 The Physical Eigenstates	32
3.5.1 Right Polynomial Eigenstates	32
3.5.2 Left Generalized Eigenstates	33
3.6 Validity of the Spectral Decomposition	39
4 Other One-Dimensional Maps	45
4.1 An Algebraic Technique Utilizing Symmetry	45
4.1.1 The Tent Map	46
4.1.2 The V Map and Reflected Bernoulli Map	51
4.2 Degeneracies and Jordan Decompositions	54
4.2.1 Degeneracies and Diagonalizability	54
4.2.2 Non-diagonalizability and Modified Exponential Decay	57
4.2.3 Polynomial Shift States	62
4.3 Fractal Repellors	67
4.4 Topologically Conjugate Maps	72

4.4.1	Decomposition of the Logistic Map	74
4.4.2	Other Uses of Conjugacy	77
5	Intrinsic Irreversibility	81
5.1	The Baker Transformation	81
5.2	The Generalized Spectral Decomposition	84
5.3	Irreversibility and Test Spaces	90
6	Deterministic Diffusion	93
6.1	Dynamics of Diffusion	93
6.2	The Multi-Bernoulli Map	95
6.3	The Generalized Spectral Decomposition	97
6.4	Transport as an Exact Dynamical Property	102
6.5	Eigenfunctionals of Diffusion	106
6.6	The Multi-baker Map	110
7	Afterword	115
A	Appendices	117
A.1	Complex Microstructure of Phase Space	117
A.2	More on Mixing	119
A.3	Isometry of U_B^\dagger	121
A.4	Dual States	122
A.5	The Resolvent Formalism	123
A.6	Rescaled Legendre Polynomials	125
A.7	Formal Expression for the Eigenstates	128
A.8	Explicit Evaluation of Eigenpolynomials	129
A.9	Bernoulli Polynomials	131
A.10	Generating Function Technique	133
A.11	Jordan States	137
A.12	Dual States of Jordan States	140
A.13	Shift Polynomial Duals	141
A.14	Symmetries in a Class of One-Dimensional Maps	142
A.15	Invariant Measure of the Cantor Map	146
A.16	Explicit Form of $\eta_n(x)$	147
A.17	Decomposition with Asymptotic Periodicity	148
A.18	Frobenius–Perron Operator of the Baker Map	157
A.19	Green–Kubo Formalism for the Multi-Bernoulli map	158
A.20	Frobenius–Perron Operator of the Multi-Bernoulli map	160
A.21	Eigenstates of the Full Multi-Bernoulli Map	161
Index		162

Foreword

I am very pleased and privileged to write a short foreword for the monograph of Dean Driebe: *Fully Chaotic Maps and Broken Time Symmetry*. Despite the technical title this book deals with a problem of fundamental importance. To appreciate its meaning we have to go back to the tragic struggle that was initiated by the work of the great theoretical physicist Ludwig Boltzmann in the second half of the 19th century.

Ludwig Boltzmann tried to emulate in physics what Charles Darwin had done in biology and to formulate an evolutionary approach in which past and future would play different roles. Boltzmann's work has lead to innumerable controversies as the laws of classical mechanics (as well as the laws of quantum mechanics) as traditionally formulated imply symmetry between past and future. As is well known, Albert Einstein often stated that "Time is an illusion". Indeed, as long as dynamics is associated with trajectories satisfying the equations of classical mechanics, explaining irreversibility in terms of trajectories appears, as Henri Poincaré concluded, as a logical error. After a long struggle, Boltzmann acknowledged his defeat and introduced a probability description in which all microscopic states are supposed to have the same a priori probability. Irreversibility would then be due to the imperfection of our observations associated only with the "macroscopic" state described by temperature, pressure and other similar parameters. Irreversibility then appears devoid of any fundamental significance.

However today this position has become untenable. Nonequilibrium physics has shown that the flow of time plays an essential constructive role as it leads to nonequilibrium structures; often called "dissipative structures" to distinguish them from equilibrium structures such as crystals. It becomes absurd to imagine that we, through our approximations, are at the origin of the arrow of time found at all levels of observation. A time-reversible world would also be a world we could not learn how to describe as every experiment implies a difference between past and future.

What then is the way out? Gradually I was driven to the conclusion that the traditional formulations of classical and quantum mechanics have to be extended to include time symmetry breaking.¹ This, however, requires the construction of a new mathematical formulation which reduces to the usual formulation of classical or quantum mechanics in simple situations.

¹I. Prigogine, *From Being to Becoming* (W.H. Freeman and Company, New York, 1980); I. Prigogine and I. Stengers, *Order Out of Chaos* (Bantam, New York, 1983); I. Prigogine, *The End of Certainty* (The Free Press, New York, 1997).

While the physical ideas have been clear for a considerable length of time² a precise mathematical formulation has emerged only during the past few years. The simplest example where we can at present extend the laws of classical dynamics is precisely deterministic chaos, the subject of this book.

The essential point is that dynamics can be formulated either on the level of individual trajectories or in terms of ensembles as introduced by Gibbs and Einstein in their fundamental work on thermodynamics. Traditionally ensembles were associated with ignorance. It was always assumed that from the dynamical point of view the two descriptions are equivalent. However – and that is the most interesting conclusion described in this book – this is not so for chaotic systems. The probabilistic description in terms of ensembles is properly formulated with operator theory extended to generalized functional spaces. Then the ensemble description leads to new solutions irreducible to the usual description in terms of trajectories. That is what we mean by the “extension” of classical dynamics. Thanks to this recent development, we may consider that Boltzmann’s time paradox has found its natural resolution. It is no more necessary to make any reference to extra-dynamical features such as coarse graining or environmental noise as has been done in the past.

Chaotic maps are only one example where the individual description in terms of trajectories and the ensemble description lead to different formulations. Thermodynamic systems form another class. This class has been studied elsewhere.³ Dean Driebe’s presentation is limited to chaotic maps but even so it makes fascinating reading as it shows how to solve a long-standing paradox, which has been hotly debated for over a hundred years.

Dean Driebe is especially well-prepared to write this monograph as he has made a number of original contributions to the subject. I am sure that his book will be of great interest to all scientists, philosophers and engineers who are interested in the perennial questions of the limits of determinism and the meaning of time.

Ilya Prigogine

²I. Prigogine, *Nonequilibrium Statistical Mechanics* (Wiley-Interscience, New York, 1962).

³T. Petrosky and I. Prigogine, “Poincaré resonances and the extension of classical dynamics,” *Chaos, Solitons & Fractals* **7**, 441 (1996); “The Liouville space extension of quantum mechanics,” in *Advances in Chemical Physics*, **99**, (John Wiley, New York, 1997).

Preface

This book originated from notes for a series of lectures given by the author at the University of Chile in December 1994. The purpose of the lectures was to present some of the recent work, mainly of the groups directed by I. Prigogine in Austin and Brussels, on the time evolution of densities in chaotic systems and its relevance to the problem of irreversibility. The emphasis was on the construction of new spectral decompositions of time evolution operators in generalized functional spaces. These decompositions allow for a detailed study of nonequilibrium processes and an understanding of time-symmetry breaking. The approach realizes part of the goal of the Prigogine group to understand irreversibility as an intrinsic property of unstable dynamical systems.

The book deals only with fully chaotic maps, where complete, exact spectral decompositions have been obtained. Besides the intrinsic interest of these systems – even if they don't display generic behavior from a physical point of view – they elucidate the main assertion that dynamical instability is the root of irreversibility. Several advances have been made in the last couple of years, mainly in explicit results obtained for a variety of one-dimensional maps and the discovery of an unexpectedly rich variety of spectra found in a class of simple one-dimensional piecewise-linear maps. These new results, some of which have not yet been published, have been included so that the book gives an up-to-date presentation. The purpose though has not been to give an exhaustive review of the subject but to write an introduction for students and research workers who want to know how the generalized spectral decompositions are obtained and the range of systems that have been considered. The presentation does not strive for mathematical rigor, rather it emphasizes ideas, results and calculational tools. The reader interested in mathematical details may refer to the literature cited as well as the forthcoming monograph by I. Antoniou.

The first two chapters essentially cover background material. In Chapter 1 the motivation for the approach used is discussed as pertinent to the dynamical understanding of irreversibility. An introduction to the concept of probability densities in the phase space of a chaotic system is given and the hierarchy of types of behavior in phase space is presented. In Chapter 2 a more detailed discussion of nonequilibrium statistical mechanics of chaotic maps is given and time correlation functions of observables is discussed in the context of how their behavior reflects on the spectral properties of the time evolution operator of the system.

The heart of the book begins in Chapter 3 where the simple one-dimensional

Bernoulli map is studied and the construction of the spectral decomposition of its Frobenius–Perron operator is given in detail. In this and the following chapter one-dimensional systems with non-invertible trajectory dynamics are considered. These systems are irreversible from the beginning but they share many key features with the invertible systems considered later in the book. In Chapter 4 a variety of maps of the unit interval are discussed. An algebraic technique utilizing symmetry is used to obtain the explicit spectral decomposition of some maps, including the well-known tent map. Also, a map with a fractal repeller is considered and the decomposition of topologically conjugate maps is discussed and applied to obtain the decomposition of the logistic map with unit height.

Chapter 5 is devoted to the baker transformation as the paradigm system to elucidate the time-symmetry breaking of the generalized spectral decomposition. The trajectory dynamics of the baker map is invertible so the associated time evolution operators for densities or observables are unitary in a Hilbert space setting. The group evolution in Hilbert space splits into two distinct semigroups in the generalized representation. In Chapter 6 a model system of deterministic diffusion is considered. Transport properties are identified in the exact spectrum of the full time evolution operator of the system and quite interesting generalized eigenstates with fractal properties appear.

There are several appendices collected at the end of the book. This material expands on some topics discussed in the main text and fills in details of some of the calculations. At the end of each chapter appear bibliographical notes with comments on what can be found in the relevant books and papers. No attempt has been made to be exhaustive in the referencing. Also, in the text itself there do not generally appear specific reference citations. I feel that this is appropriate for a book presentation.

I am grateful to Enrique Tirapegui for inviting me to Santiago to give the lectures and write this book. My utmost gratitude goes to I. Prigogine for his support and encouragement and for his kindness in writing the foreword. I thank Hiroshi H. Hasegawa from whom I learnt many of the methods presented in this book. Many of the recent results presented in Chapter 4 have been obtained in collaboration with Gonzalo Ordóñez. My progress in the subject benefitted over the years from discussions with Ioannis Antoniou, Oscar Bandtlow, Francisco Bosco, Pierre Gaspard, Donal MacKernan, Bill Saphir and Shuichi Tasaki. I also acknowledge Irene Burghardt, David Daems, Brian LaCour and Suresh Subbiah for their comments on draft versions of the manuscript. Thanks is due Annie Harding for typing the original manuscript and David Leonard for assistance in preparing the figures.

Chapter 1

Chaos and Irreversibility

In contrast to the manifest irreversibility of nearly all systems we observe in nature, the basic dynamical laws of physics, be they classical or quantum, are time reversible. It has been a long-standing problem in physics to reconcile these two facts. The recent realization that unstable or chaotic dynamical systems are the most typical in nature has given fresh insight into this problem. We begin in this chapter with an informal discussion of the relation of unstable dynamics to the problem of irreversibility. We then discuss some general aspects of the evolution of probability densities in chaotic systems.

1.1 Irreversibility and Complexity

Traditional approaches to the explanation of irreversibility have always included extra-mechanical elements, such as coarse graining, which are difficult to justify and introduce subjectivity into the description of the time evolution of systems. These extra-mechanical elements have been considered necessary because the evolution laws for trajectories (or wavefunctions) are time reversible and the operators describing the evolution of ensembles are unitary so that time-oriented eigenmodes cannot be obtained in regular functional spaces.

The main idea of the Prigogine school of nonequilibrium statistical mechanics is to extend the formulation of the laws of dynamics to include irreversibility on the fundamental level. This goal was inspired by the realization that irreversible processes are ubiquitous in nature and play a constructive role on many levels. Quoting from Prigogine's book *From Being to Becoming*: "Irreversibility corresponds not to some supplementary approximation introduced into the laws of dynamics but to an embedding of dynamics

within a vaster formalism.” Of course, this new formalism should reduce to the well-known reversible laws of dynamics for simple systems displaying, for example, periodic motion, such as harmonic oscillation or two-body attractive central force motion. Irreversibility should occur only if the system is sufficiently complex.

Complex behavior has traditionally been associated with systems of many degrees of freedom. As all statistical mechanics textbooks state: to solve Hamilton’s equations for a system of N interacting particles, where N corresponds to a macroscopic sample so that $N \gtrsim 10^{23}$, is a hopelessly complicated task. In practice one then considers not the set of trajectories of the particles but a statistical description involving an ensemble distribution. From the point of view of describing the macroscopic behavior of a system, especially in equilibrium situations, this approach is generally valid since such behavior usually doesn’t depend on details of the microscopic motions. If though one would like to understand the emergence of irreversible behavior from reversible microscopic dynamics, the bridge between these levels requires deeper considerations.

As is now well known, it is by no means necessary for a system to have many degrees of freedom to exhibit “complex” behavior. For a discrete time system, only one degree of freedom is necessary for chaotic behavior. Chaos means that the system displays “sensitivity to initial conditions.” This means that two closely-spaced initial trajectories will spread exponentially in time under the dynamics.

Why should chaos be related to irreversibility? Let us quote David Ruelle from his book *Chaotic Evolution and Strange Attractors*. Speaking of chaos he states that “...the exponential growth of errors makes the time evolution self-independent from its past history and then nondeterministic in any practical sense.” This statement certainly suggests that the applicability of time-reversibility for a system whose evolution makes it self-independent from its past is in doubt. But Ruelle implies that this problem is only of a practical nature. For us, chaos leads to a formulation of dynamics transcending traditional theoretical approaches and allows for an understanding of irreversibility as an intrinsic property of chaotic systems.

A simple picture of chaotic evolution associated with diverging trajectories doesn’t tell the whole story. In fact, the phase space of strongly chaotic systems in general has points (i.e., initial conditions) leading to regular (periodic) motion densely distributed among points leading to chaotic motion. (See Appendix A.1 for more on this.) This is in contrast to stable systems where different types of motion occur in finite regions of phase space with distinct boundaries between the regions.

The complex motion in chaotic systems naturally generates densities on the phase space. (If we follow the motion of a typical trajectory for a long time it will wander all over the chaotic region with the relative time spent in various parts of the region yielding a density, i.e., we consider ergodic systems – more about this later.) An initial nonequilibrium density may correspond to some uncertainty in the specification of the initial condition or may be thought of as representing an ensemble of systems with different initial conditions. A smooth density is supported on a finite region of phase space and so its evolution contains some non-local information that is missing in a point dynamical description.

For stable systems exhibiting regular motion the description of the dynamics in terms of the evolution of a density is generally reducible to a point density corresponding to an evolving trajectory. This is because in such a system the density may sample a region containing only one typical kind of trajectory behavior. For example, if for a pendulum we consider a smooth density supported on a region away from the separatrix we may reduce the density successively to a typical point in its support without a qualitative change in its behavior. But for chaotic systems the reduction from a smooth density corresponding to a statistical ensemble to a point density is wrought with inherent difficulties because the complex microstructure in phase space doesn't allow for an unambiguous limit. Quoting from Prigogine again: "Is this difficulty practical or theoretical in nature? I would support the view that this result has important theoretical and conceptual significance because it forces us to transgress the limits of a purely dynamical description." As we will see, the natural description for the time evolution in chaotic systems will be in terms of densities that are *irreducible* to trajectories. This representation of the time evolution operator involves generalized functional spaces. This will yield an intrinsically irreversible description for systems that nevertheless have time-reversible trajectory dynamics.

1.2 Densities in Chaotic Maps

In this book we are going to concentrate on the analysis of chaotic maps. Maps are discrete-time dynamical processes that may arise in several different contexts. A map may arise directly from the statement of a physical problem; for instance, a system that is kicked periodically and follows free motion between kicks. A map may also be constructed by taking a slice in phase space of a continuous-time system. Our interest in chaotic maps is that they are the simplest systems that have relevant features of chaotic

Hamiltonian systems. We use them as models to explore the dynamics and statistical mechanics of chaotic systems.

A map is specified by a dynamical law that determines how an initial point, x_0 , evolves. (The dimension of the space of points to which x belongs may be greater than 1.) The map tells how to evolve one time step and to get t steps we apply an iterative procedure; thus, $x_t = S(x_{t-1}) = S(S(x_{t-2})) = \dots = S_t(x_0)$, where S is the rule for the map. This procedure yields a trajectory for the system. There now exists a huge literature on trajectory dynamics in chaotic systems. The principal characterization of chaotic trajectory dynamics is given by the values of the positive Lyapunov exponents, which determine the rate of exponential spreading of nearby trajectories.

An alternative picture of the dynamics may be obtained from a statistical mechanics approach by considering an ensemble description. If we pick N initial points: $x_0^1, x_0^2, \dots, x_0^N$ and apply the map to each point we obtain N new points: $x_1^1, x_1^2, \dots, x_1^N$. A density, $\rho(x, t)$, at time step t , will describe this ensemble of N points if

$$\int_{\Delta} dx \rho(x, t) \simeq \frac{1}{N} \sum_{j=1}^N \chi_{\Delta}(x_t^j), \quad (1.1)$$

where

$$\chi_{\Delta}(y) = \begin{cases} 1, & y \in \Delta \\ 0, & y \notin \Delta \end{cases}$$

is the characteristic function of a small set Δ .

To determine the rule for the evolution of densities given the rule for points (i.e., trajectories) consider the evolution of a density corresponding to a trajectory. The point x_0 evolving to $S(x_0)$ after one iteration is equivalent to the singular density described by a Dirac delta function, $\delta(x - x_0)$, evolving to $\delta(x - S(x_0))$. The new density may be written in terms of the original one as

$$\delta(x - S(x_0)) = \int dx' \delta(x - S(x')) \delta(x' - x_0). \quad (1.2)$$

The evolution of a smooth density may be obtained then just by superposition. Since $\rho(x, t) = \int dx_0 \delta(x - x_0) \rho(x_0, t)$ we obtain

$$\rho(x, t+1) = \int dx' \delta(x - S(x')) \rho(x', t) \equiv U \rho(x, t), \quad (1.3)$$

where we have defined the operator U , called the Frobenius–Perron operator, which evolves densities. Thus, in order to obtain the density at time t from

an initial density at time $t = 0$ the Frobenius–Perron operator is applied t times as $\rho(x, t) = U^t \rho(x, 0)$.

A very important fact we may notice immediately is that U is a linear operator. This is in contrast to the trajectory evolution which proceeds by an iterative process that is highly nonlinear. We may thus employ linear operator theory to study chaotic dynamics from the point of view of evolving densities. Even though the evolution of a density is determined by superposing trajectories, we will see later that we may nevertheless construct spectral decompositions of U that are irreducible to trajectories.

The behavior of trajectories and densities in a given system may be strikingly different. For a uniformly chaotic system a typical trajectory will wander around in the phase space in an apparently random fashion. Even in systems with non-invertible trajectory dynamics, a time series of the trajectory may look qualitatively similar forward or backward in time. In contrast, the evolution of a density will usually be obviously time-oriented and will often approach an attracting equilibrium state. These two types of behavior are illustrated in Figures 1.1 and 1.2 for the simple example of the one-dimensional dyadic Bernoulli map on the interval $[0, 1)$. This system will be studied in detail in Chapter 3.

We note then a somewhat complementary character of trajectories versus densities. For a system with very chaotic or irregular trajectory behavior the density will normally show a quite regular behavior. On the other hand, for regular motion, such as periodic trajectories, the density behavior will generally mirror the trajectory behavior.

Discussions of the approach to equilibrium in simple chaotic systems are not very prevalent in the literature. In many places where the Frobenius–Perron operator is discussed it is used just to obtain the invariant density of the system. In fact, many authors discuss invariant densities and even show pictures of them generated numerically and comment how they were obtained “after neglecting transients.” For us the so-called transients are our main interest.

1.3 Types of Behavior in Phase Space

The dynamics of a system in phase space may be classified according to its behavior over long times. A hierarchy of behavior may be identified and the Frobenius-Perron operator is useful for the classification. In the next chapter we will discuss in more detail how to do statistical mechanics of chaotic maps. For the present discussion it is only necessary to know that

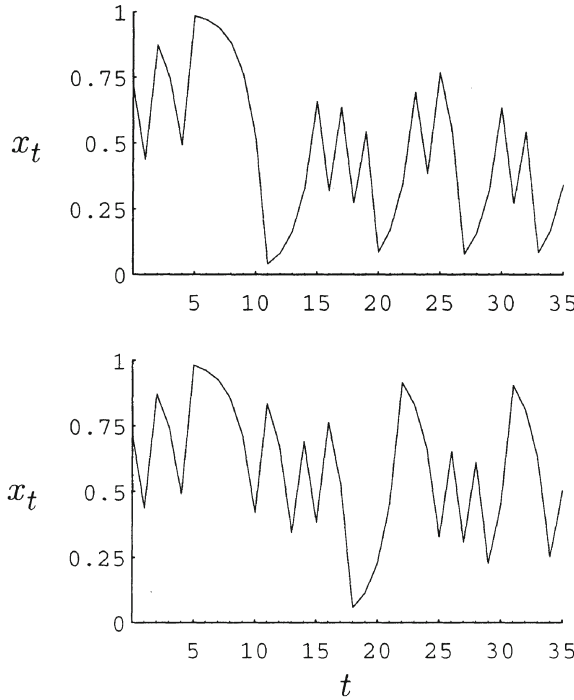


Figure 1.1: Evolution of two initially close trajectories evolving under the Bernoulli map: $x_t = 2x_{t-1} \bmod 1$. After about 10 time steps the trajectories follow completely different paths illustrating the sensitivity to initial conditions of the trajectory dynamics.

averages of observables are calculated from the probability density by using it as a weight function and integrating over the phase space.

The first type of systems we consider are ergodic systems. A system is ergodic when long time averages may be replaced by phase space averages. The time average of some function, $B(x)$, of the phase space variable x is

$$\langle B \rangle^{\text{TA}} \equiv \lim_{T \rightarrow \infty} \frac{1}{T} \sum_{\tau=0}^{T-1} B(x_\tau). \quad (1.4)$$

But we may rewrite $B(x_\tau)$ as

$$B(x_\tau) = B(S_\tau(x_0)) = \int dx \delta(x - S_\tau(x_0)) B(x). \quad (1.5)$$

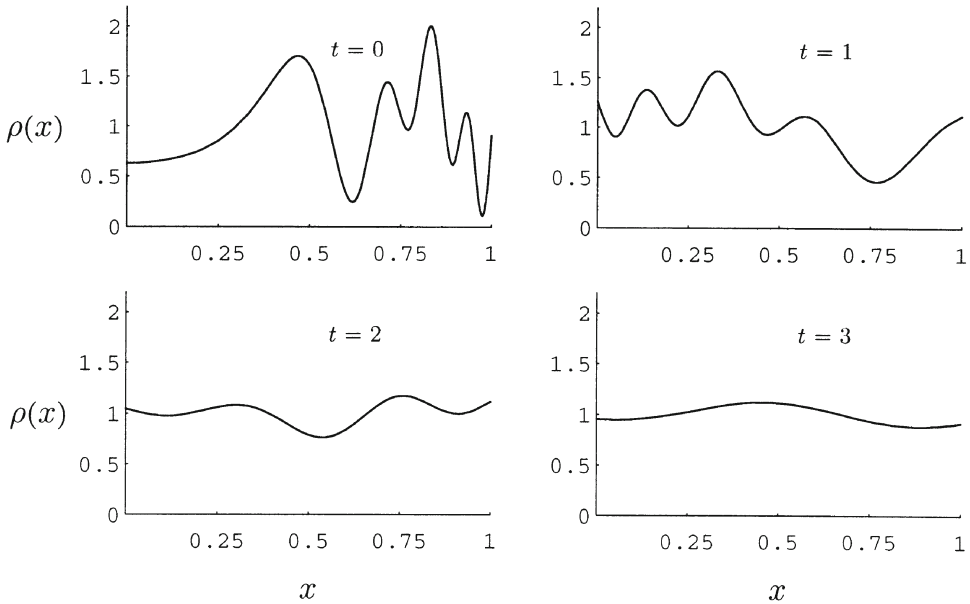


Figure 1.2: Evolution of an initial nonequilibrium density in the Bernoulli Map. After just three time steps the density has nearly approached the equilibrium density, which is uniform for this system.

Using this in (1.4) and assuming that the integration and the infinite summation may be interchanged gives that $\langle B \rangle^{\text{TA}} = \langle B \rangle^{\text{eq}}$ where

$$\langle B \rangle^{\text{eq}} \equiv \int dx B(x) \rho^{\text{eq}}(x), \quad (1.6)$$

and the equilibrium density is defined operationally here from the time average of trajectory iterates as

$$\rho^{\text{eq}}(x) = \lim_{T \rightarrow \infty} \frac{1}{T} \sum_{\tau=0}^{T-1} \delta(x - S_\tau(x_0)). \quad (1.7)$$

Of course, in general this expression could depend strongly on x_0 if, for example, $S_\tau(x_0)$ is eventually periodic. For the systems we will consider, which are fully chaotic, for almost all x_0 (i.e., except for a zero measure set of initial conditions) the above time average will yield the “physical” $\rho^{\text{eq}}(x)$ of the system.

The average in (1.4) or (1.6) is the time-independent equilibrium average of the quantity B . More generally, we are interested in averages with respect to a nonequilibrium density, $\rho(x, t)$, as

$$\begin{aligned}\langle B \rangle_t &= \int dx B(x) \rho(x, t) \\ &\equiv \langle B(x) | \rho(x, t) \rangle \\ &= \langle B(x) | U^t \rho(x, 0) \rangle,\end{aligned}\quad (1.8)$$

where in the second line we have introduced an obvious bracket notation. Ergodicity of the system means that for $\langle B \rangle_t$ its time average is equivalent to a phase space average as

$$\lim_{T \rightarrow \infty} \frac{1}{T} \sum_{\tau=0}^{T-1} \langle B(x) | U^\tau \rho(x, 0) \rangle = \langle B(x) | \rho^{\text{eq}}(x) \rangle. \quad (1.9)$$

It is not necessary for a system to be chaotic to be ergodic; it is only required that the density, if it is concentrated in some region, will travel throughout phase space over time with the relative frequency to visit various regions given by $\rho^{\text{eq}}(x)$.

Note that the condition of ergodicity does not imply anything about the approach of the nonequilibrium average of an observable to its equilibrium average. In fact, densities themselves (or observables) are not necessarily approaching equilibrium in ergodic systems, i.e., $\lim_{t \rightarrow \infty} \rho(x, t)$ does not itself have to approach $\rho^{\text{eq}}(x)$ for (1.9) to hold. In this sense a satisfactory theory of the general approach to equilibrium (i.e., nonequilibrium statistical mechanics) can not be based on just the study of ergodic systems. A simple example of an ergodic transformation is the one-dimensional map on the unit interval given by

$$x_{t+1} = x_t + \alpha \bmod 1, \quad (1.10)$$

where α is an irrational number. This system is not chaotic.

The second type of behavior we consider is exhibited by so-called mixing systems. In these systems there is the stronger condition that phase space averages themselves approach equilibrium values, i.e.,

$$\lim_{t \rightarrow \infty} \langle B(x) | U^t \rho(x, 0) \rangle = \langle B(x) | \rho^{\text{eq}}(x) \rangle. \quad (1.11)$$

Of course, for a given system one would not expect this condition to be satisfied for any $B(x)$ (or any initial density) and considerations of the class of functions for which it is satisfied will play a role in our later analysis.

Mixing systems are usually characterized (when the phase space dimension is greater than one) by densities tending to filament throughout the phase space. This implies some stretching, which may not be exponential so mixing doesn't necessarily imply chaotic dynamics, but the mixing systems we will consider are chaotic. As with ergodicity, it is not necessary that the density in mixing systems strongly approach the equilibrium density. An example of a chaotic mixing transformation is the baker map acting on the unit square as

$$(x_{t+1}, y_{t+1}) = \begin{cases} (2x_t, y_t/2), & 0 \leq x_t < \frac{1}{2} \\ (2x_t - 1, y_t/2 + 1/2) & \frac{1}{2} \leq x_t < 1. \end{cases} \quad (1.12)$$

Mixing systems are necessarily ergodic.

Finally, there are so-called exact systems where any initial density strongly approaches to the equilibrium density, i.e.,

$$\lim_{t \rightarrow \infty} \| U^t \rho(x, 0) - \rho^{\text{eq}}(x) \| = 0, \quad (1.13)$$

where we mean the L^1 norm here and elsewhere if not otherwise specified. The dyadic Bernoulli map, $x_{t+1} = 2x_t \bmod 1$, is an example of an exact system. Exact systems are mixing and thus ergodic also.

Our interest is in time-dependent properties, such as the rate of the approach to equilibrium, and not just that a system will approach equilibrium. Thus we consider systems which are at least mixing since these are the ones for which observables approach equilibrium. Exact systems are also important for us since some mixing systems, especially the ones which we shall consider, are composed of a combination of dynamics where one of the elements is an exact dynamical system.

Bibliographical Notes

Full references for the two books quoted in Section 1.1 are:

- I. Prigogine, *From Being to Becoming* (W.H. Freeman and Company, New York, 1980).
- D. Ruelle, *Chaotic Evolution and Strange Attractors* (Cambridge University Press, Cambridge, 1989).

Prigogine's book is an insightful and fresh reassessment of the foundations of physics and chemistry from the perspective of time and complexity as fundamental to our understanding of the world around us. Ruelle's little book gives a concise overview of chaos and its statistical aspects by one of the masters of the subject. A general presentation of the recent work of the Prigogine group is in

- I. Prigogine, *The End of Certainty* (The Free Press, New York, 1997).

A good reference discussing the physical motivation for considering chaotic maps and a little about the Frobenius-Perron operator is

- H.G. Schuster, *Deterministic Chaos* (VGH Publishers, Berlin, 1989).

The derivation in Section 1.2 of the Frobenius–Perron operator by superposing densities corresponding to trajectories is adapted from this book.

The best general reference I have seen on the behavior of densities in chaotic systems is

- A. Lasota and M. Mackey, *Chaos, Noise and Fractals* (Springer-Verlag, New York, 1994).

The first edition of this book was published with the more revealing title *Probabilistic Properties of Deterministic Systems* (Cambridge University Press, Cambridge, 1985). Also of interest is the concise presentation of much of the material in that book, with relevance to the problem of irreversibility, in

- M. Mackey, *Time’s Arrow: The Origins of Thermodynamic Behavior* (Springer-Verlag, New York, 1992).

Chapter 2

Statistical Mechanics of Chaotic Maps

We give now a more precise formulation of some of the ideas mentioned in the first chapter. The basic tools needed for a statistical mechanics approach to chaotic dynamics are given. Resonances are discussed by considering the various types of correlation decay in mixing systems.

2.1 Statistical Mechanics

The setting for a modern discussion of dynamics starts with a phase space M with a σ -algebra \mathcal{A} of sets and a measure function μ . Since we will not discuss detailed measure-theoretic aspects of the systems we will study it is not necessary for us to give the precise definitions of a σ -algebra or a measure function. It is more than sufficient to know that a σ -algebra is a collection of sets closed under the formation of complements and countable unions and a measure function is a non-negative and countably additive set function. A measure space is the setting for modern probability theory so this is a natural framework for the investigation of the probabilistic aspects of dynamical systems.

In most of the examples we will treat, the phase space will either be the unit interval or the unit square and the sets in the σ -algebra we will consider will be intervals for $M = [0, 1]$ and Cartesian products of intervals (rectangles) for $M = [0, 1] \times [0, 1]$. The measure will often be Lebesgue, i.e., for a set $A \in \mathcal{A}$, $\mu_L(A) = \int_A dx$, giving the length of an interval in one dimension or the area of a rectangular patch in two dimensions. A measure absolutely continuous with respect to Lebesgue measure involves a density

obtainable from a continuously differentiable function $\alpha(x)$ as $\rho(x) = d\alpha/dx$ so that

$$\mu_\rho(A) = \int_A d\alpha = \int_A dx \frac{d\alpha}{dx} = \int_A dx \rho(x). \quad (2.1)$$

Singular measures will also be encountered; in which case we can only go so far as the second term in (2.1) so that the measure will be in terms of a Riemann–Stieltjes integral. We will always deal with a bounded phase space so we will take the measure of the whole phase space normalized to unity.

The dynamics on M is given by a law $S_t : M \rightarrow M$ which maps points in M to points in M . Since we will only discuss maps which are discrete time processes, t will only take integer values. (For $t = 1$ we usually drop the subscript i.e., $S \equiv S_1$.) The dynamical law may or may not be invertible. In any case, our main interest is in measure-preserving transformations. These are transformations such that for an arbitrary set $A \in \mathcal{A}$ there is an invariant measure, μ , satisfying $\mu(S^{-1}(A)) = \mu(A)$. Here $S^{-1}(A)$ is the inverse image of the set A , which is well-defined (it being the set of all points x such that $S(x) \in A$) even if the dynamical law is non-invertible. The density defining the invariant measure is called the invariant (or equilibrium) density. Measure-preserving transformations (which include the phase-space transformation generated by Hamiltonian dynamics) are important for us because they preserve probability and in this sense are not dissipative systems where irreversible behavior is trivial.

The systems we will deal with that have a strong approach of their density to an equilibrium density are so-called exact systems as was discussed in Section 1.3. The measure-theoretic way to express exactness is provided by the condition

$$\lim_{t \rightarrow \infty} \mu(S_t(A)) = 1, \quad (2.2)$$

for all sets A of nonzero measure. Note that this condition involves the forward iteration of the set A , so that it may be satisfied by a measure-preserving transformation. But if a measure-preserving transformation is invertible then $\mu(S(A)) = \mu(S^{-1}(S(A))) = \mu(A)$ so that $\mu(S_t(A)) = \mu(A)$ and such a system cannot be exact. Of course, for the elucidation of irreversibility in systems governed, for instance by Hamiltonian dynamics, we need to consider invertible dynamical laws. As we will see though, the investigation of non-invertible dynamical laws already contains features relevant to invertible systems.

In the classical mechanics context in which we are working, an observable, \mathcal{O} is simply a function of the phase space variables that gives a real number as a result, i.e., $\mathcal{O} : M \rightarrow \mathbb{R}$. For example, the “position” is an observable

where $\mathcal{O}(x) = x$.

In a statistical mechanics context, the state of a system at time t is characterized by a probability density, $\rho(x, t)$. The only primitive requirements for a density is that it be non-negative and integrable. This means that it is an L^1 function, i.e., $\int_M |\rho(x, t)| dx < \infty$ and it is usually taken to have unit L^1 norm: $\|\rho\| = \int_M |\rho(x, t)| dx = 1$. Using the density we may calculate expectation values of observables by an integration weighted with the density as

$$\langle \mathcal{O} \rangle \equiv \int_M dx \mathcal{O}(x) \rho(x). \quad (2.3)$$

The time evolution of an expectation value may be determined by either evolving the density or the observable. (The two viewpoints correspond to the Schrödinger or Heisenberg picture, respectively, in quantum dynamics.) From the way expectations are calculated, it is natural to consider $\mathcal{O}(x)$ and $\rho(x)$ to be members of an inner product space. Traditionally, they are taken as elements of the self-dual space, L^2 , of square-integrable functions. We will see later in detail why this is not the best functional space for the elucidation of many physical features of the dynamics. Nevertheless, we can regard it as a starting point.

Densities evolve by the (linear) Frobenius-Perron operator, U , defined by

$$\begin{aligned} \rho(x, t+1) &= U\rho(x, t) \equiv \int_M dx' \delta(x - S(x')) \rho(x', t) \\ &= \sum_{x': S(x')=x} \frac{\rho(x', t)}{|dS(x')/dx'|}, \end{aligned} \quad (2.4)$$

where the sum is taken over the inverse branches of the possibly many-to-one map S . The final line above comes just from how the delta function with its argument being a function evaluates under integration. When the phase space is more than one-dimensional the denominator is the Jacobian of the transformation. In the case that the map is invertible and the Jacobian is one we have simply that $U\rho(x, t) = \rho(S^{-1}x, t)$. Note that the forward evolution of the density involves the backward evolution of phase points. This is intuitive when one realizes that the density at x at time $t+1$ equals the density at the inverse image of x at time t .

An important property of U is that it is a contractive operator as

$$\|Uf\| \leq \|f\|, \quad (2.5)$$

for any $f \in L^1$. (If $f \geq 0$ (2.5) is an equality as it then expresses conservation of probability.) The contractive property of U means that under successive

applications of U on two different functions the norm of their difference may decrease or remain constant but will never increase.

The evolution of observables is governed by the Koopman operator, K , which acts as

$$K\mathcal{O}(x) \equiv \int dx' \delta(x' - S(x)) \mathcal{O}(x') = \mathcal{O}(S(x)). \quad (2.6)$$

The Koopman operator is the adjoint of the Frobenius-Perron operator so we usually just denote it as U^\dagger .¹ (The adjoint of U is given by the operator that satisfies $\langle f|Ug \rangle = \langle U^\dagger f|g \rangle$.)

As an aside, we note that in Hamiltonian, continuous-time systems, the time evolution operator for probability densities is given by $U^t = e^{iLt}$, where L , the Liouvillian, is the generator of evolution given by the Poisson bracket with the Hamiltonian as $L \cdot \equiv i\{H, \cdot\}$. In a Hilbert space setting, L is an Hermitian operator so that U is unitary, i.e., $U^\dagger = U^{-1}$.

Returning to maps, if the transformation is measure-preserving, the Koopman operator will be isometric, i.e., $\|U^\dagger f\| = \|f\|$ (for an arbitrary function f) so that $UU^\dagger = 1$. If the transformation is invertible as well then both $U^\dagger U = UU^\dagger = 1$ so that U is unitary.

Unitary, or isometric operators, are norm-preserving so they may only have eigenvalues of modulus 1 in normed spaces. To see this, consider an eigenfunction, f , of an isometric operator V . Then $\|Vf\| = \|\lambda f\| = |\lambda| \|f\|$, where λ is the eigenvalue. By isometry though, $\|Vf\| = \|f\|$, thus $|\lambda| = 1$. Hence, we can already anticipate that we need to go outside usual function spaces to obtain decay eigenfunctions of the time evolution operators we will consider.

2.2 Decay of Correlations and Resonances

An important signature of chaotic evolution may be obtained from the consideration of correlations of dynamical variables. The time correlation of two observables $\sigma(x)$ and $\eta(x)$ is defined by

$$\hat{C}_{\sigma,\eta}(t) = \lim_{T \rightarrow \infty} \frac{1}{T} \sum_{\tau=0}^{T-1} \sigma(x_{t+\tau}) \eta(x_\tau). \quad (2.7)$$

¹In books on ergodic theory the Koopman operator is often referred to as the “induced” operator of a transformation and is often denoted by U . Since we are interested in the dynamics of the system from the point of view of statistical mechanics we take the Frobenius-Perron operator as the primary time evolution operator and so denote it as U .

It tells us how much observables determined by iterates t steps apart “know about each other” on average. (Of course, the initial value, x_0 , should be a generic initial condition, not a special one leading to periodic motion.) The correlation is accessible from experimental data or numerically from the time series x_t . Qualitatively, one would expect chaotic dynamics to yield a rapid decorrelation of most observables, such as the trajectory iterates.

If the transformation is ergodic we can replace the time average by a phase space average to give

$$\begin{aligned}\hat{C}_{\sigma,\eta}(t) &= \int_M dx \sigma(S_t(x)) \eta(x) \rho^{\text{eq}}(x) \\ &= \langle (U^\dagger)^t \sigma | \eta \rho^{\text{eq}} \rangle = \langle \sigma | U^t (\eta \rho^{\text{eq}}) \rangle.\end{aligned}\quad (2.8)$$

If the transformation is mixing we then have that

$$\begin{aligned}\lim_{t \rightarrow \infty} \langle \sigma | U^t (\eta \rho^{\text{eq}}) \rangle &= \langle \sigma | \rho^{\text{eq}} \rangle \langle 1 | \eta \rho^{\text{eq}} \rangle \\ &= \langle \sigma \rangle^{\text{eq}} \langle \eta \rangle^{\text{eq}},\end{aligned}\quad (2.9)$$

where the first line may be derived from the measure-theoretic definition of mixing:

$$\lim_{t \rightarrow \infty} \mu(S_{-t}(D) \cap E) = \mu(D)\mu(E), \quad (2.10)$$

where D and E are two sets of nonvanishing measure. (See Appendix A.2 for more on mixing, a proof of (2.9), and the relation of (2.10) to the mixing property (1.11).)

Thus, for mixing systems correlations decay to their equilibrium values and it is convenient to define the correlation with its equilibrium value subtracted off so that it decays to zero as

$$\lim_{t \rightarrow \infty} C_{\sigma,\eta}(t) \equiv \lim_{t \rightarrow \infty} [\hat{C}_{\sigma,\eta}(t) - \langle \sigma \rangle^{\text{eq}} \langle \eta \rangle^{\text{eq}}] = 0. \quad (2.11)$$

In general the decay may be very complicated. For some classes of systems though, it has been demonstrated that this decay may be decomposed into a sum of well-defined types of behavior.

To consider the decay properties it is useful to introduce the spectral function, $P(\omega)$, which corresponds to the Fourier transform of the correlation function $C(t)$. For noninvertible systems correlations are only defined for $t \geq 0$ and for invertible systems the correlation functions are even functions of t , i.e., $C(t) = C(|t|)$. Thus, we define the spectral function by the cosine transform of $C(t)$ as

$$P(\omega) = \sum_{t=0}^{\infty} C(t) \cos \omega t. \quad (2.12)$$

Then $C(t)$ is expressed in terms of $P(\omega)$ by

$$C(t) = \frac{1}{\pi} \int_{-\pi}^{\pi} d\omega e^{-i\omega t} P(\omega) - C(0)\delta_{t,0}, \quad (2.13)$$

If the system is chaotic, the dynamics is beyond a superposition of periodic motions so it is natural to have a continuous spectrum. By considering the analytic continuation of $P(\omega)$ into the complex plane of the frequency $z = \omega$ we may find simple singularities around which the integration contour can be deformed to determine well-defined discrete decay components. For example, a contribution to $C(t)$ like $e^{(-\gamma_j t - i\omega_j t)}$ will be obtained from a simple pole, $P(z) \sim (z - z_0)^{-1}$, where $z_0 = \omega_j - i\gamma_j$. From a multiple pole, $P(z) \sim (z - z_0)^{-m}$, we will obtain a contribution like $t^{m-1} e^{(-\gamma_j t - i\omega_j t)}$.

The poles, giving the decay rates of approach to equilibrium of the correlation, are intrinsic to the dynamical system and are naturally interpreted as resonances. These resonances have been discussed by Ruelle and others for certain classes of chaotic systems. From our point of view the resonances are physically observed so they should be explicit in the spectral decomposition of the time evolution operator, i.e., the Frobenius–Perron or Koopman operator. This viewpoint corresponds to the Heisenberg program in quantum mechanics. But, as mentioned, the time evolution operators are unitary for invertible systems, or at least the Koopman operator is isometric in non-invertible measure-preserving systems, so they do not have spectral decompositions with decay modes in ordinary functional spaces. In order to obtain decay modes, and the spectrum incorporating the resonances, we will see that we need to consider the operators in generalized functional spaces.

Bibliographical Notes

Ergodic theory has been a fertile subject for mathematicians and much of the literature is highly technical. The classic book on ergodic theory, written at an accessible level for physicists is

- V.I. Arnold and A. Avez, *Ergodic Problems of Classical Mechanics*, (W.A. Benjamin, New York, 1968).

Also recommended is the short and clearly written book

- P. Halmos, *Lectures on Ergodic Theory*, (Math. Soc. of Japan, Tokyo, 1956).

The book of Lasota and Mackey referenced in Chapter 1 covers well for a physicist many of the aspects we have touched on.

The discussion about singularities in the analytic continuation of the spectral function is adapted from:

- P. Gaspard, “What is the role of chaotic scattering in irreversible processes?” *Chaos*, **3**, 427 (1993).

This paper also gives a clear physical motivation for considering generalized spectral decompositions. It discusses several of the systems studied in this book.

A nice account of correlation decay in a mixing system and how the decay properties depend on the type of observables considered is

- J.D. Crawford and J.R. Cary, “Decay of correlations in a chaotic measure-preserving transformation” *Physica D*, **6**, 223 (1983).

Some references to work on resonances in chaotic systems are

- D. Ruelle, “Resonances of Chaotic Dynamical Systems” *Physical Review Letters*, **56**, 405 (1986).
- D. Ruelle, “Locating Resonances for Axiom A Dynamical Systems” *Journal of Statistical Physics*, **44**, 281 (1987).
- S. Isola, “Resonances in Chaotic Dynamics” *Communications in Mathematical Physics*, **116**, 343 (1988).

The paper by Isola gives a simple discussion of resonances with illustrations from numerical calculations.

The appearance of resonances in quantum mechanical decay problems has a long history. Several workers have given alternative mathematical formulations of quantum mechanics that include explicitly the resonances. One approach, given by Böhm and collaborators, leads to a rigged Hilbert space formulation of quantum mechanics and is presented in

- A. Böhm and M. Gadella, *Dirac Kets, Gamow Vectors and Gelfand Triplets* (Springer-Verlag, Berlin, 1989).

Another approach, due to Sudarshan and collaborators, is to consider analytic continuation of the conventional spectra leading to quantum mechanics in dual spaces. A recent reference discussing this approach is

- E.C.G. Sudarshan, “Quantum mechanics in dual spaces” *Physical Review A*, **50**, 2006 (1994).

Chapter 3

The Bernoulli Map

In this chapter we study in detail the simplest example of a chaotic transformation for which we may construct a spectral decomposition of the Frobenius–Perron operator that explicitly incorporates the discrete, physical decay modes of the system. As we will see, this decomposition has elements belonging to a generalized functional space, which implies a restriction of the domain of the Frobenius–Perron operator to smooth densities. We give full details of the construction for this system since the main aspects of the analysis will be applicable to all the systems we will consider.

3.1 The System

The one-dimensional dyadic Bernoulli map acts in the phase space, $M = [0, 1]$, of the unit interval. The dynamical law is $x_{t+1} = S_B(x_t)$ where

$$S_B(x) = 2x \bmod 1 = \begin{cases} 2x & 0 \leq x < \frac{1}{2} \\ 2x - 1 & \frac{1}{2} \leq x < 1. \end{cases} \quad (3.1)$$

The map is shown in Figure 3.1. The uniform stretching factor of 2 means that this map has a global Lyapunov exponent of $\log 2$. This system is not invertible since S_B has two inverse branches: $(S_B^{-1})_1 = x/2$ and $(S_B^{-1})_2 = x/2 + 1/2$. It preserves Lebesgue measure in that the inverse image of an interval, say $[a, b]$, where $0 \leq a < b < 1$, is the union of the two intervals $[a/2, b/2]$ and $[a/2 + 1/2, b/2 + 1/2]$ so that $\mu([a, b]) = b - a$ and $\mu(S^{-1}[a, b]) = b/2 - a/2 + (b/2 + 1/2) - (a/2 + 1/2) = b - a$. Some aspects of trajectory evolution in this system are discussed in Appendix A.1.

Densities in this system evolve by the Frobenius–Perron operator, U_B ,

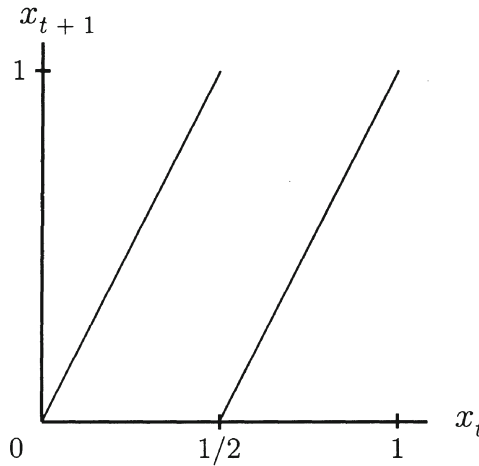


Figure 3.1: The Bernoulli map.

which acts on a density as

$$\rho(x, t+1) = U_B \rho(x, t) = \frac{1}{2} \left[\rho\left(\frac{x}{2}, t\right) + \rho\left(\frac{x+1}{2}, t\right) \right]. \quad (3.2)$$

The action of the Frobenius–Perron operator here is quite simple. It takes the first half of the density defined on $[0, 1/2]$, stretches it to $[0, 1]$, and adds to it the second half of the density defined on $[1/2, 1]$, which has been also stretched to $[0, 1]$. This stretching of the density arises from the unstable trajectory motion. By repeated applications of U_B initial inhomogeneities in the density will be smoothed out as was seen in Figure 1.2. It is easily seen that the invariant density $\rho^{\text{eq}}(x) = 1$ in this system. This state corresponds to the eigenstate of U_B with eigenvalue 1.

The Bernoulli map is an exact system (and thus mixing and ergodic). Exactness is easily demonstrated in this system since $\rho(x, t)$ in terms of $\rho(x, 0)$ from t applications of the Frobenius–Perron operator is

$$\rho(x, t) = U_B^t \rho(x, 0) = \frac{1}{2^t} \sum_{k=0}^{2^t-1} \rho\left(\frac{k+x}{2^t}, 0\right). \quad (3.3)$$

In the limit of $t \rightarrow \infty$ the right hand side here becomes just a Riemann integral so we have that

$$\lim_{t \rightarrow \infty} \rho(x, t) = \int_0^1 dx \rho(x, 0) = 1, \quad (3.4)$$

showing that the density strongly approaches to the equilibrium density.

Observables evolve by the Koopman operator, U_B^\dagger , as

$$U_B^\dagger \mathcal{O}(x) = \begin{cases} \mathcal{O}(2x) & 0 \leq x < \frac{1}{2} \\ \mathcal{O}(2x - 1) & \frac{1}{2} \leq x < 1. \end{cases} \quad (3.5)$$

Note that U_B^\dagger is an isometric operator (in $L^p(0, 1)$). (See Appendix A.3 for proofs.) Thus, in these normed spaces it only admits eigenstates with eigenvalues of modulus 1.

3.2 Exponential Correlation Decay

The Bernoulli map belongs to the class of strongly chaotic systems displaying exponential decay of correlations to their equilibrium values. In this system it is easy to directly calculate, for instance, the auto-correlation of the observable corresponding to the trajectory. We have

$$\begin{aligned} \hat{C}(t) &= \lim_{T \rightarrow \infty} \frac{1}{T} \sum_{\tau=0}^{T-1} x_{t+\tau} x_\tau \\ &= \int_0^1 dx_0 x_t x_0 \rho^{\text{eq}}(x_0) \\ &= \langle (U_B^\dagger)^t x | x \rho^{\text{eq}} \rangle = \langle x | U_B^t x \rangle, \end{aligned} \quad (3.6)$$

where the ergodicity of the system was used to replace the time average by a phase space average with $\rho^{\text{eq}} = 1$. We may calculate $\hat{C}(t)$ by deriving a simple recursion relation as

$$\begin{aligned} \hat{C}(t) &= \langle (U_B^\dagger)^{t-1} x | U_B x \rangle \\ &= \langle (U_B^\dagger)^{t-1} x | \frac{1}{2} [\frac{x}{2} + (\frac{1+x}{2})] \rangle \\ &= \frac{1}{2} \langle (U_B^\dagger)^{t-1} x | x \rangle + \frac{1}{4} \langle (U_B^\dagger)^{t-1} x | 1 \rangle \\ &= \frac{1}{2} \hat{C}(t-1) + \frac{1}{8}, \end{aligned} \quad (3.7)$$

where we used $\langle (U_B^\dagger)^{t-1} x | 1 \rangle = \langle x | U_B^{t-1} 1 \rangle = \int_0^1 dx x = 1/2$. Iterating this relation gives

$$\hat{C}(t) = \frac{\hat{C}(0)}{2^t} + \frac{1}{8} \sum_{k=0}^{t-1} \frac{1}{2^k} = \frac{1}{3} \frac{1}{2^t} + \frac{1}{4} \left(1 - \frac{1}{2^t} \right) = \frac{1}{12} e^{-(\log 2)t} + \frac{1}{4}, \quad (3.8)$$

where we used that $\hat{C}(0) = \int_0^1 dx x^2 = 1/3$, and wrote the time dependence so as to stress the exponential decay with the decay rate of $\log 2$. The constant $1/4$ is the equilibrium value of the auto-correlation as $\langle x \rangle^{\text{eq}} \langle x \rangle^{\text{eq}} = (1/2)(1/2) = 1/4$, so we take $C(t) \equiv \hat{C}(t) - 1/4$.

The spectral function, as defined by (2.12), corresponding to this correlation function is

$$P(\omega) = \frac{1}{6} \frac{2 - \cos \omega}{5 - 4 \cos \omega}. \quad (3.9)$$

This function, for ω real, is shown in Figure 3.2. The exponential decay of $C(t)$ corresponds to a simple pole of $P(\omega)$ off the real axis. The pole(s) at $\omega = \tilde{\omega}$ can be found from the zeros of the denominator above as $5 - 4 \cos \tilde{\omega} = 0$. This gives $\tilde{\omega} = \pm i \log 2$. The pole at $-i \log 2$ corresponds to exponential decay of $C(t)$ for $t > 0$. The other pole at $i \log 2$ is due to the symmetric extension of $C(t)$ for $t < 0$ by the transform. Since the map is non-invertible this pole is spurious.

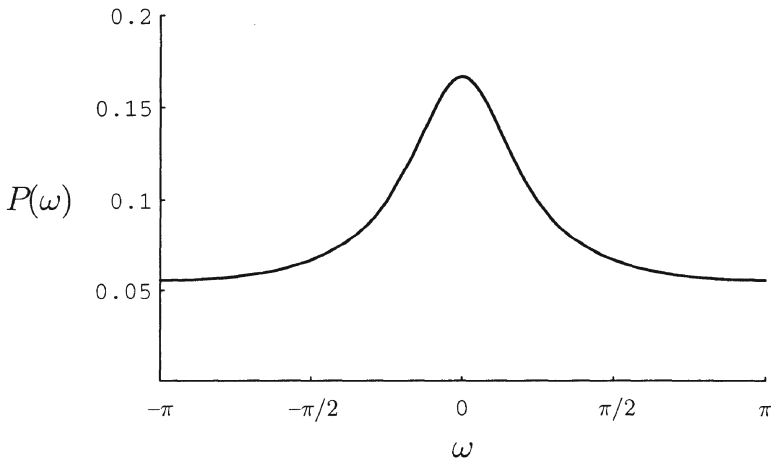


Figure 3.2: The spectral function, (3.9), of the x auto-correlation in the Bernoulli map.

As discussed in Chapter 2, from the point of view of the spectral function we may decompose the time evolution of $C(t)$ in terms of an integration on the real axis of ω or else we may deform the contour to pick up the pole contribution at the complex value of $\tilde{\omega}$. In practice it is useful to change the spectral variable to $z = e^{-i\omega}$ so that the integration is either on the unit circle or deformed to pick up the pole inside the unit circle (here at $z = 1/2$). Only

the x auto-correlation has been considered here but a general correlation function in this system will normally have a spectral function with a richer analytic structure.

These alternative ways of decomposing the time evolution of the correlation function correspond to alternative spectral decompositions of the time evolution operator. We will first consider a spectral decomposition corresponding to the continuous spectrum and point out its shortcomings. We then will construct the spectral decomposition that corresponds to discrete decay modes and show that it provides a description of the time evolution that enables us to better understand time-oriented behavior.

3.3 The Continuous Spectrum

Consider U_B acting in the Hilbert space, $L^2[0, 1]$, of square-integrable functions on the unit interval. From the way U_B acts we may expect that a function which has some symmetry with respect to $x = 1/2$ will behave in a special way. This motivates us to consider the Fourier basis states $\exp[2\pi ikx]$, where k is an integer. Any nonzero integer k can be written uniquely as $k = 2^n(2l + 1)$, where $n \geq 0$ and $-\infty < l < \infty$ are integers. Let us then write the Fourier basis states as

$$e_{n,l}(x) \equiv \exp[2\pi i 2^n(2l + 1)x], \quad (3.10)$$

where we also need the constant state 1, corresponding to $k = 0$, to complete the basis.

The Frobenius-Perron operator acts on these states as

$$\begin{aligned} U_B e_{n,l}(x) &= \frac{1}{2} \left\{ \exp \left[2\pi i 2^n(2l + 1) \left(\frac{x}{2} \right) \right] + \exp \left[2\pi i 2^n(2l + 1) \left(\frac{x+1}{2} \right) \right] \right\} \\ &= \frac{1}{2} \{ e_{n-1,l}(x) + e_{n-1,l}(x) \exp [\pi i 2^n(2l + 1)] \}, \end{aligned} \quad (3.11)$$

but

$$\exp [\pi i 2^n(2l + 1)] = \begin{cases} -1 & n = 0 \\ 1 & n > 0. \end{cases}$$

Thus,

$$U_B e_{n,l}(x) = \begin{cases} 0 & n = 0 \\ e_{n-1,l}(x) & n > 0, \end{cases} \quad (3.12)$$

showing that $e_{n,l}(x)$ are “shift states” for U_B . This shift action expresses the smoothing action of U_B as it acts successively on a function as illustrated in

Figure 1.2. Each application of the operator lowers, by a factor of $1/2$, the frequencies of each of the components of the Fourier expansion of a density.

The shift action of U_B on $e_{n,l}(x)$ is reminiscent of the action of the quantum mechanical annihilation operator on energy eigenstates of the harmonic oscillator. Like the coherent eigenstates in the quantum mechanical problem, we may easily construct “coherent” eigenstates of U_B from the shift states as

$$\phi_{z,l}(x) = \sum_{n=0}^{\infty} z^n e_{n,l}(x). \quad (3.13)$$

To see that this is an eigenstate we operate with U_B on $\phi_{z,l}(x)$

$$\begin{aligned} U_B \phi_{z,l}(x) &= \sum_{n=0}^{\infty} z^n U_B e_{n,l}(x) \\ &= \sum_{n=1}^{\infty} z^n e_{n-1,l}(x) \\ &= z \sum_{n=0}^{\infty} z^n e_{n,l}(x) = z \phi_{z,l}(x), \end{aligned} \quad (3.14)$$

showing that $\phi_{z,l}(x)$ is an eigenstate of U_B with eigenvalue z . Since $|e_{n,l}(x)| \leq 1$ the series defining $\phi_{z,l}(x)$ converges for all $|z| < 1$. Hence the spectrum¹ of U_B (in this function space) is the unit disk in the complex z -plane. Thus no specific time scales are selected in this spectrum.

The eigenstates $\phi_{z,l}(x)$ are for nearly all values of z somewhat “irregular” functions. In fact, for $1/2^{m+1} < |z| < 1/2^m$ the state $\phi_{z,l}(x)$ is everywhere m -times differentiable with respect to x and nowhere $m+1$ -times differentiable. In particular, for $1/2 < |z| < 1$ it is a continuous but non-differentiable function.

Since coherent states may be constructed with any decay rate, we may from them construct a density with any decay rate. This density will generally inherit the irregular nature of the coherent states. Physically though, a non-differentiable density implies that point information is accessible. If this is so then we are essentially considering a trajectory description and gain no fundamentally new information from the density.

¹In this book we use the physicist’s definition of the spectrum of an operator to be the set (discrete or continuous) of eigenvalues of the operator under consideration acting in a specified function space. The spectrum of a given operator may (and in fact will for the examples we consider) be different when the operator is considered in different function spaces.

We want a spectral decomposition of the Frobenius–Perron operator so we can write its action on a density as a sum (or integral) over the eigenstates. The coefficients of the expansion are determined from the dual states, which are eigenstates of the Koopman operator U_B^\dagger . (See Appendix A.4 for a discussion of dual states.) But we cannot construct eigenstates of U_B^\dagger with eigenvalues inside the unit disk in $L^2[0, 1]$ because it is an isometric operator in that space. The action of U_B^\dagger on a function gives two copies of the function as illustrated in Figure 3.3. Successive action as $(U_B^\dagger)^n$ gives 2^n copies. On the shift states $e_{n,l}(x)$ we have that

$$U_B^\dagger e_{n,l}(x) = e_{n+1,l}(x) \quad (3.15)$$

and no eigenstate like that constructed for U_B can be constructed here from the shift states. From (3.12) and (3.15) it is clear that for functions expandable in terms of the shift states that $U_B U_B^\dagger = 1$ but $U_B^\dagger U_B \neq 1$.

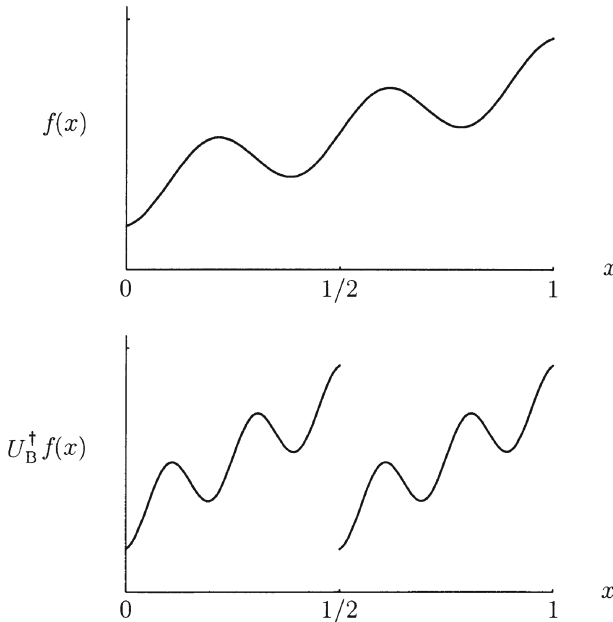


Figure 3.3: The action of U_B^\dagger on a function yields two rescaled copies of the function.

It is known that correlation functions (for a class of observables) in this system decay as a sum of exponential contributions where the coefficients

depend on the observable but the decay rates are intrinsic to the system. Our goal is to construct a spectral decomposition that is composed of these discrete decay modes. For this very simple system with uniform stretching factor we may expect the Lyapunov time, being the inverse of the Lyapunov exponent, to be a characteristic time scale for the decay. This was seen in the previous section where the x auto-correlation function was decaying at the rate of $\log 2$, which is the Lyapunov exponent in this system.

3.4 The Generalized Spectral Decomposition

We now turn to the construction of the spectral decomposition of U_B composed of discrete decay modes. The construction may be performed by several methods. Because of its generality we will employ a resolvent formalism. This formalism is widely used in modern nonequilibrium statistical mechanics as well as in quantum mechanics in the guise of the Green's function.

We begin by writing the time evolution of a density in terms of the resolvent, $1/(z - U_B)$, of U_B as

$$\rho(x, t) = \frac{1}{2\pi i} \oint_{|z|=1} dz \frac{z^t}{z - U_B} \rho(x, 0), \quad (3.16)$$

where the contour is taken outside the unit circle inside of which all singularities of the resolvent are located. (See Appendix A.5 for a discussion of the resolvent formalism and a derivation of this expression.) Our first task is to determine the analytic structure of the resolvent, i.e., its singularities. If they are simple poles we can get eigenstates from them (as will be shown below) by calculating residues.

We have already seen that using a trigonometric basis U_B has a continuous spectrum inside the unit circle. We want to get directly time evolution modes with exponential decay like we saw for the x auto-correlation function. Because U_B acts essentially as a scale transformation and preserves the degree of a polynomial it acts on, it is natural to consider a polynomial basis. Knowing that the invariant density is just the constant 1, it is convenient to use a basis of polynomials which are orthogonal with 1 as the weight function. On the interval $[-1, 1]$ the Legendre polynomials are a suitable basis but to use them on $[0, 1]$ they must be rescaled.

The rescaled Legendre polynomials $\hat{P}_n(x)$ are given in terms of the standard Legendre polynomials $P_n(x)$ as

$$\hat{P}_n(x) = \sqrt{2n+1} P_n(2x - 1). \quad (3.17)$$

They are discussed in Appendix A.6. Their orthonormality and completeness are expressed as

$$\begin{aligned}\langle \hat{P}_m | \hat{P}_n \rangle &\equiv \langle m | n \rangle \\ &= \int_0^1 dx \hat{P}_m^*(x) \hat{P}_n(x) = \delta_{m,n},\end{aligned}\quad (3.18a)$$

and

$$\sum_{n=0}^{\infty} |n\rangle \langle n| = \mathbf{1}, \quad (3.18b)$$

where $\mathbf{1}$ is the unit operator in the space where they are complete and a shorthand notation for the Legendre basis states has been introduced. We are also using a Dirac-style bra-ket notation for the states and their inner product and in the following will freely switch to such a notation when it is convenient. (For states that are real we will generally not explicitly indicate that the complex conjugate of the left state in the inner product needs to be taken.)

The matrix elements of U_B in this basis are

$$\begin{aligned}\langle m | U_B | n \rangle &= \int_0^1 dx \hat{P}_m(x) U_B \hat{P}_n(x) \\ &= \int_0^1 dx \hat{P}_m(x) \left\{ \frac{1}{2} \left[\hat{P}_n\left(\frac{x}{2}\right) + \hat{P}_n\left(\frac{x+1}{2}\right) \right] \right\} \\ &= \frac{1}{2} I_{m,n} + \frac{1}{2} (-1)^{m+n} I_{m,n},\end{aligned}\quad (3.19)$$

where

$$\begin{aligned}I_{m,n} &= \int_0^1 dx \hat{P}_m(x) \hat{P}_n\left(\frac{x}{2}\right) \\ &= \begin{cases} d_{mn} & m < n \\ 1/2^m & m = n \\ 0 & m > n. \end{cases}\end{aligned}\quad (3.20)$$

The explicit value of d_{mn} is not needed for us to carry on; it is given in Appendix A.6. Since the matrix elements vanish for $m > n$, U_B is upper-triangular in this basis. A triangular matrix already has its eigenvalues along the diagonal so we will write the diagonal values as $e^{-\gamma_m} \equiv 1/2^m$, because we want to emphasize that the associated eigenstates are exponentially decaying in time. The decay rates are $\gamma_m = m \log 2$.

To proceed, U_B is decomposed into its diagonal, U_0 , and off-diagonal part, δU , as

$$U_B = U_0 + \delta U, \quad (3.21)$$

where

$$U_0 \equiv \sum_m |m\rangle\langle m|U_B|m\rangle\langle m| = \sum_m \frac{1}{2^m} |m\rangle\langle m|, \quad (3.22a)$$

and

$$\delta U \equiv \sum_{m < n} |m\rangle\langle m|U_B|n\rangle\langle n|, \quad (3.22b)$$

where $m < n$ due to the upper-triangularity of U_B . Thus δU acting on a state $|n\rangle$ (a polynomial of degree n) will yield a linear combination of states less than $|n\rangle$ (a polynomial of degree $< n$). We refer to this as the non-recurrence property of δU since once δU acts on a state that state does not occur again through any further actions of δU or U_B .

Using this decomposition we may express the resolvent of U_B as

$$\begin{aligned} \frac{1}{z - U_B} &= \frac{1}{z - U_B} \left[(z - U_0) \frac{1}{z - U_0} \right] \\ &= \frac{1}{z - U_B} \left[(z - U_B + \delta U) \frac{1}{z - U_0} \right] = \left[1 + \frac{1}{z - U_B} \delta U \right] \frac{1}{z - U_0}. \end{aligned} \quad (3.23)$$

By iterating this expression we obtain the well-known expansion formula

$$\frac{1}{z - U_B} = \sum_{k=0}^{\infty} \left(\frac{1}{z - U_0} \delta U \right)^k \frac{1}{z - U_0}. \quad (3.24)$$

This type of expansion is commonly employed in perturbation calculations when δU includes a small parameter so that the expansion may be truncated at some level to get approximate results.

Now, we write the resolvent in terms of the Legendre polynomial basis by inserting complete sets of states on both sides of it as

$$\frac{1}{z - U_B} = \sum_{m,n} |m\rangle\langle m| \frac{1}{z - U_B} |n\rangle\langle n|. \quad (3.25)$$

We then use the expansion (3.24) of the resolvent in the matrix elements as

$$\langle m | \frac{1}{z - U_B} | n \rangle = \sum_{k=0}^{\infty} \langle m | \left(\frac{1}{z - U_0} \delta U \right)^k \frac{1}{z - U_0} | n \rangle. \quad (3.26)$$

Due to the non-recurrence property of δU the sum over k above will terminate when $k > n - m$. Hence, we don't need to artificially truncate the series since it truncates itself and will allow us to get exact results.

To determine the analytic structure of the matrix elements of the resolvent a complete set of states is inserted before each δU in a representative term of (3.26) as

$$\begin{aligned} \langle m | \left(\frac{1}{z - U_0} \delta U \right)^k \frac{1}{z - U_0} | n \rangle \\ = \sum_{j_1, j_2, \dots, j_{k-1}, j_k} \langle m | \frac{1}{z - U_0} \delta U | j_1 \rangle \langle j_1 | \frac{1}{z - U_0} \delta U | j_2 \rangle \langle j_2 | \\ \dots \delta U | j_{k-1} \rangle \langle j_{k-1} | \frac{1}{z - U_0} \delta U | j_k \rangle \langle j_k | \frac{1}{z - U_0} | n \rangle \\ = \sum_{j_1 < j_2 < \dots < j_{k-1}} \frac{1}{z - e^{-\gamma_m}} \langle m | \delta U | j_1 \rangle \frac{1}{z - e^{-\gamma_{j_1}}} \langle j_1 | \delta U | j_2 \rangle \langle j_2 | \\ \dots \delta U | j_{k-1} \rangle \frac{1}{z - e^{-\gamma_{j_{k-1}}}} \langle j_{k-1} | \delta U | n \rangle \frac{1}{z - e^{-\gamma_n}}, \end{aligned} \quad (3.27)$$

where the fact that $j_1 < j_2 < \dots < j_{k-1}$ is due to the non-recurrence property of δU . This means that the poles in (3.27) are simple poles. The matrix elements of the full resolvent (3.26) are given by a sum of terms like (3.27) and so have only simple poles located at the eigenvalues $z = e^{-\gamma_j}$ for $m \leq j \leq n$ and no other singularities. Because of the simple analytic structure of the resolvent the contour in (3.16) may be deformed into the unit circle and the integration may be written as a sum of terms obtained from successively encircling each of the isolated poles. This is illustrated in Figure 3.4. Each term will be a projection operator (see Appendix A.5) that may be separated into right and left eigenstates of U_B as will be seen below.

After shrinking the contour and encircling each of the poles we may write the time evolution of $\rho(x, t)$ as a sum of contributions from each pole as

$$\rho(x, t) = \sum_{j=0}^{\infty} \frac{1}{2\pi i} \oint_{z=e^{-\gamma_j}} dz \frac{z^t}{z - U_B} \rho(x, 0) = \sum_{j=0}^{\infty} e^{-\gamma_j t} \Pi^{(j)} \rho(x, 0), \quad (3.28)$$

where the time dependence comes from z^t being evaluated at the pole and

$$\Pi^{(j)} \equiv \frac{1}{2\pi i} \oint_{z=e^{-\gamma_j}} dz \frac{1}{z - U_B} \quad (3.29)$$

is the projection operator² satisfying $U_B \Pi^{(j)} = \Pi^{(j)} U_B = e^{-\gamma_j} \Pi^{(j)}$. Since $\Pi^{(j)}$ just projects onto a one-dimensional subspace we may formally write it

²Readers familiar with the Brussels–Austin subdynamics formalism will recognize $\Pi^{(j)}$

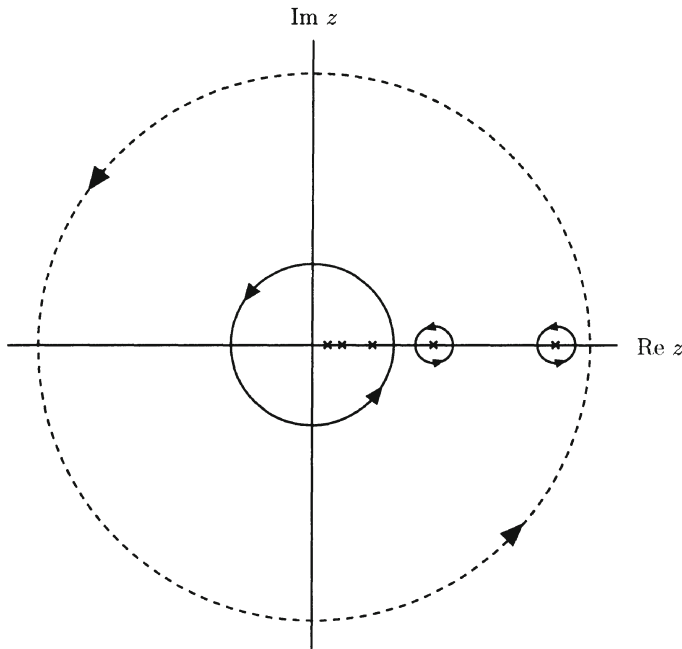


Figure 3.4: The original contour of (3.16) just outside the unit circle is shown as the dashed circle. After partial shrinking the contour is shown encircling individually the first two poles with the rest of the contour encircling the remaining poles (of which only three are shown).

in terms of the right and left eigenstates of U_B associated with the eigenvalue $e^{-\gamma_j}$ as $\Pi^{(j)} = |\gamma_j\rangle\langle\tilde{\gamma}_j|$. To get expressions for the eigenstates themselves we just need to act on something with $\Pi^{(j)}$ that doesn't vanish after the projection. The simplest choice is to act on the unperturbed state $|j\rangle$. Thus, $\Pi^{(j)}|j\rangle = |\gamma_j\rangle\langle\tilde{\gamma}_j|j\rangle$ and $\langle j|\Pi^{(j)} = \langle j|\gamma_j\rangle\langle\tilde{\gamma}_j|$. We will see shortly that $\langle j|\gamma_j\rangle = \langle\tilde{\gamma}_j|j\rangle = 1$, so the right and left eigenstates of U_B corresponding to the eigenvalue $e^{-\gamma_j}$ are given by

$$|\gamma_j\rangle = \frac{1}{2\pi i} \oint_{z=e^{-\gamma_j}} dz \frac{1}{z - U_B} |j\rangle, \quad (3.30a)$$

as the fundamental operator of that theory. In this approach $\Pi^{(j)}$ is decomposed into operators that create, destroy and time evolve correlation components. References that use this approach for chaotic maps are cited in this and following chapters.

and

$$\langle \tilde{\gamma}_j | = \frac{1}{2\pi i} \oint_{z=e^{-\gamma_j}} dz \langle j | \frac{1}{z - U_B}, \quad (3.30b)$$

respectively.

In order to evaluate these integrals we again use the operator expansion, (3.24), of the resolvent. For the right eigenstate we have

$$\begin{aligned} |\gamma_j\rangle &= \frac{1}{2\pi i} \oint_{z=e^{-\gamma_j}} dz \sum_{k=0}^{\infty} \left(\frac{1}{z - U_0} \delta U \right)^k \frac{1}{z - U_0} |j\rangle \\ &= \frac{1}{2\pi i} \oint_{z=e^{-\gamma_j}} dz \sum_{k=0}^{\infty} \left(\frac{1}{z - U_0} \delta U \right)^k |j\rangle \frac{1}{z - e^{-\gamma_j}}. \end{aligned} \quad (3.31)$$

Because of the non-recurrence property of δU the simple pole at $z = e^{-\gamma_j}$ that has been made explicit doesn't occur again in the sum over k . The integral is then trivial to evaluate using Cauchy's theorem. But from (3.24) we may rewrite the sum over k as

$$\begin{aligned} \sum_{k=0}^{\infty} \left(\frac{1}{z - U_0} \delta U \right)^k &= \frac{1}{z - U_B} (z - U_0) = \frac{1}{z - U_B} (z - U_B + \delta U) \\ &= 1 + \frac{1}{z - U_B} \delta U. \end{aligned} \quad (3.32)$$

So the right eigenstate is formally given by

$$|\gamma_j\rangle = \left(1 + \frac{1}{e^{-\gamma_j} - U_B} \delta U \right) |j\rangle. \quad (3.33)$$

A similar calculation gives for the left eigenstate

$$\langle \tilde{\gamma}_j | = \langle j | \left(1 + \delta U \frac{1}{e^{-\gamma_j} - U_B} \right). \quad (3.34)$$

From these expressions our assertion that $\langle j | \gamma_j \rangle = \langle \tilde{\gamma}_j | j \rangle = 1$ is seen to be true. These states are also bi-orthonormal in that $\langle \tilde{\gamma}_j | \gamma_k \rangle = \delta_{jk}$. See Appendix A.7 for a direct verification of these formal expressions for the eigenstates and a proof of their bi-orthonormality.

The only fact we used to get (3.33) and (3.34) was that the resolvent of U_B had discrete simple poles. Thus these expressions are valid whenever the resolvent of the operator under consideration has such an analytic structure. They will be used again later for other maps.

3.5 The Physical Eigenstates

The eigenstates, $|\gamma_j\rangle$ and $\langle\tilde{\gamma}_j|$, we have obtained correspond to the eigenvalue $e^{-\gamma_j} = 1/2^j$. The decay rate, $\gamma_j = j \log 2$, is a multiple of the Lyapunov exponent in this system. These are the physical decay rates observed experimentally (on the computer), at least for polynomial observables, so we call the eigenstates physical. The right and left eigenstates are quite different so we discuss each of them separately.

3.5.1 Right Polynomial Eigenstates

In order to evaluate the eigenstates explicitly we write recursion relations for them. For the right eigenstates, starting from (3.33), we have

$$\begin{aligned} |\gamma_j\rangle &= |j\rangle + \frac{1}{e^{-\gamma_j} - U_B} \delta U |j\rangle \\ &= |j\rangle + \sum_{i=0}^{j-1} |i\rangle \langle i| \frac{1}{e^{-\gamma_j} - U_B} \delta U |j\rangle. \end{aligned} \quad (3.35)$$

But

$$\begin{aligned} \langle i| \frac{1}{e^{-\gamma_j} - U_B} \delta U |j\rangle &= \langle i| \frac{1}{e^{-\gamma_j} - U_0} (e^{-\gamma_j} - U_0) \frac{1}{e^{-\gamma_j} - U_B} \delta U |j\rangle \\ &= \frac{1}{e^{-\gamma_j} - e^{-\gamma_i}} \langle i| (e^{-\gamma_j} - U_B + \delta U) \frac{1}{e^{-\gamma_j} - U_B} \delta U |j\rangle \\ &= \frac{1}{e^{-\gamma_j} - e^{-\gamma_i}} \langle i| \delta U (1 + \frac{1}{e^{-\gamma_j} - U_B} \delta U) |j\rangle \\ &= \frac{1}{e^{-\gamma_j} - e^{-\gamma_i}} \langle i| \delta U |\gamma_j\rangle. \end{aligned} \quad (3.36)$$

Thus, $|\gamma_j\rangle$ satisfies the self-consistent equation (discrete analog of an integral equation)

$$|\gamma_j\rangle = |j\rangle + \sum_{i=0}^{j-1} \frac{1}{e^{-\gamma_j} - e^{-\gamma_i}} |i\rangle \langle i| \delta U |\gamma_j\rangle. \quad (3.37)$$

To carry out an explicit evaluation it is convenient to put a complete set of states between δU and $|\gamma_j\rangle$ for which only states between $i+1$ and j will contribute because of the upper triangularity of δU . We then have

$$|\gamma_j\rangle = |j\rangle + \sum_{i=0}^{j-1} \left[\frac{1}{e^{-\gamma_j} - e^{-\gamma_i}} \sum_{k=i+1}^j \langle i| \delta U |k\rangle \langle k| \gamma_j \rangle \right] |i\rangle. \quad (3.38)$$

There is no problem with $|\gamma_j\rangle$ appearing on the right hand side of this expression. Using that $\langle j|\gamma_j\rangle = 1$, the other components of $|\gamma_j\rangle$ needed for its explicit evaluation are available if one does the successive evaluations of the states starting with $|\gamma_0\rangle$ (see Appendix A.8). If the expansion (3.38) is written out and the components $\langle k|\gamma_j\rangle$ are put in we find that the i th component of $|\gamma_j\rangle$ contains all possible series of transitions from $\langle i|$ to $|j\rangle$. We see then that $|\gamma_j\rangle$ is just a linear combination of the basis states up to $|j\rangle$ and thus a polynomial in x of degree j .

Explicit evaluation of the right eigenstates will yield polynomials that are multiples of the so-called Bernoulli polynomials. Since an eigenstate may be multiplied by any non-zero constant and remain an eigenstate, we take the standard Bernoulli polynomials as the right eigenstates of U_B . In Appendix A.9 the Bernoulli polynomials are discussed. The explicit forms of the first six eigenpolynomials of U_B are

$$\begin{aligned} B_0(x) &= 1 \\ B_1(x) &= x - \frac{1}{2} \\ B_2(x) &= x^2 - x + \frac{1}{6} \\ B_3(x) &= x^3 - \frac{3}{2}x^2 + \frac{1}{2}x \\ B_4(x) &= x^4 - 2x^3 + x^2 - \frac{1}{30} \\ B_5(x) &= x^5 - \frac{5}{2}x^4 + \frac{5}{3}x^3 - \frac{1}{6}x \end{aligned} \quad (3.39)$$

The first few eigenpolynomials are illustrated in Figure 3.5. Since all of the eigenpolynomials except $B_0(x)$ decay in time we have that $\int_0^1 dx B_n(x) = \delta_{0,n}$, as must be the case for conservation of probability in this system. Furthermore, the eigenpolynomials are seen to be symmetric with respect to the midpoint of the unit interval as

$$B_n(1-x) = (-1)^n B_n(x). \quad (3.40)$$

This symmetry of the eigenstates will be exploited in the next chapter.

3.5.2 Left Generalized Eigenstates

A calculation of the self-consistent equation for $\langle\tilde{\gamma}_j|$ analogous to (3.37) gives

$$\langle\tilde{\gamma}_j| = \langle j| + \sum_{i=j+1}^{\infty} \frac{1}{e^{-\gamma_j} - e^{-\gamma_i}} \langle\tilde{\gamma}_j|\delta U|i\rangle\langle i|. \quad (3.41)$$

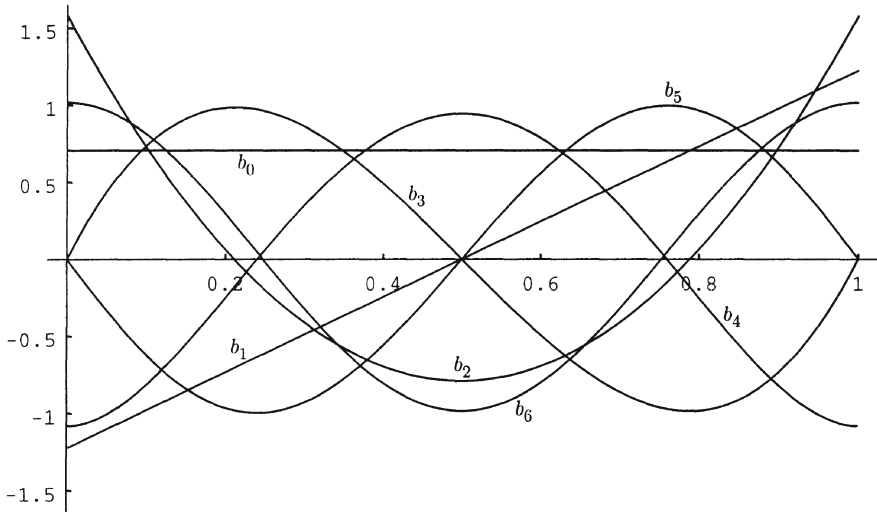


Figure 3.5: The first seven Bernoulli polynomials. They have been renormalized so that their L^2 norm equals $1/\sqrt{2}$. This normalization leads to $b_{2n}(x) \rightarrow \pm \cos(2\pi x)$ and $b_{2n+1}(x) \rightarrow \pm \sin(2\pi x)$ as $n \rightarrow \infty$. Note that unlike the Legendre polynomials the number of axis crossings (zeros) of the Bernoulli polynomials does not increase as the degree of the polynomial increases.

The recursion relation for $\langle \tilde{\gamma}_j |$ yields an infinite series, and thus a polynomial of infinite order (power series) in x , beginning at x^j . Furthermore, the series of coefficients of the expansion is diverging, essentially as i^{2j} for large i . Anyway, we know that $\langle \tilde{\gamma}_j |$ cannot be an element of an ordinary functional space like L^p because it is an eigenstate of U_B^\dagger with eigenvalue less than 1. Realizing that a divergent series can sometimes have a meaning under integration with another function motivates us to see if that is the case here.

We thus consider $\langle \tilde{\gamma}_j |$ with an arbitrary function, f , expanded in terms of the original basis as

$$\langle \tilde{\gamma}_j | f \rangle = \sum_{k=0}^{\infty} \langle \tilde{\gamma}_j | k \rangle \langle k | f \rangle, \quad (3.42)$$

where terms with $k < j$ vanish since $\langle \tilde{\gamma}_j |$ starts at $\langle j |$, as can be seen from (3.41). We won't use (3.41) but rather obtain $\langle \tilde{\gamma}_j | k \rangle$ by formally expanding the matrix element of U_B^T with respect to the Legendre polynomial basis in

terms of the left and right eigenstates of U_B as

$$\begin{aligned}
 \langle j|U_B^\tau|k\rangle &= \sum_{p=0}^{\infty} \langle j|U_B^\tau|\gamma_p\rangle \langle \tilde{\gamma}_p|k\rangle \\
 &= \sum_{p=j}^k \langle j|\gamma_p\rangle e^{-\gamma_p\tau} \langle \tilde{\gamma}_p|k\rangle \\
 &= \langle j|\gamma_j\rangle e^{-\gamma_j\tau} \langle \tilde{\gamma}_j|k\rangle \\
 &\quad + \sum_{p=j+1}^k \langle j|\gamma_p\rangle e^{-\gamma_p\tau} \langle \tilde{\gamma}_p|k\rangle.
 \end{aligned} \tag{3.43}$$

Using, $\langle j|\gamma_j\rangle = 1$, multiplying both sides by $e^{\gamma_j\tau}$ and rearranging gives

$$\begin{aligned}
 \langle \tilde{\gamma}_j|k\rangle &= e^{\gamma_j\tau} \langle j|U_B^\tau|k\rangle \\
 &\quad - \sum_{p=j+1}^k e^{(\gamma_j-\gamma_p)\tau} \langle j|\gamma_p\rangle \langle \tilde{\gamma}_p|k\rangle.
 \end{aligned} \tag{3.44}$$

Since the left hand side of this equation doesn't depend on τ it equals the right hand side for any value of τ . Now, $\gamma_j - \gamma_p = (j-p) \log 2 < 0$, since $p \geq j+1$, so in the limit $\tau \rightarrow \infty$ the second term will vanish giving

$$\begin{aligned}
 \langle \tilde{\gamma}_j|k\rangle &= \lim_{\tau \rightarrow \infty} 2^{j\tau} \langle j|U_B^\tau|k\rangle \\
 &= \lim_{\tau \rightarrow \infty} 2^{j\tau} \langle (U_B^\dagger)^\tau j|k\rangle.
 \end{aligned} \tag{3.45}$$

We have written $\langle \tilde{\gamma}_j|k\rangle$ in terms of U_B^\dagger here because it gives us a more intuitive grasp in the following as to how the eigenstate of U_B^\dagger arises.

The action of $\langle \tilde{\gamma}_j|$ on a function is then, using (3.45) in (3.42), given by

$$\begin{aligned}
 \langle \tilde{\gamma}_j|f\rangle &= \sum_k \lim_{\tau \rightarrow \infty} 2^{j\tau} \langle (U_B^\dagger)^\tau j|k\rangle \langle k|f\rangle \\
 &= \lim_{\tau \rightarrow \infty} 2^{j\tau} \langle (U_B^\dagger)^\tau j|f\rangle \\
 &= \lim_{\tau \rightarrow \infty} \int_0^1 dx 2^{j\tau} \hat{P}_j(2^\tau x \bmod 1) f(x),
 \end{aligned} \tag{3.46}$$

where we assumed that we could interchange the limit of $\tau \rightarrow \infty$ and the sum over the complete set of states. In the integration, starting from $x = 0$, for each advance of x by $1/2^\tau$ the argument, $2^\tau x \bmod 1$, of \hat{P}_j goes from zero to one. This is illustrated in Figure 3.6 where $2^{j\tau} \hat{P}_j(2^\tau x \bmod 1)$ is plotted

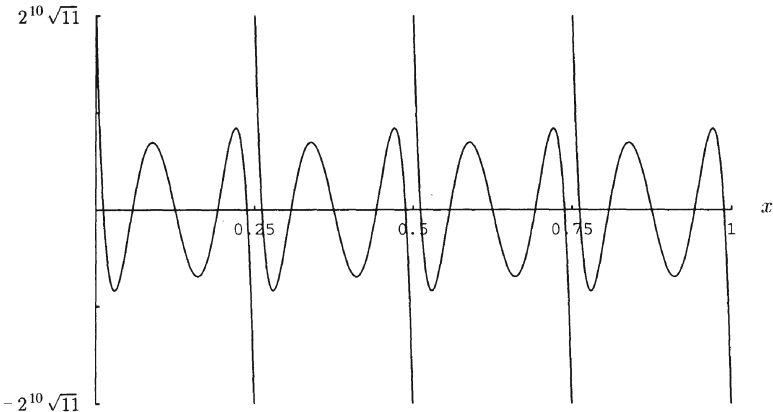


Figure 3.6: The term $2^{j\tau} \hat{P}_j(2^\tau x \bmod 1)$ when $j = 5$ and $\tau = 2$ appearing in the expression (3.46) for the left eigenstate of U_B .

for $j = 5$ and $\tau = 2$. This motivates us to divide the unit interval into 2^τ intervals as

$$\int_0^1 dx 2^{j\tau} \hat{P}_j(2^\tau x \bmod 1) f(x) = \sum_{k=0}^{2^\tau-1} \int_{\frac{k}{2^\tau}}^{\frac{k+1}{2^\tau}} dx 2^{j\tau} \hat{P}_j(2^\tau x - k) f(x). \quad (3.47)$$

Assuming $f(x)$ is j -times differentiable at $x = k/2^\tau$, we may expand f in a Taylor series (with remainder) as:

$$f(x) = \sum_{q=0}^j \frac{f^{(q)}(k/2^\tau)}{q!} \left(x - \frac{k}{2^\tau}\right)^q + \frac{f^{(j+1)}(c)}{(j+1)!} \left(x - \frac{k}{2^\tau}\right)^{j+1}, \quad (3.48)$$

where $f^{(q)}$ denotes the q -th derivative of f and we have written the remainder in the Lagrange form where $0 < c < k/2^\tau$. Using (3.47) and the Taylor expansion in (3.46) gives

$$\begin{aligned} \langle \tilde{\gamma}_j | f \rangle &= \lim_{\tau \rightarrow \infty} \sum_{k=0}^{2^\tau-1} \left\{ \sum_{q=0}^j \frac{2^{(j-q)\tau}}{2^\tau} \frac{f^{(q)}(k/2^\tau)}{q!} \int_0^1 dy \hat{P}_j(y) y^q \right. \\ &\quad \left. + \frac{1}{2^{2\tau}} \frac{f^{(j+1)}(c)}{(j+1)!} \int_0^1 dy \hat{P}_j(y) y^{j+1} \right\}, \end{aligned} \quad (3.49)$$

where we have made the substitution of $y = 2^\tau x - k$. For $q < j$ the integration over y vanishes because the Legendre polynomial of order l is orthogonal to

all monomials of degree $< l$ (see Appendix A.6). In the limit of $\tau \rightarrow \infty$ the term coming from the remainder of the Taylor series vanishes because of the $1/2^{2\tau}$ factor. Thus, only the $q = j$ term survives and the sum turns into an integral as

$$\langle \tilde{\gamma}_j | f \rangle = a_j \lim_{\tau \rightarrow \infty} \sum_{k=0}^{2^\tau - 1} \frac{1}{2^\tau} f^{(j)}\left(\frac{k}{2^\tau}\right) = a_j \int_0^1 dx f^{(j)}(x), \quad (3.50)$$

where

$$a_j = \frac{1}{j!} \int_0^1 dx \hat{P}_j(x) x^j. \quad (3.51)$$

The expression (3.50) tells us how $\langle \tilde{\gamma}_j |$ acts on a function but we want an expression for $\langle \tilde{\gamma}_j |$ itself. The derivative of a function inside an integral can be reinterpreted (using integration by parts) as the derivative of the Dirac delta function times the function we are considering. Thus we have

$$\langle \tilde{\gamma}_j | f \rangle = a_j \int_0^1 dx (-1)^{j-1} \left[\delta_-^{(j-1)}(x-1) - \delta_+^{(j-1)}(x) \right] f(x). \quad (3.52)$$

for $j \geq 1$ where the action of δ_\pm is given by

$$\int_a^b dx \delta_\pm^{(m)}(x-c) f(x) = \lim_{\epsilon \rightarrow 0} (-1)^m f^{(m)}(c \pm \epsilon), \quad (3.53)$$

for $a \leq c \leq b$ and ϵ is a positive infinitesimal. In our case $f(x)$ is defined only on $[0, 1]$ so for $c = 0$ we need the right-sided limit and for $c = 1$ the left-sided limit. So the left eigenstates (corresponding to decay modes) of U_B are generalized functions. This is why we refer to the spectral decomposition with these states as the generalized spectral decomposition. As a generalized function has meaning only when integrated with a function belonging to the test space, the left eigenstate is an eigenfunctional. We will sometimes refer though to the kernel of the eigenfunctional as the eigenstate.

The standard Bernoulli polynomials were chosen as the right eigenstates, so in order to form an orthonormal set with them we need to multiply the left eigenstate that we have obtained by $(j! a_j)^{-1}$. We thus have

$$\tilde{B}_j(x) = \frac{(-1)^{j-1}}{j!} \left[\delta_-^{(j-1)}(x-1) - \delta_+^{(j-1)}(x) \right], \quad (3.54a)$$

for $j \geq 1$ and

$$\tilde{B}_0(x) = 1. \quad (3.54b)$$

The left eigenstate $\langle \tilde{B}_j |$ acts on a function expandable in terms of the Bernoulli polynomials then as

$$\langle \tilde{B}_j | f \rangle = \frac{1}{j!} \left[f^{(j-1)}(1) - f^{(j-1)}(0) \right], \quad (3.55a)$$

for $j \geq 1$ and when $j = 0$

$$\langle \tilde{B}_0 | f \rangle = \int_0^1 dx f(x). \quad (3.55b)$$

The left eigenstate may also be written as

$$\tilde{B}_j(x) = \frac{1}{j!} \frac{d^j}{dx^j}. \quad (3.56)$$

This form is often useful in explicit calculations. For example, we may use it to verify that $\tilde{B}_j(x)$ is the left eigenstate of U_B (right eigenstate of U_B^\dagger) as

$$\begin{aligned} \langle U_B^\dagger \tilde{B}_j | f \rangle &= \langle \tilde{B}_j | U_B f \rangle \\ &= \int_0^1 dx \frac{1}{j!} \frac{d^j}{dx^j} \frac{1}{2} \left[f\left(\frac{x}{2}\right) + f\left(\frac{x+1}{2}\right) \right] \\ &= \frac{1}{2} \left[2 \int_0^{1/2} dx' \frac{1}{2^j} \frac{1}{j!} \frac{d^j}{dx'^j} f(x') + 2 \int_{1/2}^1 dx'' \frac{1}{2^j} \frac{1}{j!} \frac{d^j}{dx''^j} f(x'') \right] \\ &= \frac{1}{2^j} \int_0^1 dx \frac{1}{j!} \frac{d^j}{dx^j} f(x) = \frac{1}{2^j} \langle \tilde{B}_j | f \rangle. \end{aligned} \quad (3.57)$$

In summary, we have constructed the complete spectral decomposition of U_B in the space of functions spanned by the Bernoulli polynomials and so may write the time evolution of a density evolving under the Bernoulli map as

$$\rho(x, t) = U_B^t \rho(x, 0) = \sum_{j=0}^{\infty} e^{-\gamma_j t} B_j(x) \langle \tilde{B}_j | \rho \rangle. \quad (3.58)$$

We note that the general r -adic map defined by $S_r(x) = rx \bmod 1$, where r is an integer greater than or equal to 2, has the Frobenius–Perron operator U_r given by

$$U_r \rho(x) = \frac{1}{r} \sum_{m=0}^{r-1} \rho\left(\frac{x+m}{r}\right). \quad (3.59)$$

The dyadic Bernoulli map we have been considering corresponds to $r = 2$. For any r the operator U_r has the same right and left eigenstates we have

obtained for the $r = 2$ case. The eigenvalues for the r -adic map are r^{-n} . For the Bernoulli polynomials this means that

$$\frac{1}{r} \sum_{m=0}^{r-1} B_n \left(\frac{x+m}{r} \right) = r^{-n} B_n(x). \quad (3.60)$$

In the special function literature on Bernoulli polynomials this relation is known as the multiplication theorem.

3.6 Validity of the Spectral Decomposition

Since the right eigenstates of U_B we have determined are a complete set of polynomials, it is obvious that any polynomial observable or density may be expanded in terms of them. For example, the time dependence of the x auto-correlation, (3.8), is determined using the generalized spectral decomposition as

$$\hat{C}(t) = \int_0^1 dx x U_B^t x = \int_0^1 dx x \left[\langle \tilde{B}_0 | x \rangle B_0(x) + \frac{1}{2^t} \langle \tilde{B}_1 | x \rangle B_1(x) \right], \quad (3.61)$$

where $\langle \tilde{B}_n | x \rangle = 0$ for $n > 1$. Since $\langle \tilde{B}_0 | x \rangle = 1/2$ and $\langle \tilde{B}_1 | x \rangle = 1$ we obtain

$$\hat{C}(t) = \int_0^1 dx x \left[\frac{1}{2} + \frac{1}{2^t} \left(x - \frac{1}{2} \right) \right] = \frac{1}{4} + \frac{1}{12} \frac{1}{2^t}, \quad (3.62)$$

which is the result (3.8) obtained previously from the recursion relation obeyed by $\hat{C}(t)$.

The left eigenstates give us more direct information about the types of functions for which the generalized spectral representation is valid. The most important condition on the functions is that they must be infinitely differentiable; this excludes trajectories, which correspond to non-differentiable point densities and is consistent with the qualitatively different behavior of trajectories and smooth densities. As was illustrated in Figures 1.1 and 1.2, trajectories wander but smooth densities approach an equilibrium state. It is important to note that the approach to equilibrium that we have for smooth densities with the generalized spectral decomposition does not depend on some width of the distribution or any subjective feature one would have to introduce for a coarse-grained description. The decay rates are determined, as will be seen below, from the differentiability of ρ and are multiples of the Lyapunov exponent for this simple system with uniform stretching.

A more precise specification of the class of functions for which the generalized decomposition is valid requires topological considerations beyond the

scope of our presentation. Interested readers may refer to the papers cited in the bibliographic notes at the end of the chapter. One characterization of the function space is immediate from some theorems on the expansion of analytic functions in polynomials. This is discussed in Appendix A.10 where an alternative approach to obtaining the spectral decomposition by first determining the class of eigenpolynomials and their generating function is given. For our purposes it is sufficient to think of the decomposition being valid for the space \mathcal{P} of polynomials. The eigendistributions are then members of the dual space \mathcal{P}^\dagger of linear functionals on \mathcal{P} .

It is natural to ask what are the types of densities for which one may determine just the first few decay modes. This question is answered when we consider the connection between the expansion of U_B associated with the continuous spectrum, as discussed in Section 3.3, and the generalized spectral decomposition with an infinite number of discrete decay modes.

Consider an arbitrary density belonging to $L^2[0, 1]$ expanded in terms of the shift states $e_{n,l}(x)$, given by (3.10), and the constant state 1 (i.e., a Fourier decomposition) as

$$\begin{aligned} U_B^t \rho(x) &= \langle 1 | \rho \rangle + \sum_{n=0}^{\infty} \sum_{l=-\infty}^{\infty} e_{n,l}(x) \langle e_{n,l} | U_B^t \rho \rangle \\ &= \langle 1 | \rho \rangle + \sum_{n,l} e_{n,l}(x) \langle e_{n+t,l} | \rho \rangle, \end{aligned} \quad (3.63)$$

where for the second line we used that $(U_B^\dagger)^t e_{n,l}(x) = e_{n+t,l}(x)$. The expansion coefficients are given by

$$\begin{aligned} \langle e_{n+t,l} | \rho \rangle &= \int_0^1 dx e^{-2\pi i 2^{n+t}(2l+1)x} \rho(x) \\ &= \frac{-1}{2\pi i 2^{n+t}(2l+1)} \left\{ e^{-2\pi i 2^{n+t}(2l+1)x} \rho(x) \Big|_0^1 - \int_0^1 dx e^{-2\pi i 2^{n+t}(2l+1)x} \frac{d\rho(x)}{dx} \right\} \\ &= \frac{1}{2^t} \frac{-1}{2\pi i 2^n(2l+1)} \left\{ \rho(1) - \rho(0) - \langle e_{n+t,l} | \rho^{(1)} \rangle \right\}, \end{aligned} \quad (3.64)$$

where an integration by parts has been performed assuming that the density is differentiable i.e., that $d\rho/dx \in L^2$. The boundary term here may be written in terms of the first-order left eigenstate of the generalized decomposition as

$$\rho(1) - \rho(0) = \int_0^1 dx \frac{d\rho}{dx} = \langle \tilde{B}_1 | \rho \rangle. \quad (3.65)$$

This term can go outside the summation in (3.63) and then we have that

$$\sum_{n=0}^{\infty} \sum_{l=-\infty}^{\infty} \frac{-e_{n,l}(x)}{2\pi i 2^n (2l+1)} = \sum_{k \neq 0} \frac{-e^{2\pi i k x}}{2\pi i k} = B_1(x). \quad (3.66)$$

(The Fourier representation of the Bernoulli polynomials is discussed in Appendix A.9) The summation of the term from (3.64) involving the derivative of ρ is

$$\begin{aligned} & \sum_{n=0}^{\infty} \sum_{l=-\infty}^{\infty} \frac{-e_{n,l}(x)}{2\pi i 2^n (2l+1)} \int_0^1 dx' e_{n+t,l}^*(x') \frac{d\rho(x')}{dx'} \\ &= \sum_{k \neq 0} \int_0^1 dx' \frac{e^{2\pi i k (x - 2^t x')}}{2\pi i k} \frac{d\rho(x')}{dx'} \\ &= \int_0^1 dx' B_1(x - 2^t x') \frac{d\rho(x')}{dx'}, \end{aligned} \quad (3.67)$$

where, as noted before, the argument of the Bernoulli polynomial is taken modulo 1. Thus, for $d\rho/dx' \in L^2$ we obtain

$$\begin{aligned} U_B^t \rho(x) &= \langle 1 | \rho \rangle + \frac{1}{2^t} B_1(x) \langle \tilde{B}_1 | \rho \rangle + \frac{1}{2^t} \int_0^1 dx' B_1(x - 2^t x') \frac{d\rho(x')}{dx'} \\ &= \sum_{m=0}^1 e^{-\gamma_m t} B_m(x) \langle \tilde{B}_m | \rho \rangle + e^{-\gamma_1 t} R_1(x, t), \end{aligned} \quad (3.68)$$

where $\|R_1(x, t)\| \leq \|d\rho/dx\|$. Hence, by restricting the domain of U_B to functions which are one-time differentiable, we have made explicit one uniquely determined discrete decay mode and separated out a remainder term which includes all quicker decay contributions.

By restricting the domain of U_B to M -times differentiable functions (i.e., $d^M \rho / dx^M \in L^2$) we may repeatedly integrate by parts to obtain

$$U_B^t \rho(x) = \sum_{m=0}^M e^{-\gamma_m t} B_m(x) \langle \tilde{B}_m | \rho \rangle + e^{-\gamma_M t} R_M(x, t), \quad (3.69)$$

where

$$R_M(x, t) = \frac{1}{2^M} \int_0^1 dx' B_M(x - 2^t x') \frac{d^M \rho(x')}{dx'^M}. \quad (3.70)$$

Hence, by imposing the condition of differentiability we extract discrete decay modes corresponding to the states of the generalized spectral decomposition. This result is consistent with the fact, already mentioned in Section 3.3,

that for $1/2^{m+1} < |z| < 1/2^m$ the eigenstates $\phi_{z,l}(x)$ are m -times differentiable but not $m + 1$ -times differentiable. Taking $M \rightarrow \infty$ we have the complete generalized decomposition, (3.58), for C^∞ functions.

For $t = 0$ (3.69) corresponds to the so-called Euler–Maclaurin expansion (with remainder). It is quite similar to a Taylor series expansion but involves the values of the derivatives of the function at two points. The Euler–Maclaurin expansion is used often in numerical calculations for the evaluation of integrals (it is essentially the trapezoidal rule) and yields an efficient method for evaluating slowly convergent series by means of an integral. We will use the expansion later to get closed form expressions for the left eigenstates of some systems.

Bibliographical Notes

The simple proof of exactness of the Bernoulli map given in Section 3.1 is from the book of Lasota and Mackey cited in Chapter 1. The first published papers on the explicit generalized spectral decomposition of the Bernoulli map are:

- H. Hasegawa and W. Saphir, “Decaying eigenstates for simple chaotic systems,” *Physics Letters A* **162**, 471 (1992).
- P. Gaspard, “r-adic one-dimensional maps and the Euler summation formula,” *Journal of Physics A* **25**, L483 (1992).
- I. Antoniou and S. Tasaki, “Spectral decomposition of the Renyi map,” *Journal of Physics A* **26**, 73 (1993).

Haswgawa and Saphir use the resolvent technique in conjunction with a subdynamics formalism. Gaspard’s concise discussion characterizes the class of functions valid for the decomposition. Antoniou and Tasaki give a thorough presentation, including the connection of the coherent states and the eigenpolynomials, with full mathematical details. A more complete presentation of the subdynamics approach of Hasegawa and Saphir, including the spectral decomposition of the baker map to be discussed in Chapter 5, is

- H. Hasegawa and W. Saphir, “Unitarity and Irreversibility in Chaotic Systems,” *Physical Review A*, **46**, 7401 (1992).

A semi-popular presentation of some of the original work of the Brussels–Austin groups on generalized spectral decompositions of chaotic maps and its relevance to irreversibility appeared in French as

- I. Prigogine, *Les Lois du Chaos* (Flammarion, Paris, 1994).

The resolvent technique is well presented in

- T. Kato, *Perturbation theory for linear operators* (Springer-Verlag, Berlin, 1966).

A good general reference for the properties of polynomial sets, including Legendre, Bernoulli and the Euler polynomials used in the next chapter is

- E. Rainville, *Special Functions* (Chelsea Publishing Company, New York, 1960).

The discussion of the validity of the spectral decomposition in Section 3.6 is adapted from

- H.H. Hasegawa and D.J. Driebe, “Intrinsic irreversibility and the validity of the kinetic description of chaotic systems,” *Physical Review E*, **50**, 1781 (1994).

This paper constructs the spectral decompositions of a variety of maps and considers the physical conditions for their validity.

Chapter 4

Other One-Dimensional Maps

In this chapter the generalized spectral decomposition of a variety one-dimensional maps is presented. An algebraic technique is introduced and applied to determine the spectral decomposition of the tent map. Some maps with non-diagonalizable decompositions are presented, including a map whose resolvent has an essential singularity. A map that does not preserve Lebesgue measure and where the dynamics settles onto a strange attractor is analyzed. Finally, the decompositions of maps related by a simple change of variables are discussed and the decomposition of the logistic map with unit height is determined from the decomposition of the tent map.

4.1 An Algebraic Technique Utilizing Symmetry

The resolvent technique, as employed in Chapter 3 for the Bernoulli map, enables the construction of the generalized spectral decomposition for a variety of maps. But the construction is a somewhat lengthy procedure and it is not always easy to know whether the eigenpolynomials for a given map are related to one of the standard polynomial sets. It is worthwhile to be able to obtain more directly the decomposition, especially for systems that are simply related to a case that has been worked out, such as the Bernoulli or r -adic map.

As is familiar from quantum mechanics, the symmetries of an operator are often useful in obtaining its eigenstates. We noted in Section 3.5.1 that the eigenstates of the Bernoulli map, the Bernoulli polynomials, are symmetric with respect to the midpoint of the unit interval. This could have

been anticipated by noticing that U_B commutes with the reflection operator, R , defined by

$$Rf(x) \equiv Rf(1-x), \quad (4.1)$$

i.e., $U_B R = RU_B$. Since the eigenstates of U_B are non-degenerate this tells us that they are eigenstates of R as well.¹

It is useful in this context to introduce the projection operators, P_+ and P_- defined by

$$P_{\pm} \equiv \frac{1 \pm R}{2}, \quad (4.2)$$

which project onto the even and odd parts of a function. If the Frobenius–Perron operator U commutes with R (such as U_B) it also commutes with P_{\pm} and since $P_+ P_- = P_- P_+ = 0$ the dynamics governed by U evolves independently in the two subspaces defined by the P_{\pm} projections.

We now apply symmetry considerations to get the spectral decomposition of some maps simply related to the Bernoulli map.

4.1.1 The Tent Map

The tent map on the unit interval is defined by

$$S_T(x) = \begin{cases} 2x & 0 \leq x < \frac{1}{2} \\ 2 - 2x & \frac{1}{2} \leq x < 1. \end{cases} \quad (4.3)$$

This map (sometimes called the hat map) is frequently cited, like the Bernoulli map, as the canonical example of the simplest chaotic system. The map is shown in Figure 4.1. It also has a global Lyapunov exponent of $\log 2$. Unlike the exponential decay of the Bernoulli map, the x auto-correlation function for the tent map is delta correlated. This will be seen below after obtaining the spectral decomposition.

The Frobenius–Perron operator, U_T , acts on a density as

$$U_T \rho(x) = \frac{1}{2} \left[\rho\left(\frac{x}{2}\right) + \rho\left(1 - \frac{x}{2}\right) \right]. \quad (4.4)$$

Since this map is so similar to the dyadic Bernoulli map we seek a solution which uses our knowledge of the Bernoulli map solution. From (4.4)

¹To see this use first the commutation of U_B and R and then that $B_n(x)$ is an eigenstate of U_B as $U_B[RB_n(x)] = RU_BB_n(x) = 2^{-n}[RB_n(x)]$. Because of the nondegeneracy, $B_n(x)$ is the only eigenstate of U_B with eigenvalue 2^{-n} so that $RB_n(x) \propto B_n(x)$; hence, $B_n(x)$ is an eigenstate of R as well.

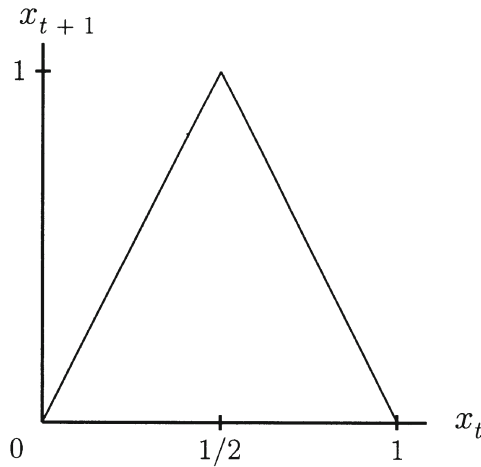


Figure 4.1: The tent map.

polynomial eigenstates, $T_n(x)$, of U_T satisfy

$$\frac{1}{2} \left[T_n\left(\frac{x}{2}\right) + T_n\left(1 - \frac{x}{2}\right) \right] = c_n T_n(x), \quad (4.5)$$

where c_n are the associated eigenvalues. First of all we see that any polynomial of odd parity with respect to the midpoint of the unit interval satisfies this equation with $c_n = 0$. Thus zero is an eigenvalue of infinite multiplicity with linearly independent eigenstates for each occurrence of the eigenvalue. Any complete set of odd-parity polynomials may be chosen as the associated eigenstates. A set will be chosen below after determining the even-order eigenstates. The fact that the subspace defined by the P_- projection is spanned by eigenstates corresponding to the zero eigenvalue may also be seen by noticing that $U_T P_- = 0$.

The eigenstate equation for the Bernoulli map, satisfied by the Bernoulli polynomials, is

$$\frac{1}{2} \left[B_m\left(\frac{x}{2}\right) + B_m\left(\frac{1+x}{2}\right) \right] = 2^{-m} B_m(x). \quad (4.6)$$

Letting $x \rightarrow x/2$ this equation becomes

$$\frac{1}{2} \left[B_m\left(\frac{x/2}{2}\right) + B_m\left(\frac{1+x/2}{2}\right) \right] = 2^{-m} B_m(x/2). \quad (4.7)$$

The even-degree Bernoulli polynomials have even parity so for m even

$$B_m\left(\frac{1+x/2}{2}\right) = B_m\left(1 - \frac{1+x/2}{2}\right) = B_m\left(\frac{1-x/2}{2}\right). \quad (4.8)$$

Taking $m = 2n$ and using this in (4.7) gives

$$\frac{1}{2} \left[B_{2n}\left(\frac{x/2}{2}\right) + B_{2n}\left(\frac{1-x/2}{2}\right) \right] = 2^{-2n} B_{2n}(x/2). \quad (4.9)$$

This equation is precisely the form of the eigenstate equation (4.5) for the tent map with $T_{2n}(x) = B_{2n}(x/2)$ and $c_{2n} = 2^{-2n}$.

The above derivation used both the symmetry properties of the Bernoulli polynomials (arising from the symmetry of the Bernoulli map) and the relation of the tent map to the Bernoulli map. The relation of between U_T and U_B can be made explicit by reconsidering the above derivation in terms of operators. We denote the operation of $x \rightarrow x/2$ by D as

$$Df(x) \equiv f\left(\frac{x}{2}\right). \quad (4.10)$$

In P_+ space then we see that

$$U_T D P_+ = D U_B P_+. \quad (4.11)$$

Now we notice that in fact $D P_+ = U_T$ and since U_B commutes with P_+ we see that (4.11) may be written as

$$U_T U_T = U_T U_B. \quad (4.12)$$

From this intertwining relation the result for the even-order eigenpolynomials of U_T is obtained by operating both sides of the relation on an even-order Bernoulli polynomial, $B_{2n}(x)$, and using that it is an eigenstate of U_B with eigenvalue 2^{-2n} . This gives

$$U_T [U_T B_{2n}(x)] = 2^{-2n} [U_T B_{2n}(x)]. \quad (4.13)$$

Thus, $U_T B_{2n}(x) = B_{2n}(x/2)$ is an eigenpolynomial of U_T with eigenvalue 2^{-2n} .

The even-order left eigenstates of U_T may also be obtained from the intertwining relation (4.12). Taking the adjoint of the relation gives

$$U_B^\dagger U_T^\dagger = U_T^\dagger U_B^\dagger. \quad (4.14)$$

Multiplying both sides of this equation by the unknown eigenstate, $\tilde{T}_{2n}(x)$, with eigenvalue 2^{-2n} gives

$$U_B^\dagger \tilde{T}_{2n}(x) = 2^{-2n} \tilde{T}_{2n}(x). \quad (4.15)$$

Thus, $\tilde{T}_{2n}(x)$ is an eigenstate of U_B^\dagger with eigenvalue 2^{-2n} and so it is equivalent (up to a constant) with $\tilde{B}_{2n}(x)$. The constant may be fixed by requiring that the left and right eigenstates of U_T form an orthonormal basis. This gives $\tilde{T}_{2n}(x) = 2^{2n} \tilde{B}_{2n}(x)$.

As noted, we are completely free to choose the odd-order eigenpolynomials spanning P_- to be any complete set in that subspace. Of course, it makes sense to choose them so that the functional space spanned by the set should be the same type of space as is spanned by the even-order eigenpolynomials. So we don't want to choose a family like the Legendre polynomials. One obvious choice is to take the odd-order Bernoulli polynomials. But for this choice the associated odd-order left eigenstates have a rather cumbersome form. (Because of the degeneracy of the zero eigenvalue the dual states would not be $\tilde{B}_{2n-1}(x)$.)

A good choice for the odd-order eigenpolynomials, which yields simple associated left eigenstates, are the so-called Euler polynomials. These polynomials, $E_n(x)$, may be defined by their generating function

$$\frac{2e^{xp}}{e^p + 1} = \sum_{n=0}^{\infty} \frac{E_n(x)}{n!} p^n. \quad (4.16)$$

The dual states, $\tilde{E}_n(x)$, of the full set of Euler polynomials may be determined by integration over the unit interval with the generating function as

$$\int_0^1 dx \tilde{E}_m(x) \frac{2e^{xp}}{e^p + 1} = \sum_{n=0}^{\infty} \frac{p^n}{n!} \int_0^1 dx \tilde{E}_m(x) E_n(x) \quad (4.17)$$

$$= \frac{p^m}{m!}, \quad (4.18)$$

where we imposed that $\int_0^1 dx \tilde{E}_m(x) E_n(x) = \delta_{mn}$. Thus, it is easily verified that the dual states are

$$\tilde{E}_n(x) = \frac{(-1)^n}{2(n!)} \left[\delta_-^{(n)}(x-1) + \delta_+^{(n)}(x) \right]. \quad (4.19)$$

These states, for n odd, are of course duals for our choice of the Euler polynomials as the odd-order eigenpolynomials, but they are not orthogonal

to the even-order eigenpolynomials, $B_{2n}(x/2)$. To determine the correct odd-order left eigenstates we may employ the completeness of the full set of eigenstates.

Formally, in the space spanned by the full set of eigenstates, we have the completeness relation

$$\sum_{m=0}^{\infty} |T_{2m}\rangle \langle \tilde{T}_{2m}| + \sum_{m=1}^{\infty} |T_{2m-1}\rangle \langle \tilde{T}_{2m-1}| = 1. \quad (4.20)$$

Since $\langle \tilde{E}_{2n-1}|T_{2m-1}\rangle = \langle \tilde{E}_{2n-1}|E_{2m-1}\rangle = \delta_{n,m}$, we can extract an expression for $\langle \tilde{T}_{2n-1}|$ from the completeness relation by acting on (4.20) with $\langle \tilde{E}_{2n-1}|$ and then rearranging. This yields

$$\langle \tilde{T}_{2n-1}| = \langle \tilde{E}_{2n-1}| - \sum_{m=0}^{\infty} \langle \tilde{E}_{2n-1}|T_{2m}\rangle \langle \tilde{T}_{2m}|, \quad (4.21)$$

where $n \geq 1$. Now,

$$\begin{aligned} \langle \tilde{E}_{2n-1}|T_{2m}\rangle &= \int_0^1 dx \frac{(-1)^{2n-1}}{2(2n-1)!} \left[\delta_-^{(2n-1)}(x-1) + \delta_+^{(2n-1)}(x) \right] 2^{2m} B_{2m}\left(\frac{x}{2}\right) \\ &= \frac{(-1)^{2n-1}}{2(2n-1)!} \frac{(-1)^{2n-1}(2m)! 2^{2m}}{2^{2n-1}(2m-2n)!} \\ &\quad \times \left[B_{2m-2n+1}\left(\frac{1}{2}\right) - B_{2m-2n+1}(0) \right] \\ &= -n\delta_{n,m}, \end{aligned} \quad (4.22)$$

where we used that $B_{2m-2n+1}\left(\frac{1}{2}\right) = 0$ and $B_{2m-2n+1}(0) = -\frac{1}{2}\delta_{n,m}$. Inserting this in (4.21) then gives

$$\begin{aligned} \tilde{T}_{2n-1}(x) &= \frac{(-1)^{2n-1}}{2(2n-1)!} \left[\delta_-^{(2n-1)}(x-1) + \delta_+^{(2n-1)}(x) \right] \\ &\quad + \frac{n(-1)^{2n-1}}{2(2n)!} \left[\delta_-^{(2n-1)}(x-1) - \delta_+^{(2n-1)}(x) \right] \\ &= \frac{-1}{(2n-1)!} \delta_-^{(2n-1)}(x-1). \end{aligned} \quad (4.23)$$

The time evolution of a density under U_T , expandable in the generalized decomposition, is thus

$$U_T^t \rho(x) = \sum_{n=0}^{\infty} \left(\frac{1}{2^{2n}} \right)^t B_{2n}\left(\frac{x}{2}\right) 2^{2n} \langle \tilde{B}_{2n}|\rho\rangle + \sum_{n=1}^{\infty} \delta_{t,0} E_{2n-1}(x) \langle \tilde{T}_{2n-1}|\rho\rangle. \quad (4.24)$$

Since P_- is the null space of U_T , after just one application of U_T any component in P_- is annihilated. For example, the x auto-correlation function for the tent map evolves as

$$\langle x|U_T^t|x\rangle = \int_0^1 dx x \left[\langle \tilde{B}_0|x\rangle B_0\left(\frac{x}{2}\right) + \delta_{t,0} \langle \tilde{T}_1|x\rangle E_1(x) \right]. \quad (4.25)$$

But $\langle \tilde{B}_0|x\rangle = \int_0^1 dx x = 1/2$ and $\langle \tilde{T}_1|x\rangle = -\int_0^1 dx \delta(x-1)x = 1$ so that

$$\begin{aligned} \langle x|U_T^t|x\rangle &= \int_0^1 dx x \left[\frac{1}{2} + \delta_{t,0}(x-\frac{1}{2}) \right] \\ &= \frac{1}{4} + \frac{1}{12}\delta_{t,0}. \end{aligned} \quad (4.26)$$

In contrast, the x auto-correlation of the Bernoulli map, (3.62), decayed exponentially. Here the delta-correlation is due to the symmetry of the tent map and is not due to the tent map being in any sense more chaotic than the Bernoulli map. Of course, correlations of higher degree polynomials in x will generally contain components including the exponentially decaying even-order polynomial eigenstates.

4.1.2 The V Map and Reflected Bernoulli Map

The map shown in Figure 4.2 we call the “V” map. Its Frobenius–Perron operator is given by

$$U_V\rho(x) = \frac{1}{2} \left[\rho\left(\frac{1-x}{2}\right) + \rho\left(\frac{1+x}{2}\right) \right]. \quad (4.27)$$

Considering U_V and R acting successively gives

$$U_V R = U_V, \quad (4.28a)$$

and

$$R U_V = U_T. \quad (4.28b)$$

The above two relations just mean that U_V and U_T are related by a similarity transformation as

$$R^{-1} U_V R = U_T, \quad (4.29a)$$

or

$$R U_T R^{-1} = U_V, \quad (4.29b)$$

where we used that $R^{-1} = R$. Also, (4.28a) tells us that the null space of U_V is spanned by P_- , just like the tent map.

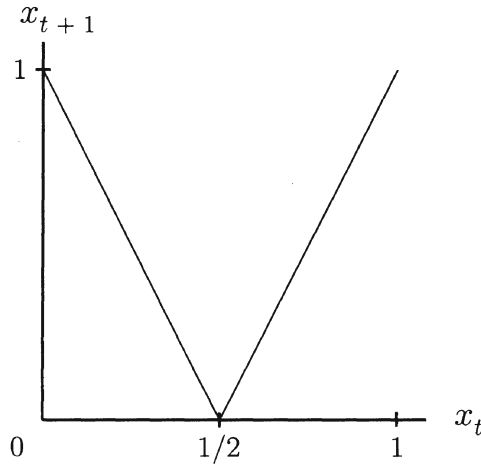


Figure 4.2: The V map.

Since U_V and U_T are related by a similarity transformation, their eigenvalues are the same. The eigenstates, $V_n(x)$, of U_V may be obtained by acting with both sides of (4.29a) on the eigenstates of U_T as

$$R^{-1}U_VRB_{2n}\left(\frac{x}{2}\right) = U_TB_{2n}\left(\frac{x}{2}\right),$$

or,

$$R^{-1}U_VB_{2n}\left(\frac{1-x}{2}\right) = 2^{-2n}B_{2n}\left(\frac{x}{2}\right). \quad (4.30)$$

Multiplying this expression by R gives

$$U_VB_{2n}\left(\frac{1-x}{2}\right) = 2^{-2n}RB_{2n}\left(\frac{x}{2}\right) = 2^{-2n}B_{2n}\left(\frac{1-x}{2}\right). \quad (4.31)$$

So the even-order eigenpolynomials, $V_{2n}(x)$, of U_V are

$$V_{2n}(x) = B_{2n}\left(\frac{1-x}{2}\right). \quad (4.32)$$

Since, $U_VU_B = U_VU_V$, we may take the adjoint of this relation as

$$U_B^\dagger U_V^\dagger = U_V^\dagger U_V^\dagger. \quad (4.33)$$

Then we see, following the same steps as for the tent map, that the even-order left eigenstates, $\tilde{V}_{2n}(x) = 2^{2n}\tilde{B}_{2n}(x)$.

As for the tent map, a very simple form for the odd-order left states is obtained if we choose the odd-order eigenpolynomials to be Euler polynomials, i.e., $V_{2n-1}(x) = E_{2n-1}(x)$. The odd-order left eigenstates may also be obtained from the completeness relation as was done for the tent map, or by using the adjoint of (4.28b) with (4.23). The result here is

$$\tilde{V}_{2n-1}(x) = \frac{-1}{(2n-1)!} \delta^{(2n-1)}(x). \quad (4.34)$$

The Frobenius–Perron operator of the reflected Bernoulli map, shown in Figure 4.3, may be obtained from successive operations of R and U_B in either order, i.e.,

$$RU_B = U_B R \equiv U_R, \quad (4.35)$$

and so U_B and U_R themselves commute.

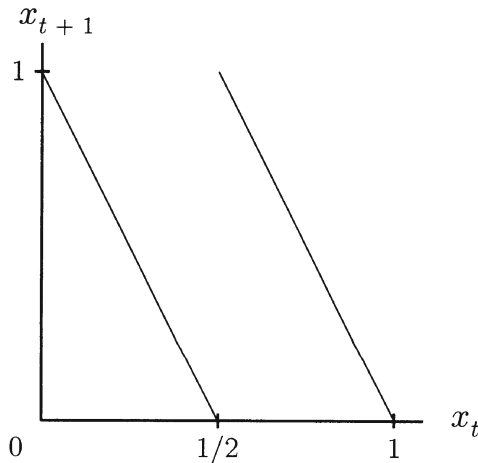


Figure 4.3: The reflected Bernoulli map.

The operator U_R acts on a density as

$$U_R \rho(x) = \frac{1}{2} [\rho(\frac{1-x}{2}) + \rho(1 - \frac{x}{2})]. \quad (4.36)$$

The eigenstates, $R_n(x)$, of U_R the same as those of U_B as

$$U_R B_n(x) = R U_B B_n(x) = 2^{-n} R B_n(x) = (-1)^n 2^{-n} B_n(x). \quad (4.37)$$

It is seen that the associated eigenvalue of the odd-order Bernoulli polynomials is negative. The left eigenstates are $\tilde{B}_n(x)$ since the right eigenpolynomials are $B_n(x)$.

4.2 Degeneracies and Jordan Decompositions

The tent and V maps studied in the previous section both had an infinite degeneracy of the zero eigenvalue. But there was a linearly independent eigenstate associated with each member of the degenerate set so the Frobenius–Perron operator was still fully diagonalizable. In the case that there are not linearly independent eigenstates for each occurrence of a degenerate eigenvalue the spectral decomposition will contain Jordan blocks. The resolvent formalism is well suited for determining if a degenerate eigenvalue is associated with a non-trivial Jordan block. If the eigenvalue, even if it is degenerate, is associated only with a simple pole of the resolvent, then there are as many independent eigenvectors as the multiplicity of the degeneracy. A multiple pole will be associated with a block of size of the order of the pole. Jordan blocks will appear in our analysis of the baker map in the next chapter, so it is good preparation to understand their appearance in the simpler one-dimensional map presented in this section.

We first present the spectral decomposition of two maps with the same spectrum containing non-zero degenerate eigenvalues. One of the maps is fully diagonalizable and the other has Jordan blocks. We also analyze a map with an infinitely degenerate zero eigenvalue associated with an infinite size Jordan block.

4.2.1 Degeneracies and Diagonalizability

Consider first the map defined by

$$S_N(x) = \begin{cases} 3x & 0 \leq x < \frac{1}{3} \\ 2 - 3x & \frac{1}{3} \leq x < \frac{2}{3} \\ 3x - 2 & \frac{2}{3} \leq x < 1. \end{cases} \quad (4.38)$$

This map, which we refer to as the “N” map, and the map we will consider later in this section are shown in Figure 4.4.

The Frobenius–Perron operator of this map, U_N , acts on a density as

$$U_N \rho(x) = \frac{1}{3} \left[\rho\left(\frac{x}{3}\right) + \rho\left(\frac{2-x}{3}\right) + \rho\left(\frac{2+x}{3}\right) \right]. \quad (4.39)$$

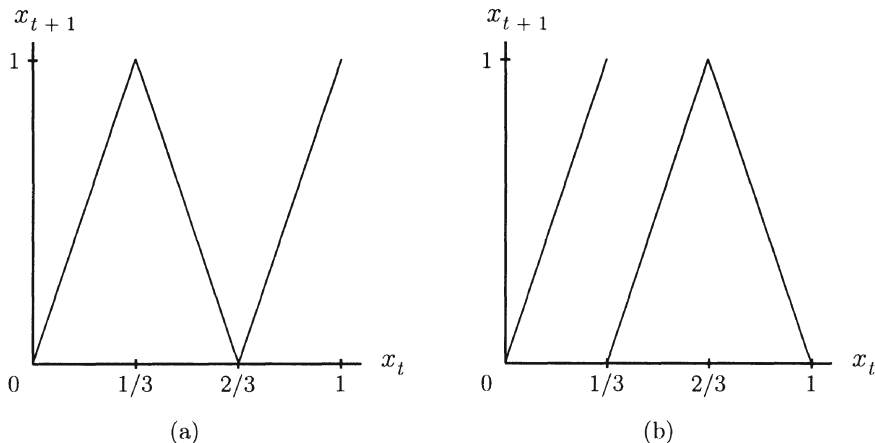


Figure 4.4: Two three-branch maps with the same spectrum are shown. The map (a) is fully diagonalizable. The map (b) has a 2×2 Jordan block associated with each two-fold degenerate eigenvalue.

The simplest way to get the eigenvalues of U_N (or any of the maps with polynomial eigenstates we have been considering) is to act on the monomial x^n . The coefficient of x^n after U_N acts is the eigenvalue associated with the n -th degree eigenpolynomial. Except for the first eigenvalue of 1, corresponding to the invariant uniform density, they are found to be two-fold degenerate. The eigenpolynomials of order $2n - 1$ and $2n$, where $n \geq 1$, both have the associated eigenvalues of 3^{-2n} .

The algebraic technique, along with symmetry considerations may be used here to determine the spectral decomposition of U_N . The operator U_N intertwines with the Frobenius–Perron operator of the 3-adic map, U_3 , (given by (3.59) with $r = 3$) and the tent map, U_T as

$$U_N U_T = U_T U_3. \quad (4.40)$$

Operating both sides of (4.40) on an even-order Bernoulli polynomial, $B_{2n}(x)$, and using that it is an eigenstate of U_3 with eigenvalue 3^{-2n} we then obtain

$$U_N U_T B_{2n}(x) = 3^{-2n} U_T B_{2n}(x). \quad (4.41)$$

Thus, $U_T B_{2n}(x) = B_{2n}(x/2)$ is an eigenpolynomial of U_N with eigenvalue 3^{-2n} . But this eigenpolynomial is not uniquely determined. Since the eigenpolynomial of order $2n - 1$ has the same eigenvalue we may add any multiple

of this lower-order polynomial to $B_{2n}(x/2)$ to obtain different eigenstates of order $2n$.

The intertwining relation (4.40) is not directly useful to obtain the odd-order eigenstates because the odd-order Bernoulli polynomials, which are eigenstates of U_3 , are in the null space of U_T . We may obtain the odd-order eigenstates using the symmetry of U_N , i.e., that U_N commutes with R . Realizing this tells us that $RB_{2n}(x/2)$ is also an eigenstate of U_N , with eigenvalue 3^{-2n} . Hence any linear combination of $B_{2n}(x/2)$ and $RB_{2n}(x/2)$ is an eigenstate as well. Using that the simultaneous eigenstates of two commuting operators form a complete set if the operators considered separately admit complete sets of eigenstates, we may form a complete set of right eigenstates of U_N by making them a complete set of eigenstates of R also. Such states may be constructed using the projections $P_{\pm} \equiv (1 \pm R)/2$ as

$$P_+ B_{2n}\left(\frac{x}{2}\right) = 2^{-2n} B_{2n}(x), \quad (4.42a)$$

and

$$P_- B_{2n}\left(\frac{x}{2}\right) = -n 2^{-2n} E_{2n-1}(x), \quad (4.42b)$$

where we used that $P_+ B_{2n}(x/2) = U_B B_{2n}(x)$ and $E_{2n-1}(x)$ is the Euler polynomial of order $2n-1$. (For the even-order states n starts at 0 and for the odd-order states at 1.) The Euler polynomials are defined by the generating function (4.16) given in Section 4.1.1. For (4.42b) we used the relation of the Euler and Bernoulli polynomials given by

$$E_{n-1}(x) = \frac{2^n}{n} \left\{ B_n\left(\frac{1+x}{2}\right) - B_n\left(\frac{x}{2}\right) \right\}. \quad (4.43)$$

For convenience we choose the coefficient of the highest power of x in the eigenpolynomials to be 1. The eigenpolynomials of U_N are thus taken as, $B_{2n}(x)$ and $E_{2n-1}(x)$.

The even-order states, $\tilde{B}_{2n}(x)$, are all orthogonal to the odd-order Euler polynomials and the odd-order states, $\tilde{E}_{2n-1}(x)$, are all orthogonal to the even-order Bernoulli polynomials. Thus, the complete set of orthonormal duals are given by $\tilde{B}_{2n}(x)$ and $\tilde{E}_{2n-1}(x)$. The spectral decomposition of U_N is then

$$U_N = |B_0\rangle\langle\tilde{B}_0| + \sum_{n=1}^{\infty} \frac{1}{3^{2n}} \left[|B_{2n}\rangle\langle\tilde{B}_{2n}| + |E_{2n-1}\rangle\langle\tilde{E}_{2n-1}| \right]. \quad (4.44)$$

4.2.2 Non-diagonalizability and Modified Exponential Decay

Now consider the map shown in Figure 4.4(b)

$$S_J(x) = \begin{cases} 3x & 0 \leq x < \frac{1}{3} \\ 3x - 1 & \frac{1}{3} \leq x < \frac{2}{3} \\ 3 - 3x & \frac{2}{3} \leq x < 1. \end{cases} \quad (4.45)$$

The Frobenius–Perron operator for this map is given by

$$U_J \rho(x) = \frac{1}{3} \left[\rho\left(\frac{x}{3}\right) + \rho\left(\frac{1+x}{3}\right) + \rho\left(\frac{3-x}{3}\right) \right], \quad (4.46)$$

The eigenvalues of U_J are the same as those of U_N , i.e., the simple eigenvalue 1 and the eigenvalues 3^{-2n} of double multiplicity. We were able to fully diagonalize U_N because there were independent eigenvectors associated with each occurrence of the degenerate eigenvalues. For U_J this is not the case; there are no even-order polynomial eigenstates, so that the spectral decomposition takes a Jordan block form.

In terms of the resolvent, Jordan blocks correspond to multiple poles. As we have seen in Chapter 3 simple poles of the resolvent yield pure exponential decay contributions to $\rho(t)$. Let us suppose that the resolvent has a double pole at $z = \lambda_l$ so we may write this contribution to the resolvent as $F(z)/(z - \lambda_l)^2$, where $F(z)$ is an operator valued function of z regular at $z = \lambda_l$. Evaluating the residue from this contribution yields

$$\begin{aligned} \rho_2^{(l)}(t) &= \frac{1}{2\pi i} \oint_{z=\lambda_l} dz z^t \frac{F(z)}{(z - \lambda_l)^2} \rho(0) \\ &= \frac{d}{dz} [z^t F(z)] \Big|_{z=\lambda_l} \rho(0) \\ &= [\lambda_l^t F'(\lambda_l) + t \lambda_l^{t-1} F(\lambda_l)] \rho(0). \end{aligned} \quad (4.47)$$

Thus, we see that the double pole leads to a mode with both pure exponential decay ($\lambda_l^t = e^{-(\log \lambda_l)t}$) and exponential decay modified by a coefficient linear in t . This mode is essentially the contribution of a Jordan vector,² as will be seen explicitly below.

We can expect that the decomposition of U_J in terms of eigenpolynomials will include left eigenstates that are generalized functions, as we have seen

²Various terminology is found in linear algebra texts for what we call a Jordan vector. Some other terms are principal vector, root vector and generalized eigenvector (not to be confused with generalized in the sense we use it in this book for a generalized function).

for the systems studied so far in this book. A suitable bi-orthonormal basis to begin the construction of the spectral decomposition is thus the basis of eigenstates of the Bernoulli map, i.e., the Bernoulli polynomials, $|B_n\rangle$, and their duals, $\langle\tilde{B}_n|$.

The matrix elements of U_J in the Bernoulli basis are

$$\langle\tilde{B}_n|U_J|B_m\rangle = \int_0^1 dx \tilde{B}_n(x) U_J B_m(x) = \frac{m!}{n!(m-n)!} \frac{1}{3^n} J_{n,m} \quad (4.48a)$$

where

$$J_{n,m} \equiv \int_0^{2/3} dx B_{m-n}(x) + (-1)^n \int_{2/3}^1 dx B_{m-n}(x) \quad (4.48b)$$

If $n = m$ then $J_{n,n} = 1$ for n even and $J_{n,n} = 1/3$ for n odd. Thus the diagonal elements of U_J in this basis are

$$\langle\tilde{B}_n|U_J|B_n\rangle = \begin{cases} \frac{1}{3^n} & n \text{ even} \\ \frac{1}{3^{n+1}} & n \text{ odd,} \end{cases} \quad (4.49)$$

The off-diagonal elements vanish for $n > m$ (so that U_J is upper-triangular) and for $n < m$ the integration of (4.48b) gives

$$J_{n,m} = \begin{cases} 0 & n \text{ even} \\ \frac{1}{m-n+1} [2B_{m-n+1}(\frac{2}{3}) - B_{m-n+1}(0) - B_{m-n+1}(1)] & n \text{ odd.} \end{cases} \quad (4.50)$$

The eigenvalues of U_J are given by the diagonal elements (4.49) and, as we noted, are the same as for the N map, i.e., except for the first simple eigenvalue of 1 there is a two-fold degeneracy of $\lambda_{2n} \equiv 3^{-2n}$.

To proceed we decompose U_J into its diagonal part, U_0 , and off-diagonal part, δU , as $U_J = U_0 + \delta U$, where

$$\begin{aligned} U_0 &\equiv \sum_n |B_n\rangle\langle\tilde{B}_n|U_J|B_n\rangle\langle\tilde{B}_n| \\ &= |B_0\rangle\langle\tilde{B}_0| + \sum_{n=1}^{\infty} \lambda_{2n} \left[|B_{2n-1}\rangle\langle\tilde{B}_{2n-1}| + |B_{2n}\rangle\langle\tilde{B}_{2n}| \right], \end{aligned} \quad (4.51)$$

and

$$\delta U \equiv \sum_{n < m} |B_n\rangle\langle\tilde{B}_n|U_J|B_m\rangle\langle\tilde{B}_m|, \quad (4.52)$$

where $n < m$ due to the upper-triangularity of U_J .

Matrix elements of the resolvent of U_J with a double pole can be found by employing an expansion like (3.26). If the transition between the two

basis states $|B_{2n}\rangle$ and $\langle \tilde{B}_{2n-1}|$ is nonvanishing then, for example, a double pole is found in

$$\begin{aligned} \langle \tilde{B}_{2n-1} | \frac{1}{z - U_J} | B_{2n} \rangle &= \langle \tilde{B}_{2n-1} | \frac{1}{z - U_0} \delta U \frac{1}{z - U_0} | B_{2n} \rangle \\ &= \frac{1}{(z - \lambda_{2n})^2} \langle \tilde{B}_{2n-1} | \delta U | B_{2n} \rangle \end{aligned} \quad (4.53)$$

The co-diagonal matrix elements of odd-numbered rows are

$$\begin{aligned} \langle \tilde{B}_{2n-1} | U_J | B_{2n} \rangle &= \frac{2n}{3^{2n-1}} \left[\int_0^{2/3} dx B_1(x) - \int_{2/3}^1 dx B_1(x) \right] \\ &= \frac{2n}{3^{2n-1}} \left(-\frac{2}{9} \right) = -\frac{4n}{3^{2n+1}}, \end{aligned} \quad (4.54)$$

which is nonvanishing so that the resolvent of U_J has double poles at 3^{-2n} . The corresponding matrix elements of U_N are vanishing so that its resolvent only has simple poles, despite the degeneracy of the eigenvalues. This is why we were able to obtain linearly independent eigenvectors for each of the degenerate eigenvalues of U_N .³

Returning to U_J , its resolvent also has simple poles associated with matrix elements with odd-order right basis states as

$$\langle \tilde{B}_l | \frac{1}{z - U_J} | B_{2n-1} \rangle = \sum_k \langle \tilde{B}_l | \left(\frac{1}{z - U_0} \delta U \right)^k | B_{2n-1} \rangle \frac{1}{z - \lambda_{2n}}, \quad (4.55)$$

where the singularity at λ_{2n} does not occur again in the sum over k due to the upper-triangularity of δU . Associated with the simple poles are odd-order eigenpolynomials, $\lambda_{2n-1}(x)$, as

$$|\lambda_{2n-1}\rangle = \frac{1}{2\pi i} \oint_{z=\lambda_{2n}} dz \frac{1}{z - U_J} |B_{2n-1}\rangle. \quad (4.56)$$

Associated with the double poles are even-order Jordan polynomial states, $\lambda_{2n}(x)$, as

$$|\lambda_{2n}\rangle = \frac{1}{\langle \tilde{B}_{2n-1} | \delta U | B_{2n} \rangle} \frac{1}{2\pi i} \oint_{z=\lambda_{2n}} dz \frac{1}{z - U_J} |B_{2n}\rangle. \quad (4.57)$$

³In the language of linear algebra, the algebraic multiplicity of the degenerate eigenvalues of U_J and U_N is 2. But the geometric multiplicity (meaning the dimension of the associated eigenspace) of the degenerate eigenvalues of U_N is 1; whereas it is 2 for U_J .

As shown in Appendix A.11 the matrix element coefficient is put here so that these states satisfy the canonical Jordan state relation

$$U_J |\lambda_{2n}\rangle = \lambda_{2n} |\lambda_{2n}\rangle + |\lambda_{2n-1}\rangle, \quad (4.58a)$$

with the odd-order eigenpolynomials satisfying

$$U_J |\lambda_{2n-1}\rangle = \lambda_{2n} |\lambda_{2n-1}\rangle. \quad (4.58b)$$

The Jordan state corresponding to λ_{2n} is not uniquely determined because any multiple of the eigenstate $|\lambda_{2n-1}\rangle$ may be added to it and the new state will still satisfy (4.58a).

As shown in Appendix A.11, evaluation of the integral in (4.57) yields the formal expression for the Jordan states of

$$\begin{aligned} |\lambda_{2n}\rangle &= \frac{1}{\langle \tilde{B}_{2n-1} | \delta U | B_{2n} \rangle} \left(1 + \frac{1}{\lambda_{2n} - U_J} \delta U \right) |B_{2n}\rangle \\ &\quad - \frac{1}{\lambda_{2n} - U_J} \left(1 + \frac{1}{\lambda_{2n} - U_J} \delta U \right) |B_{2n-1}\rangle. \end{aligned} \quad (4.59)$$

This expression contains ill-defined terms but as a whole makes sense since those terms cancel when it is evaluated. It is written this way so that it is easy to compare with the formal expression for the eigenstates. A self-consistent equation yielding a recursion relation for the Jordan state may be derived, as also shown in Appendix A.11, as

$$|\lambda_{2n}\rangle = |B_{2n}\rangle + \sum_{k=0}^{2n-2} |B_k\rangle \frac{1}{\lambda_{2n} - \lambda_k} \langle \tilde{B}_k | \left[\delta U |\lambda_{2n}\rangle - \langle \tilde{B}_{2n-1} | \delta U | B_{2n} \rangle |\lambda_{2n-1}\rangle \right]. \quad (4.60)$$

The eigenpolynomials may be determined from a recursion relation like (3.38) or, if the Jordan states are determined first, then the eigenpolynomials may be obtained from (4.58a) as $|\lambda_{2n-1}\rangle = (U_J - \lambda_{2n}) |\lambda_{2n}\rangle$.

The first four right states, with the coefficient of the highest power of x in the odd-order eigenpolynomials taken to be 1, are

$$\begin{aligned} \lambda_0(x) &= 1 \\ \lambda_1(x) &= x - \frac{1}{2} \\ \lambda_2(x) &= -\frac{27}{4}(x^2 - \frac{2}{3}x) \\ \lambda_3(x) &= x^3 - \frac{3}{2}x^2 + \frac{3}{4}x - \frac{1}{8}. \end{aligned} \quad (4.61)$$

For the left states of U_J it is the odd-order states that are Jordan states and the even-order states that are eigenstates. (See Appendix A.12 for a discussion of duals of Jordan states.) In terms of the resolvent the left states are

$$\langle \tilde{\lambda}_{2n-1} | = \frac{1}{2\pi i} \oint_{z=\lambda_{2n}} dz \langle \tilde{B}_{2n-1} | \frac{1}{z - U_J}, \quad (4.62)$$

and,

$$\langle \tilde{\lambda}_{2n} | = \frac{\langle \tilde{B}_{2n-1} | \delta U | B_{2n} \rangle}{2\pi i} \oint_{z=\lambda_{2n}} dz \langle \tilde{B}_{2n} | \frac{1}{z - U_J}. \quad (4.63)$$

They satisfy

$$\langle \tilde{\lambda}_{2n-1} | U_J = \lambda_{2n} \langle \tilde{\lambda}_{2n-1} | + \langle \tilde{\lambda}_{2n} |, \quad (4.64)$$

and

$$\langle \tilde{\lambda}_{2n} | U_J = \lambda_{2n} \langle \tilde{\lambda}_{2n} |. \quad (4.65)$$

In the basis of the λ states U_J takes the canonical Jordan block diagonal form with 2×2 blocks of 3^{-2n} on the diagonal and 1 off diagonal as

$$U_J = |\lambda_0\rangle\langle\tilde{\lambda}_0| + \sum_{n=1}^{\infty} (|\lambda_{2n-1}\rangle\langle\lambda_{2n}|) \begin{pmatrix} 3^{-2n} & 1 \\ 0 & 3^{-2n} \end{pmatrix} \begin{pmatrix} \langle\tilde{\lambda}_{2n-1}| \\ \langle\tilde{\lambda}_{2n}| \end{pmatrix}, \quad (4.66)$$

which is the spectral decomposition of U_J .

From (4.58a) the right Jordan vectors evolve in time as (compare with (4.47))

$$U_J^t |\lambda_{2n}\rangle = \lambda_{2n}^t |\lambda_{2n}\rangle + t \lambda_{2n}^{t-1} |\lambda_{2n-1}\rangle. \quad (4.67)$$

In order to isolate the modified exponential decay we may consider the correlation of $\lambda_{2n}(x)$ with another function, $G_{2n}(x)$, orthogonal to it but not to $\lambda_{2n-1}(x)$ as

$$\langle G_{2n} | U_J^t | \lambda_{2n} \rangle = t \lambda_{2n}^{t-1} \langle G_{2n} | \lambda_{2n-1} \rangle, \quad (4.68)$$

where we assumed that $\langle G_{2n} | \lambda_{2n} \rangle = 0$. For $\lambda_2(x)$ and $\lambda_1(x)$ given above an appropriate $G_2(x)$ is $-60(x^2 - \frac{6}{5}x)$ and we obtain $\langle G_2 | U_J^t | \lambda_2 \rangle = t(1/9)^{t-1}$. This correlation grows initially before decaying. Of course, even in maps that are fully diagonalizable there may be correlations that grow initially before decaying to their equilibrium values. This only would occur in such a case though if there is more than one mode contributing to the correlation. Initial growth may occur then, for example, when two decay modes with opposite sign contribute to the correlation such as $C(t) = c_1 e^{-\gamma_1 t} - c_2 e^{-\gamma_2 t}$, where $c_1 > c_2 > 0$. If γ_2 is sufficiently larger than γ_1 then $C(t)$ will grow initially.

4.2.3 Polynomial Shift States

The tent map presented in Section 4.1.1 has a zero eigenvalue of infinite degeneracy. But the map was fully diagonalizable in the eigenspace spanned by the zero eigenvalue. This meant that all elements of a density in P_- are annihilated by one application of the map. It also meant that correlation functions had components with delta correlations, as we saw for the x auto-correlation function. In this section a map that also has an infinite degeneracy of the zero eigenvalue but which is not diagonalizable is presented. Here there is the situation of not just one-time delta correlations but components that are annihilated after more than one time step.

Consider the four-branch piecewise-linear map, $x_{t+1} = S_A(x_t)$, given by

$$S_A(x) = \begin{cases} 4x & 0 \leq x < \frac{1}{4} \\ 2 - 4x & \frac{1}{4} \leq x < \frac{1}{2} \\ 3 - 4x & \frac{1}{2} \leq x < \frac{3}{4} \\ 4x - 3 & \frac{3}{4} \leq x < 1. \end{cases} \quad (4.69)$$

The map is shown in Figure 4.5. The Frobenius–Perron operator for this map acts on a density as

$$U_A \rho(x) = \frac{1}{4} \left[\rho\left(\frac{x}{4}\right) + \rho\left(\frac{2-x}{4}\right) + \rho\left(\frac{3-x}{4}\right) + \rho\left(\frac{3+x}{4}\right) \right]. \quad (4.70)$$

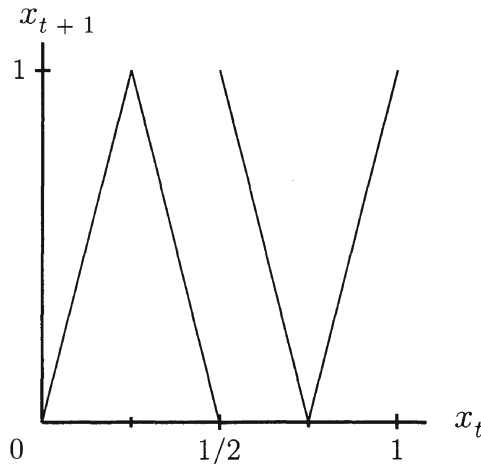


Figure 4.5: The map $S_A(x)$.

The Frobenius–Perron operator U_A commutes with R and so, as discussed in Section 4.1, the evolution is independent in the two spaces spanned by the projection operators P_+ and P_- . Acting on the monomial x^n the eigenvalues associated with even-order eigenpolynomials are seen to be $1/4^{2n}$ and 0 is the infinitely degenerate eigenvalue in P_- space. But $U_A P_- \neq 0$, which tells us that the eigenstates associated with the zero eigenvalue do not span P_- .

First, the decomposition of U_A in P_+ space is very easy to obtain using the algebraic technique. The operator U_A intertwines with P_+ and the Frobenius–Perron operator of the 4-adic map, U_4 , given by (3.59) with $r = 4$, as

$$P_+ U_A = U_4 P_+, \quad (4.71)$$

Since U_A commutes with P_+ , the dynamics of U_A in this subspace is just like the 4-adic map, so this part of their spectral decomposition is identical. The decomposition of U_A in P_+ thus has the explicit form

$$U_A P_+ = \sum_{n=0}^{\infty} \frac{1}{4^{2n}} |B_{2n}\rangle \langle \tilde{B}_{2n}|. \quad (4.72)$$

To determine whether there are distinct eigenstates associated with the degenerate zero eigenvalue of U_A we consider the nature of the singularity of its resolvent at $z = 0$. The resolvent in P_- , as spanned by the odd-degree Bernoulli polynomials and their duals, in terms of its matrix elements in this basis is

$$P_- \frac{1}{z - U_A} P_- = \sum_{m,n=0}^{\infty} |B_{2m+1}\rangle \langle \tilde{B}_{2m+1}| \frac{1}{z - U_A} |B_{2n+1}\rangle \langle \tilde{B}_{2n+1}|. \quad (4.73)$$

Expanding the resolvent in terms of the diagonal, U_0 , and off-diagonal (strictly triangular) parts, δU , of U_A in P_- gives

$$\begin{aligned} \langle \tilde{B}_{2m+1} | \frac{1}{z - U_A} | B_{2n+1} \rangle &= \sum_{n=0}^{\infty} \langle \tilde{B}_{2m+1} | \frac{1}{z - U_0} \left(\delta U \frac{1}{z - U_0} \right)^n | B_{2n+1} \rangle \\ &= \sum_{n=0}^{\infty} \langle \tilde{B}_{2m+1} | \frac{1}{z} \left(\delta U \frac{1}{z} \right)^n | B_{2n+1} \rangle, \end{aligned} \quad (4.74)$$

where we used that $P_- U_0 P_-$ is the zero matrix. Since the off-diagonal matrix elements,

$$\langle \tilde{B}_{2m+1} | \delta U | B_{2n+1} \rangle = \frac{(2n+1)! B_{2n-2m+1}(\frac{1}{4})}{4^{2m}(2m+1)!(2n-2m+1)!}, \quad (4.75)$$

are nonvanishing (for $n > m$), powers of $\frac{1}{z}$ up to $(\frac{1}{z})^{n-m+1}$ appear in (4.74). Hence, in (4.73) there appears a pole of infinite order at $z = 0$, i.e., an essential singularity. This means that U_A is not diagonalizable in this functional space but is only reducible to one Jordan block of infinite size, with zeroes on the diagonal.

When U_A acts on a polynomial in P_- of degree $2n+1$ it gives a polynomial of degree $2n-1$. Denoting a “shift” polynomial of degree $2n+1$ as $\phi_{2n+1}(x)$ we have

$$U_A \phi_{2n+1}(x) = \phi_{2n-1}(x), \quad (4.76)$$

for $n \geq 1$, where any weight factors are incorporated here into the definition of the states. The first-degree polynomial associated with the zero eigenvalue is the only eigenstate of U_A in P_- . This state is unique (up to a constant factor) and is $\phi_1(x) = x - 1/2$. We refer to this state as the vacuum state. The decomposition of U_A in P_- is formally thus

$$U_A P_- = \sum_{n=1}^{\infty} |\phi_{2n-1}\rangle \langle \tilde{\phi}_{2n+1}|. \quad (4.77)$$

To construct explicit shift states obeying (4.76) we first note that any polynomial in P_- , say $p_{2n+1}(x)$, may be used to generate a set of shift states running down to the vacuum state as $\{p_{2n+1}, U_A p_{2n+1}, U_A^2 p_{2n+1}, \dots, U_A^n p_{2n+1}\}$. Since $U_A U_A^\dagger = 1$ we may consider applying U_A^\dagger successively to $p_{2n+1}(x)$ to generate shift states above $p_{2n+1}(x)$. But these states will not be higher-degree polynomials.

Since the action of U_A reduces the degree of a shift polynomial by two, it motivates the consideration of families of shift polynomials that satisfy

$$\frac{d^2}{dx^2} \psi_{2n+1}(x) = v_{2n-1} \psi_{2n-1}(x). \quad (4.78a)$$

For states in this family U_A will act in general as a weighted shift,

$$U_A \psi_{2n+1}(x) = w_{2n-1} \psi_{2n-1}(x). \quad (4.78b)$$

The weight, w_{2n-1} , may be found by comparing the highest degree terms on the right hand sides of both (4.78a) and (4.78b);

$$w_{2n-1} = \frac{v_{2n-1}}{2 \cdot 4^{2n+1}}. \quad (4.79)$$

The fact that (4.78a) and (4.78b) are consistent may be proven from the intertwining relation between U_A and the second derivative operator:

$$\frac{d^2}{dx^2} U_A = \frac{1}{4^2} U_A \frac{d^2}{dx^2}. \quad (4.80)$$

To construct ψ_{2n+1} from ψ_{2n-1} we invert (4.78a), i.e., integrate twice, and use (4.78b) to determine the constants of integration. Suppose that the state ψ_{2n-1} is known and is expanded in terms of Bernoulli polynomials as

$$\psi_{2n-1}(x) = \sum_{j=1}^n b_{2j-1}^{(2n-1)} B_{2j-1}(x). \quad (4.81)$$

We want to find the expansion coefficients, $b_{2j-1}^{(2n+1)}$, of the next shift state, $\psi_{2n+1}(x)$. Using that $\frac{d^2}{dx^2} B_{2j+1}(x) = 2j(2j+1)B_{2j-1}(x)$ we obtain, from (4.78a)

$$b_{2j+1}^{(2n+1)} = v_{2n-1} \frac{b_{2j-1}^{(2n-1)}}{2j(2j+1)}, \quad j = 1, \dots, n. \quad (4.82)$$

The coefficient, $b_1^{(2n+1)}$, of the vacuum component of $\psi_{2n+1}(x)$ is still undetermined. Since this component is annihilated by U_A and by the second derivative operator, we need to go one more step up; that is, consider $\psi_{2n+3}(x)$ in order to determine this coefficient. The state $\psi_{2n+3}(x)$ is obtained from (4.78a) by integrating $\psi_{2n+1}(x)$ twice as,

$$\psi_{2n+3}(x) = b_1^{(2n+3)} B_1(x) + v_{2n+1} \sum_{j=0}^n b_{2j+1}^{(2n+1)} \frac{B_{2j+3}(x)}{(2j+3)(2j+2)}. \quad (4.83)$$

Using (4.78b) we extract the $B_1(x)$ component of $\psi_{2n+1}(x)$ from $\psi_{2n+3}(x)$ as

$$b_1^{(2n+1)} = \langle \tilde{B}_1 | \psi_{2n+1} \rangle = \frac{1}{w_{2n+1}} \langle \tilde{B}_1 | U_A | \psi_{2n+3} \rangle. \quad (4.84)$$

Then from (4.83), using (4.82) and that $\langle \tilde{B}_1 | U_A | B_{2j+3} \rangle = B_{2j+3}(1/4)$ we can solve for $b_1^{(2n+1)}$ to obtain

$$b_1^{(2n+1)} = -\frac{2 \cdot 4^3 v_{2n-1}}{1 - 4^{-2n}} \sum_{j=1}^n \frac{b_{2j-1}^{(2n-1)} B_{2j+3}(\frac{1}{4})}{(2j)(2j+1)(2j+3)(2j+2)}. \quad (4.85)$$

The above procedure can be written in terms of a creation operator, U_C , which acts as $U_C \psi_{2n-1}(x) = \psi_{2n+1}(x)$. The creation operator is given by

$$U_C = \sum_{j=1}^{\infty} \frac{v_{2n-1}}{2j(2j+1)} \left[|B_{2j+1}\rangle - \frac{2 \cdot 4^3}{1 - 4^{-2n}} \frac{B_{2j+3}(1/4)}{(2j+3)(2j+2)} |B_1\rangle \right] \langle \tilde{B}_{2j-1}|. \quad (4.86)$$

If we take $v_{2n-1} = (2n+1)(2n)$ then we will generate shift states which are monic polynomials. We start from the vacuum state and work our way up.

Explicit forms of the first few monic polynomial shift states generated this way are

$$\begin{aligned}\psi_1(x) &= x - \frac{1}{2} \\ \psi_3(x) &= x^3 - \frac{3}{2}x^2 + \frac{2}{3}x - \frac{1}{12} \\ \psi_5(x) &= x^5 - \frac{5}{2}x^4 + \frac{20}{9}x^3 - \frac{5}{6}x^2 + \frac{16}{135}x - \frac{1}{270} \\ \psi_7(x) &= x^7 - \frac{7}{2}x^6 + \frac{14}{3}x^5 - \frac{35}{12}x^4 + \frac{112}{135}x^3 - \frac{7}{90}x^2 - \frac{16}{8505}x + \frac{1}{68040}.\end{aligned}\tag{4.87}$$

The duals, $\tilde{\phi}_{2n+1}(x)$, of the generic shift polynomials obeying (4.76) satisfy $\langle \tilde{\phi}_{2n+1} | \phi_{2m+1} \rangle = \delta_{n,m}$. They can be obtained from successive applications of U_A^\dagger to $\tilde{\phi}_1(x)$ as $(U_A^\dagger)^n \tilde{\phi}_1(x) = \tilde{\phi}_{2n+1}(x)$. The dual of the vacuum state in terms of the duals of the Bernoulli polynomials and the expansion coefficients of the shift states is

$$\tilde{\phi}_1(x) = \frac{1}{b_1^{(1)}} \left\{ \tilde{B}_1(x) - \frac{b_1^{(3)}}{b_3^{(3)}} \tilde{B}_3(x) - \frac{1}{b_5^{(5)}} \left(b_1^{(5)} - \frac{b_3^{(5)} b_1^{(3)}}{b_3^{(3)}} \right) \tilde{B}_5(x) - \dots \right\}.\tag{4.88}$$

(This expression is derived in Appendix A.13.) We note that U_C^\dagger acts as an annihilation operator on the dual states as $U_C^\dagger \tilde{\phi}_{2n+1}(x) = \tilde{\phi}_{2n-1}(x)$.

For the families of states obeying (4.78a) the higher-order duals can be expressed simply in terms of the vacuum dual state as

$$\langle \tilde{\psi}_{2n+1} | = \prod_{k=0}^{n-1} [v_{2k+1}]^{-1} \langle \tilde{\psi}_1 | \frac{d^{2n}}{dx^{2n}}.\tag{4.89}$$

The effect of the polynomial shift dynamics can be seen on correlation functions involving observables which are polynomials in x . To see the effect of the shift dynamics we need to consider one of the observables to be at least a third degree polynomial. The simplest choice for illustration is to take $B(x) = x$ and $A(x) = \phi_{2n+1}(x)$. Then we obtain

$$C_{x \phi_{2n+1}}(t) = \langle x | U_A^t \phi_{2n+1} \rangle = \sum_{m=0}^n a_{n-m} \delta_{t,m}.\tag{4.90}$$

where $a_k \equiv \int_0^1 dx x \phi_{2k+1}(x)$. So the equilibrium value of the correlation, which here is zero, is attained for $t \geq n+1$. The spectral function, (2.12),

corresponding to this correlation is

$$P_{x \phi_{2n+1}}(\omega) = \sum_{t=0}^{\infty} \cos \omega t \sum_{m=0}^n a_{n-m} \delta_{t,m} = \sum_{m=0}^n a_{n-m} \cos m\omega. \quad (4.91)$$

It is interesting to compare the polynomial shift states of U_A with the trigonometric shift states of U_B discussed in Section 3.3. First, the trigonometric shift states of U_B were self-dual so that U_B and U_B^\dagger served as the annihilation and creation operators respectively on the same family of states. Here the shift polynomials are not self-dual and we need four operators: U_A , U_A^\dagger , U_C and U_C^\dagger . Second, from the trigonometric shift states coherent eigenstates were constructed. If we try to construct coherent eigenstates, like (3.13), from the polynomial shift states we find that the weight factors preclude the convergence of the series defining the coherent state, except when the eigenvalue is zero, in which case we recover the vacuum state.

More on the application of symmetry and the algebraic technique to one-dimensional maps is given in Appendix A.14.

4.3 Fractal Repellors

Here we consider a map where probability with respect to Lebesgue measure escapes under successive iterations. The map presented is a very simple example of chaotic dynamics settling onto a strange attractor. Some of the features of this system will return in our analysis of deterministic diffusion in Chapter 6.

Consider the map

$$S_C(x) = \begin{cases} 3x & 0 \leq x < \frac{1}{3} \\ 0 & \frac{1}{3} \leq x < \frac{2}{3} \\ 3x - 2 & \frac{2}{3} \leq x < 1, \end{cases} \quad (4.92)$$

shown in Figure 4.6, which we call the Cantor map. The reason we give it this name is because all trajectories, except for those arising from initial conditions belonging to the well-known middle-thirds Cantor set eventually “escape” from the system. The escape occurs when an iterate falls into the interval $[\frac{1}{3}, \frac{2}{3}]$.

An easy way to see how the Cantor set emerges is to consider U_C^\dagger acting on x . Since $U_C^\dagger f(x) = f(S_C(x))$ we have from (4.92) that U_C^\dagger removes the middle third of $f(x) = x$. (The graph of $f(S_C(x))$ is just Figure 4.6.) Successive applications of U_C^\dagger remove middle thirds of what is left at each

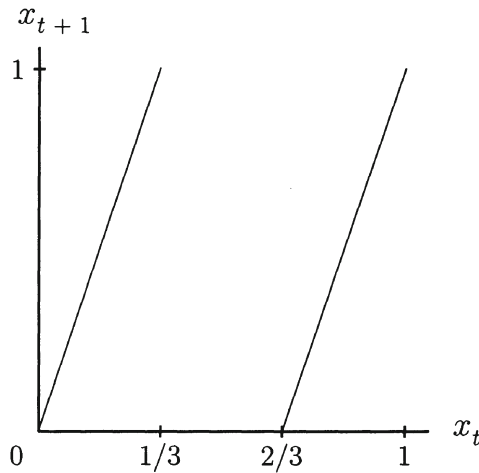


Figure 4.6: The Cantor map.

stage. Thus, $\lim_{t \rightarrow \infty} (U_C^\dagger)^t x = \{C\}$, where $\{C\}$ is the Cantor set. The same procedure applied to any other reasonable function supported on the whole unit interval will also yield the Cantor set. Thus, for long times the dynamics settles onto a fractal set of zero Lebesgue measure (with fractal dimension $\log 2 / \log 3 = 0.6309$). We may expect, by recalling the construction of the left eigenstates of the Bernoulli map in Section 3.5.2, that the left eigenstates here will involve an integration over the singular measure of the Cantor set.

The Cantor map is not measure preserving with respect to Lebesgue measure as $\mu_L(S_C^{-1}[a, b]) = \frac{2}{3}(b-a) \neq \mu_L([a, b]) = b-a$. Thus if we consider a probability density with respect to Lebesgue measure it will decay to zero as $t \rightarrow \infty$. An invariant singular measure for this map is $\mu_C([a, b]) \equiv \int_a^b dF_C(x)$, where the Cantor function, $F_C(x)$, satisfies the functional equation

$$F_C(x) = \begin{cases} \frac{1}{2}F_C(3x) & 0 \leq x < \frac{1}{3} \\ \frac{1}{2} & \frac{1}{3} \leq x < \frac{2}{3} \\ \frac{1}{2}F_C(3x-2) + \frac{1}{2} & \frac{2}{3} \leq x \leq 1. \end{cases} \quad (4.93)$$

(The proof that μ_C is invariant for F_C is given in Appendix A.15.) The function $F_C(x)$, which is shown in Figure 4.7, gives the cumulative measure on the singular Cantor set. It has slope zero almost everywhere except for discontinuous jumps at the points of the Cantor set. It is possible to consider densities with respect to the singular invariant measure but we will consider

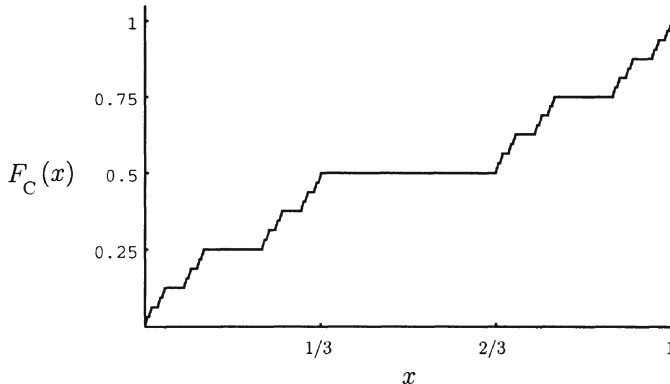


Figure 4.7: The cumulative measure, (4.93), on the Cantor set, which defines the singular invariant measure of the Cantor map.

densities with respect to Lebesgue measure, which is normally considered more physically relevant.

The Frobenius–Perron operator of the Cantor map is given by

$$U_C \rho(x) = \frac{1}{3} \left[\rho\left(\frac{x}{3}\right) + \rho\left(\frac{2+x}{3}\right) \right]. \quad (4.94)$$

The matrix elements of U_C with respect to the Bernoulli basis are

$$\langle \tilde{B}_m | U_C | B_n \rangle = \begin{cases} \frac{1}{3^m} \frac{n!}{m!(n-m+1)!} \left[B_{n-m+1}(\frac{1}{3}) - B_{n-m+1}(\frac{2}{3}) \right] & m \leq n \\ \frac{2}{3^{n+1}} & m = n \\ 0 & m > n. \end{cases} \quad (4.95)$$

The diagonal elements are the eigenvalues

$$e^{-\gamma_C^{(n)}} \equiv \frac{2}{3^{n+1}} = \frac{2}{3} e^{-n \log 3}. \quad (4.96)$$

The first eigenvalue ($n = 0$) is $2/3$, corresponding to U_C acting on a constant density so that at each time step $1/3$ of the remaining probability is lost.

Since the eigenvalues are non-degenerate, the resolvent of U_C has simple poles at the location of the eigenvalues. Formal expressions for the right and left eigenstates may thus be written down as for the Bernoulli map. The right eigenstates are polynomials whose explicit form doesn't interest us here.

The left eigenstates act as (see (3.34))

$$\langle \tilde{\gamma}_C^{(n)} | f \rangle = \langle \tilde{B}_n | f \rangle + \langle \tilde{B}_n | \delta U \frac{1}{e^{-\gamma_C^{(n)}} - U_C} | f \rangle \quad (4.97)$$

In order to get an explicit closed-form expression for the second term on the right hand side we insert to the right of δU Bernoulli basis states up to order $n+1$ and the remainder term, as given by (3.69) and (3.70) with $t=0$. This basis has the completeness relation

$$\mathbf{1}_M = \sum_{m=0}^M |B_m\rangle \langle \tilde{B}_m| - |\mathcal{B}_M\rangle \langle \mathbf{e} \tilde{B}_M|, \quad (4.98)$$

where $\mathbf{1}_M$ is the unit operator in the space of functions that are at least M -times differentiable. The remainder term doesn't have a natural decomposition into right and left vectors but we want to use bra-ket notation so we have written it as above. The meaning of the symbols is that

$$\mathcal{B}_M(x) \langle \mathbf{e} \tilde{B}_M | f \rangle = \mathcal{B}_M(x) \cdot \int_0^1 dx' \mathbf{e}^*(x') \frac{1}{M!} \frac{d^M}{dx'^M} f(x'), \quad (4.99)$$

where

$$\mathcal{B}_M(x) \cdot \mathbf{e}(x') = \sum_k B_{M,k}(x) e_k(x'), \quad (4.100)$$

and

$$B_{M,k}(x) = \frac{-M!}{(2\pi i k)^M} e_k(x) \quad (4.101)$$

for $k \neq 0$, $B_{M,0}(x) = 0$, and $e_k(x) = e^{2\pi i k x}$.

After inserting (4.98) with $M=n+1$ into the second term of (4.97) the remainder term and only the $(n+1)$ st discrete basis state contributes due to upper-triangularity. We thus obtain

$$\begin{aligned} & \langle \tilde{B}_n | \delta U \frac{1}{e^{-\gamma_C^{(n)}} - U_C} | f \rangle \\ &= \langle \tilde{B}_n | \delta U \left[|B_{n+1}\rangle \langle \tilde{B}_{n+1}| - |\mathcal{B}_{n+1}\rangle \langle \mathbf{e} \tilde{B}_{n+1}| \right] \frac{1}{e^{-\gamma_C^{(n)}} - U_C} | f \rangle. \end{aligned} \quad (4.102)$$

We may then replace δU here by U_C since the U_0 part does not contribute to the off-diagonal matrix elements. This allows us to employ the intertwining relation between U_C and n -th derivative operator:

$$\frac{d^n}{dx^n} U_C = \frac{1}{3^n} U_C \frac{d^n}{dx^n}. \quad (4.103)$$

Since $\tilde{B}_n(x) = (1/n!) d^n/dx^n$ we may pull through the derivative operator using (4.103) to obtain

$$\begin{aligned} \langle \tilde{B}_n | U_C \left[|B_{n+1}\rangle\langle\tilde{B}_{n+1}| - |\mathcal{B}_{n+1}\rangle\langle\mathbf{e}\tilde{B}_{n+1}| \right] \frac{1}{e^{-\gamma_C^{(n)}} - U_C} |f\rangle \\ = \langle 1 | \frac{U_C}{3^n} [| (n+1)B_1\rangle\langle 1| - |(n+1)\mathcal{B}_1\rangle\langle\mathbf{e}|] \frac{1}{e^{-\gamma_C^{(n)}} - \frac{U_C}{3^{n+1}}} | \frac{f^{(n+1)}}{(n+1)!} \rangle \\ \equiv \langle \xi_n | \frac{f^{(n+1)}}{n!} \rangle, \end{aligned} \quad (4.104)$$

where $\langle 1 | = \langle \tilde{B}_0 |$ is the constant state and we have defined the function $\xi_n(x)$ as

$$\xi_n(x) \equiv \frac{3}{2 - U_C^\dagger} \eta_n(x) \quad (4.105)$$

and

$$\eta_n(x) \equiv \langle 1 | U_C | B_1 \rangle - \langle 1 | U_C | \mathcal{B}_1 \rangle \mathbf{e}(x). \quad (4.106)$$

The function $\eta_n(x)$ is calculated in Appendix A.16 with the result

$$\eta_n(x) = \begin{cases} -\frac{1}{3}x & 0 \leq x < \frac{1}{3} \\ -\frac{1}{3}(1-2x) & \frac{1}{3} \leq x < \frac{2}{3} \\ -\frac{1}{3}(x-1) & \frac{2}{3} \leq x < 1, \end{cases} \quad (4.107)$$

which we notice is independent of n .

It is convenient to rewrite (4.105) to give a functional equation for $\xi_n(x)$ as

$$\xi_n(x) = \frac{1}{2} U_C^\dagger \xi_n(x) + \frac{3}{2} \eta_n(x). \quad (4.108)$$

Then using (4.107) and the explicit form of U_C^\dagger gives

$$\xi_n(x) = \begin{cases} \frac{1}{2} \xi_n(3x) - \frac{1}{2}x & 0 \leq x < \frac{1}{3} \\ -\frac{1}{2} + x & \frac{1}{3} \leq x < \frac{2}{3} \\ \frac{1}{2} \xi_n(3x-2) + \frac{1}{2} - \frac{1}{2}x & \frac{2}{3} \leq x < 1. \end{cases} \quad (4.109)$$

Going back to (4.97) we have calculated the left eigenstate as

$$\begin{aligned} \langle \tilde{\gamma}_C^{(n)} | f \rangle &= \langle 1 | \frac{f^{(n)}}{n!} \rangle + \langle \xi_n | \frac{f^{(n+1)}}{n!} \rangle \\ &= \int_0^1 dx \frac{1}{n!} \frac{d^n f}{dx^n} + \int_0^1 \xi_n(x) \frac{1}{n!} \frac{d^{n+1} f}{dx^{n+1}}. \end{aligned} \quad (4.110)$$

We can use integration by parts on the second term here and then rewrite $\langle \tilde{\gamma}_C^{(n)} | f \rangle$ as a Riemann-Stieltjes integral as

$$\langle \tilde{\gamma}_C^{(n)} | f \rangle = \int_0^1 dG_C(x) \frac{1}{n!} \frac{d^n f}{dx^n}, \quad (4.111)$$

where $G_C(x) \equiv x - \xi_n(x)$. Then $G_C(x)$ satisfies the simpler functional equation

$$G_C(x) = \begin{cases} \frac{1}{2}G_C(3x) & 0 \leq x < \frac{1}{3} \\ \frac{1}{2} & \frac{1}{3} \leq x < \frac{2}{3} \\ \frac{1}{2}G_C(3x - 2) + \frac{1}{2} & \frac{2}{3} \leq x < 1, \end{cases} \quad (4.112)$$

which is identical to the functional equation for the Cantor function, $F_C(x)$, given by (4.93). So we find that the left eigenfunctional involves an integration over the singular invariant measure of the map. In Chapter 6 we will encounter singular measures again in our study of a model of deterministic diffusion.

4.4 Topologically Conjugate Maps

Two maps related by a simple change of variables are said to be topologically conjugate. The conjugating function effecting the change should be one-to-one, onto and continuous, i.e., a homeomorphism. Knowing the spectral decomposition of one of the maps enables us, through the use of the conjugating function, to determine the spectral decomposition of the other map. In this way, we may obtain the spectral decomposition of maps that are not piecewise-linear from the results we have for piecewise-linear maps. First, we'll discuss the situation in a general context and then apply it to obtain the spectral decomposition of the well-known logistic map with unit height.

Consider the map T , i.e., $x_{t+1} = T(x_t)$. By the change of variable, $\phi(x)$, we generate a new map, S , as $\phi(x_{t+1}) = \phi(T(x_t)) \equiv S(\phi(x_t))$. The map S is obtained by using the fact that ϕ has an inverse as $\phi(T(x_t)) = \phi(T(\phi^{-1}(\phi(x_t)))) = \phi \circ T \circ \phi^{-1}(\phi(x_t))$, so that

$$S = \phi \circ T \circ \phi^{-1}. \quad (4.113)$$

The Koopman operator, K_S , corresponding to S is immediately obtained in terms of the Koopman operators corresponding to T and the conjugating

function ϕ as $K_S = K_{\phi^{-1}} K_T K_\phi$. Acting successively with K_ϕ and $K_{\phi^{-1}}$ in either order gives the identity operator so that $K_{\phi^{-1}} = K_\phi^{-1}$ and we have

$$K_S = K_\phi^{-1} K_T K_\phi. \quad (4.114)$$

The Frobenius–Perron operator, U_S , corresponding to S is the adjoint of K_S . Now, $K_S^\dagger = K_\phi^\dagger K_T^\dagger (K_\phi^{-1})^\dagger$ and since $(K_\phi^{-1})^\dagger = (K_\phi^\dagger)^{-1}$ we have

$$U_S = U_\phi U_T U_\phi^{-1}, \quad (4.115)$$

where it is also true that $U_\phi^{-1} = U_{\phi^{-1}}$. Thus we see that both the Koopman and Frobenius–Perron operators of topologically conjugate maps are related by a similarity transformation.

Let us suppose the spectral decomposition of U_T is known and that it is fully diagonal. Denoting the right and left eigenstates by $|T_n\rangle$ and $\langle \tilde{T}_n|$ with associated eigenvalue λ_n we see that

$$\begin{aligned} U_S [U_\phi |T_n\rangle] &= U_\phi U_T U_\phi^{-1} U_\phi |T_n\rangle \\ &= U_\phi U_T |T_n\rangle \\ &= \lambda_n [U_\phi |T_n\rangle]. \end{aligned} \quad (4.116)$$

Thus, the right eigenstates, $S_n(x)$, of U_S are given by

$$S_n(x) = U_\phi T_n(x) = \left. \frac{T_n(x')}{d\phi(x')/dx'} \right|_{x'=\phi^{-1}(x)} \quad (4.117)$$

with the same eigenvalues, λ_n , associated with $T_n(x)$. (Jordan states transform in the same way.)

In a similar way, using (4.114), it can be show that the left eigenstates, $\tilde{S}_n(x)$, of U_S , (i.e., the right eigenstates of K_S) are given by

$$\tilde{S}_n(x) = K_{\phi^{-1}} \tilde{T}_n(x) = \tilde{T}_n(\phi^{-1}(x)). \quad (4.118)$$

These states form an orthonormal set with the right states (4.117) as

$$\langle \tilde{S}_m | S_n \rangle = \langle K_{\phi^{-1}} \tilde{T}_m | U_\phi T_n \rangle = \langle \tilde{T}_m | U_{\phi^{-1}} U_\phi T_n \rangle = \langle \tilde{T}_m | T_n \rangle = \delta_{mn}, \quad (4.119)$$

where we used $U_{\phi^{-1}} = U_\phi^{-1}$ and the orthonormality of the T states.

Concise then, if the spectral decomposition of U_T is given by

$$U_T |\rho\rangle = \sum_n \lambda_n |T_n\rangle \langle \tilde{T}_n | \rho \rangle, \quad (4.120)$$

then the decomposition of U_S is

$$\begin{aligned} U_S|\rho\rangle &= \sum_n \lambda_n U_\phi|T_n\rangle\langle K_\phi^{-1}\tilde{T}_n|\rho\rangle \\ &= \sum_n \lambda_n U_\phi|T_n\rangle\langle\tilde{T}_n|U_\phi^{-1}|\rho\rangle. \end{aligned} \quad (4.121)$$

4.4.1 Decomposition of the Logistic Map

The logistic map of unit height on the unit interval is given by $S(x) = 4x(1-x)$. The map is shown in Figure 4.8.

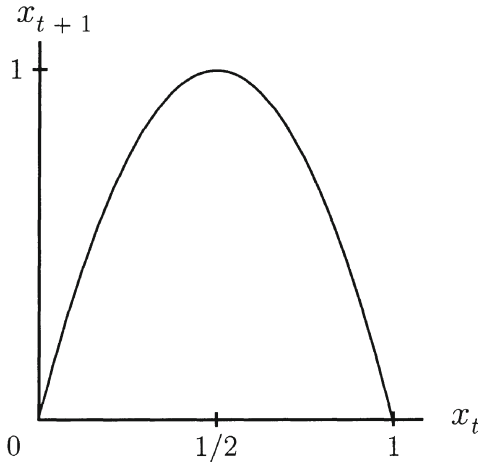


Figure 4.8: The logistic map with unit height.

The Frobenius–Perron operator acts on a density as

$$U_S\rho(x) = \frac{1}{4\sqrt{1-x}} \left[\rho \left(\frac{1-\sqrt{1-x}}{2} \right) + \rho \left(\frac{1+\sqrt{1-x}}{2} \right) \right]. \quad (4.122)$$

Clearly, there are no eigenstates of U_S that are polynomials in x , since U_S acting on a polynomial yields a non-polynomial function of x . The evolution under the logistic map of an initial nonequilibrium density (the same as in Figure 1.2 for the Bernoulli map) is given in Figure 4.9. A measure that is absolutely continuous with respect to Lebesgue measure is preserved by this map. The non-uniform invariant density, which is nearly approached by $t = 3$ in Figure 4.9, is determined below.

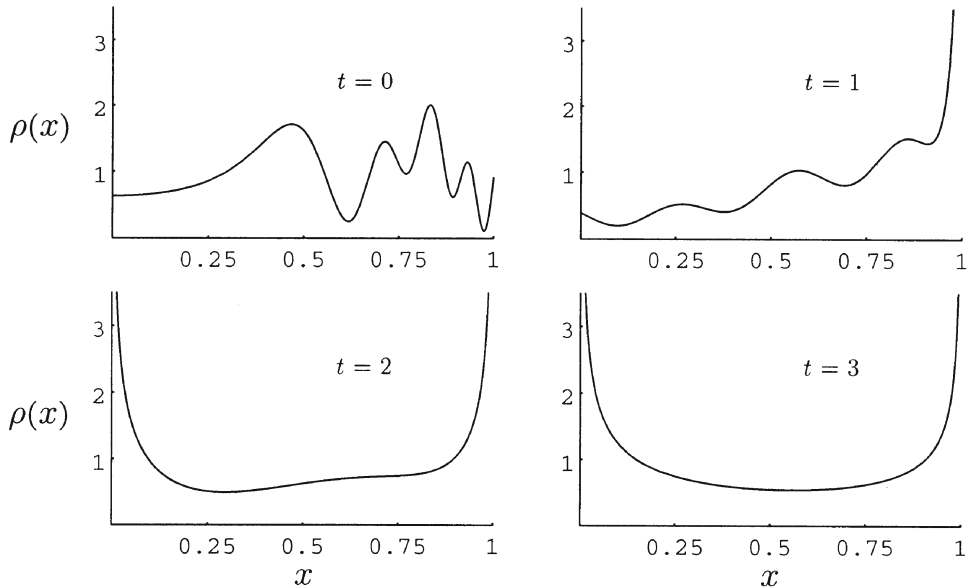


Figure 4.9: Evolution of an initial nonequilibrium density in the logistic map. The nonuniform invariant density, shown in Figure 4.10, is rapidly approached.

It is well known that the logistic map with unit height is conjugate to the tent map $T(x)$, given by (4.3). The conjugating function relating the two maps as in (4.113) is given by

$$\phi(x) = \frac{1}{2} - \frac{1}{2} \cos(\pi x). \quad (4.123)$$

The inverse of this function is

$$\phi^{-1}(x) = \frac{1}{\pi} \arccos(1 - 2x). \quad (4.124)$$

In order to calculate the right eigenstates we need the Frobenius–Perron operator corresponding to ϕ . For that we need

$$\begin{aligned} \left. \frac{d\phi(x')}{dx'} \right|_{x'=\phi^{-1}(x)} &= \frac{\pi}{2} \sin [\arccos(1 - 2x)] \\ &= \frac{\pi}{2} \sqrt{1 - (1 - 2x)^2} = \pi \sqrt{x(1 - x)}. \end{aligned} \quad (4.125)$$

So,

$$U_\phi \rho(x) = \frac{\rho \left(\frac{1}{\pi} \arccos(1 - 2x) \right)}{\pi \sqrt{x(1-x)}}. \quad (4.126)$$

Then from (4.117), using the eigenstates of the tent map from Section 4.1.1, we may obtain the logistic map eigenstates.

First, we obtain the invariant density of the logistic map from the invariant density ($T_0(x) = 1$) of the tent map as

$$S_0(x) = \frac{1}{\pi \sqrt{x(1-x)}}. \quad (4.127)$$

This function is shown in Figure 4.10. The invariant measure, absolutely

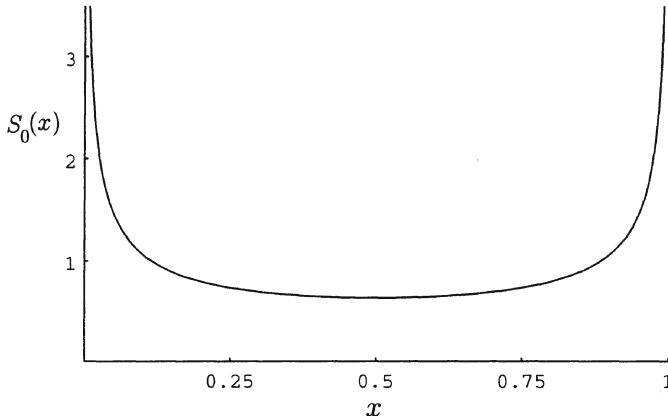


Figure 4.10: The invariant density of the logistic map.

continuous with respect to Lebesgue measure, of the logistic map is thus

$$\mu_{[a,b]} = \int_a^b \frac{dx}{\pi \sqrt{x(1-x)}} = \frac{2}{\pi} \left(\arcsin \sqrt{b} - \arcsin \sqrt{a} \right). \quad (4.128)$$

The decay eigenstates of the logistic map with non-zero eigenvalue are obtained from $T_{2n}(x) = B_{2n}(x/2)$ as

$$S_{2n}(x) = \frac{1}{\pi \sqrt{x(1-x)}} B_{2n} \left[\frac{1}{2\pi} \arccos(1 - 2x) \right]. \quad (4.129)$$

The first two are shown in Figure 4.11.

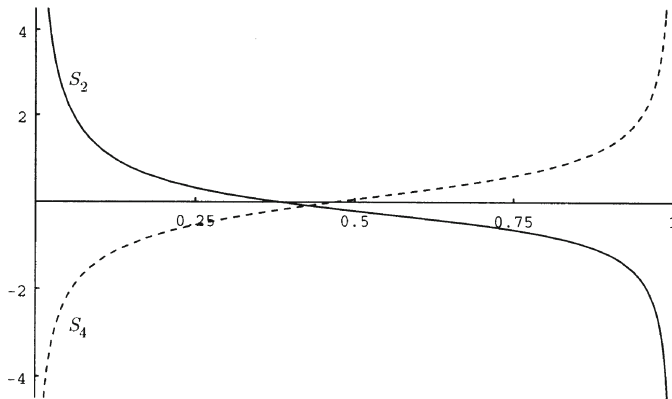


Figure 4.11: The first two decaying eigenstates of the logistic map.

The corresponding left eigenstates, using that $\tilde{T}_{2n}(x) = 2^{2n} \tilde{B}_{2n}(x)$, are

$$\begin{aligned}\tilde{S}_{2n}(x) &= 2^{2n} \tilde{B}_{2n}(\phi^{-1}(x)) \\ &= \frac{(-1)^{2n}}{(2n)!} \left\{ \delta_-^{(2n-1)} \left[\frac{1}{\pi} \arccos(1-2x) - 1 \right] \right. \\ &\quad \left. - \delta_+^{(2n-1)} \left[\frac{1}{\pi} \arccos(1-2x) \right] \right\}. \end{aligned} \tag{4.130}$$

4.4.2 Other Uses of Conjugacy

Some of the results obtained earlier in this chapter may also be obtained using conjugacy. For example, the similarity (4.29a) of the tent map and V map is an expression of the conjugacy of these maps with $1-x$ being the conjugating function corresponding to the reflection operator.

Another interesting use of conjugacy is when there is some self-similarity in a system. This is the case for the tent map with height less than unity at certain specific values of the height. In Appendix A.17 this system is studied and conjugacy is employed to determine its spectral decomposition. This system has the interesting property of being asymptotically periodic in that a general density has persistent oscillating components corresponding to

eigenstates of unit modulus (i.e., n th roots of unity) other than the invariant density.

Bibliographical Notes

The determination of the spectral decomposition of the tent and other maps using symmetry considerations and their relation to the Bernoulli map was given in

- D.J. Driebe and G.E. Ordóñez, “Using symmetries of the Frobenius–Perron operator to determine spectral decompositions,” *Physics Letters A*, **211**, 204 (1996).

The class of multi-branch tent maps, including the N map of Section 4.2.1, was treated using these methods in

- G.E. Ordóñez and D.J. Driebe, “Spectral decomposition of tent maps using symmetry considerations,” *Journal of Statistical Physics*, **84**, 269 (1996).

The simple three-branch map with Jordan blocks discussed in Section 4.2.1 has been analyzed in

- D.J. Driebe, “Jordan blocks in a one-dimensional Markov map,” *Computers and Mathematics with Applications*, **34**, 103 (1997).

The map of Section 4.2.3 with polynomial shift states is discussed in

- D.J. Driebe and G.E. Ordóñez, “Polynomial shift states of a chaotic map,” *Journal of Statistical Physics*, **89**, 1087 (1997).

Jordan block decompositions of one-dimensional maps are also discussed in

- D. Daems, “Non-diagonalizability of the Frobenius–Perron operator and transition between decay modes of the time autocorrelation function,” *Chaos, Solitons & Fractals*, **7**, 1753 (1996).

The singular invariant measures, and the spectral decomposition of the Frobenius–Perron operator with respect to such measures for a class of maps admitting fractal repellors, including the Cantor map, is discussed in

- S. Tasaki, Z. Suchanecki and I. Antoniou, “Ergodic properties of piecewise linear maps on fractal repellors,” *Physics Letters A*, **179** 103 (1993).

A thorough analysis of the generalized spectral decomposition of a class of maps with fractal repellors is in

- S. Tasaki, I. Antoniou and Z. Suchanecki, “Spectral decomposition and fractal eigenvectors for a class of piecewise linear maps,” *Chaos, Solitons & Fractals*, **4**, 227 (1994).

A nice discussion of topological conjugacy on the level of trajectory dynamics is in

- Richard A. Holmgren, *A First Course in Discrete Dynamical Systems*, (Springer, New York, 1996).

The right eigenstates of the logistic map were determined from the tent map eigenstates using conjugacy in

- R.F. Fox, “Unstable evolution of pointwise trajectory solutions to chaotic maps”, *Chaos* **5**, 619, (1995).

A general discussion of a wide class of one-dimensional maps, with a discussion of the zeta function formalism of Ruelle and others and its relation to generalized spectral decompositions is in

- D. MacKernan and G. Nicolis, “Generalized Markov coarse graining and spectral decompositions of chaotic piecewise-linear maps,” *Physical Review E*, **50**, 988, (1994).

Chapter 5

Intrinsic Irreversibility

In this chapter the baker transformation is studied as a paradigm of measure-preserving chaotic systems with invertible trajectory dynamics. We see how the generalized spectral decomposition of the Frobenius–Perron operator yields intrinsically irreversible evolution for densities even though the trajectory dynamics is time reversible.

5.1 The Baker Transformation

The baker map acts in the phase space $M = [0, 1]^2$ of the unit square as

$$S_b(x, y) = \begin{cases} (2x, y/2), & 0 \leq x < \frac{1}{2} \\ (2x - 1, y/2 + 1/2) & \frac{1}{2} \leq x < 1. \end{cases} \quad (5.1)$$

The map is shown in Figure 5.1 acting on a region in phase space. It takes the left half of the unit square, stretches it by a factor of two in the x direction and squeezes it by a factor of $1/2$ in the y direction and then cuts off the right half of the unit square, stretches and squeezes it the same way and puts it on top. The map has a positive Lyapunov exponent of $\log 2$ associated with the stretching in the x direction and a negative Lyapunov exponent of $-\log 2$ associated with the contraction in the y direction. Hence, areas in phase space are preserved under forward evolution. Figure 5.2 shows the trajectory evolution of 100 initial points randomly distributed in a small region of the phase space.

In contrast to the one-dimensional maps we have studied so far, the baker map is one-to-one so that it has an inverse. The inverse of the baker map is

$$S_b^{-1}(x, y) = \begin{cases} (x/2, 2y) & 0 \leq y < \frac{1}{2} \\ (x/2 + 1/2, 2y - 1) & \frac{1}{2} \leq y < 1. \end{cases} \quad (5.2)$$

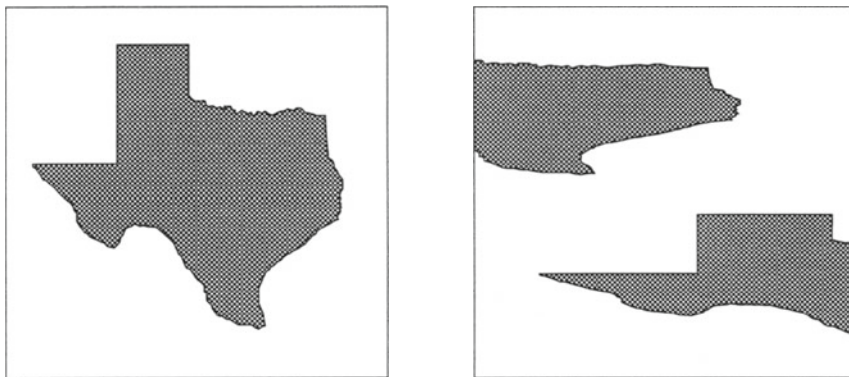


Figure 5.1: The baker map transforming a region of the unit square. Note the stretching, cutting and folding similar to a baker kneading dough.

The baker map preserves two-dimensional Lebesgue measure. Due to its invertibility it is not an exact system, and so the density does not strongly approach to an equilibrium state. But it is a mixing system so that correlations and averages of observables generally approach equilibrium.

The Frobenius-Perron operator of the baker map is given by

$$U_b \rho(x, y) = \rho(S^{-1}(x, y)) = \begin{cases} \rho(x/2, 2y) & 0 \leq y < \frac{1}{2} \\ \rho(x/2 + 1/2, 2y - 1) & \frac{1}{2} \leq y < 1. \end{cases} \quad (5.3)$$

The density uniform over the unit square is the invariant density of U_b . Thus, equilibrium values of correlations or observables are taken with respect to the uniform density. Reasonable (smooth) initial densities with finite support are successively stretched and cut under time evolution of the map and eventually become spread over the unit square so that integration with a reasonable observable and such a density is equivalent, after a long time, to integration with the uniform density.

The Koopman operator, U_b^\dagger , equals U_b^{-1} so that U_b is unitary in the Hilbert space of square integrable functions on $[0, 1]^2$. A complete spectral decomposition of U_b in Hilbert space may thus be constructed with the spectrum continuous and on the unit circle in the complex plane. Since the eigenvalues are of modulus 1 no decay modes and no specific time scales are associated with the decomposition in Hilbert space. In this representation the approach to equilibrium is time-symmetric and appears simply as a phase-mixing process. Only when a specific observable is chosen and its

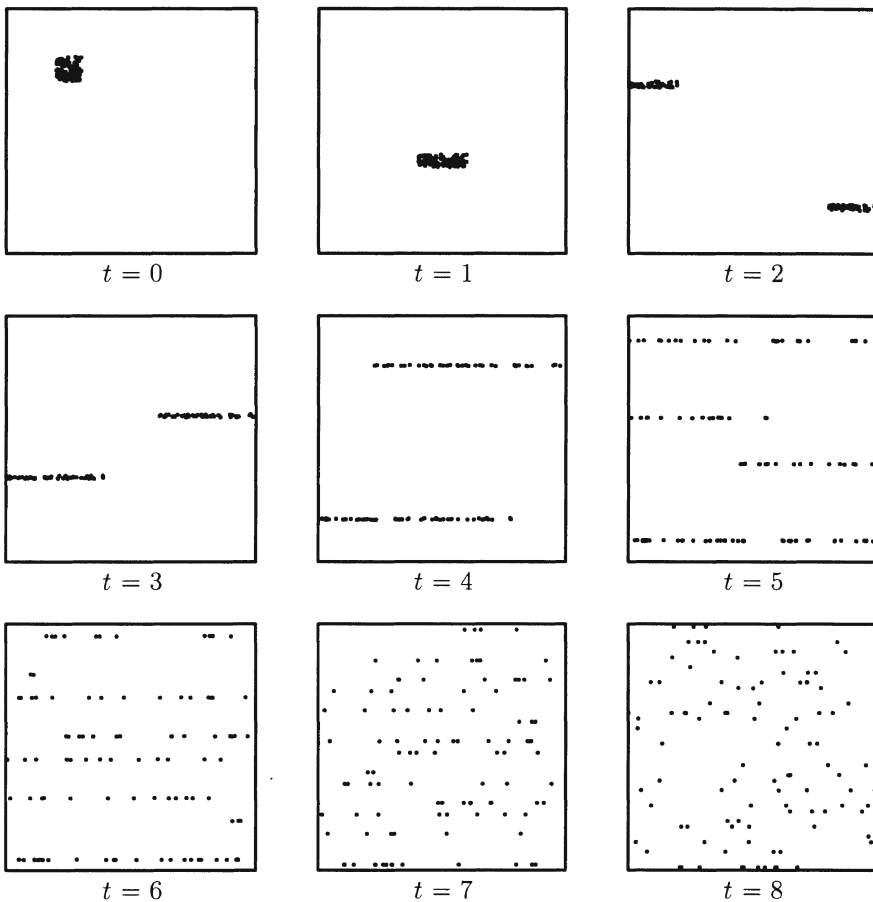


Figure 5.2: The baker map acting on 100 initial points randomly distributed in a small region of the phase space. The evolution tends to distribute the points uniformly over the phase space.

evolution is calculated by weighting it with the density and integrating over the continuous spectrum does a time scale emerge.

For one-dimensional maps we have seen that spectral decompositions in spaces of smooth functions selects the physical time scales associated with approach to equilibrium. Here we will also find that the generalized spectral decomposition of U_b contains the physical time scales and will thereby obtain a decomposition breaking the time-symmetry of the trajectory dynamics.

5.2 The Generalized Spectral Decomposition

It is useful to rewrite the Frobenius–Perron operator as

$$\begin{aligned} U_b \rho(x, y) &= [U_x U_y^\dagger + U_x r(x) r(y) U_y^\dagger] \rho(x, y) \\ &= [U_{b0} + \delta U_b] \rho(x, y), \end{aligned} \quad (5.4)$$

where U_x is the Frobenius–Perron operator of the Bernoulli map acting on the x coordinate, U_y^\dagger is the Koopman operator of the Bernoulli map acting on the y coordinate and $r(x)$ is the first Rademacher function:

$$r(x) \equiv \begin{cases} 1 & 0 \leq x < \frac{1}{2} \\ -1 & \frac{1}{2} \leq x < 1. \end{cases} \quad (5.5)$$

This way of writing U_b is derived in Appendix A.18.

By writing the operator in this form we have explicitly decomposed it into a part, U_{b0} , which is diagonal in the two-dimensional basis formed from direct products of the eigenstates of the Bernoulli map

$$\varphi_{n,m}(x, y) \equiv B_n(x) \tilde{B}_m(y), \quad \tilde{\varphi}_{n,m}(x, y) \equiv \tilde{B}_n(x) B_m(y), \quad (5.6)$$

and a part, δU_b , which is off-diagonal in this basis. The matrix elements of the diagonal part of U_b in this basis are

$$\begin{aligned} (\tilde{\varphi}_{nm}|U_{b0}|\varphi_{n'm'}) &= \int_0^1 dx \int_0^1 dy \tilde{B}_n(x) B_m(y) U_x U_y^\dagger B_{n'}(x) \tilde{B}_{m'}(y) \\ &= \left[\int_0^1 dx \tilde{B}_n(x) U_x B_{n'}(x) \right] \left[\int_0^1 dy \tilde{B}_{m'}(y) U_y B_m(y) \right], \end{aligned} \quad (5.7)$$

where in the second line we used the adjoint relation for the y integral. Now, we just use the fact that the basis states are eigenstates of U_x and U_y and the intertwining relation with the derivative operator to obtain

$$\begin{aligned} (\tilde{\varphi}_{nm}|U_{b0}|\varphi_{n'm'}) &= \left[\frac{1}{2^{n'}} \frac{n'!}{n!(n'-n)!} \int_0^1 dx B_{n'-n}(x) \right] \left[\frac{1}{2^m} \frac{m!}{m'!(m-m')!} \int_0^1 dy B_{m-m'}(y) \right] \\ &= \frac{1}{2^{n+m}} \delta_{nn'} \delta_{mm'}. \end{aligned} \quad (5.8)$$

The diagonal elements are degenerate in that

$$e^{-\gamma_{n+m}} \equiv \frac{1}{2^{n+m}} = \frac{1}{2^j} \quad \text{in } j+1 \text{ ways} \quad (5.9)$$

(e.g., $j = 3 \Rightarrow m = 0, n = 3$; or $m = 1, n = 2$; or $m = 2, n = 1$; or $m = 3, n = 0$).

The off-diagonal matrix elements are given by

$$\begin{aligned}
(\tilde{\varphi}_{nm} | \delta U_b | \varphi_{n'm'}) &= \int_0^1 dx \int_0^1 dy \tilde{B}_n(x) B_m(y) U_x r(x) r(y) U_y^\dagger B_{n'}(x) \tilde{B}_{m'}(y) \\
&= \left[\int_0^1 dx \tilde{B}_n(x) U_x r(x) B_{n'}(x) \right] \left[\int_0^1 dy \tilde{B}_{m'}(y) U_y r(y) B_m(y) \right] \\
&= \begin{cases} e^{-\gamma_{n+m'}} b_{n'-n} b_{m-m'} & n < n' \text{ and } m > m' \\ 0 & \text{otherwise,} \end{cases}
\end{aligned} \tag{5.10}$$

where

$$\begin{aligned}
b_{n'-n} &\equiv \int_0^1 dx \tilde{B}_n(x) r(x) B_{n'}(x) \\
&= \frac{n'!}{n!(n'-n)!} \left[\int_0^{1/2} dx B_{n'-n}(x) - \int_{1/2}^1 dx B_{n'-n}(x) \right] \\
&= \frac{n'!}{n!(n'-n+1)!} \left[2B_{n'-n+1}\left(\frac{1}{2}\right) - B_{n'-n+1}(0) - B_{n'-n+1}(1) \right],
\end{aligned} \tag{5.11}$$

which vanishes for $n' - n$ even but is finite otherwise.

The strict triangularity of the off-diagonal part δU_b gives us the non-recurrence property we had in the one-dimensional maps that enabled us to use an expansion of the resolvent to determine its singularities. Here we have terms with poles up to order $j + 1$ at each eigenvalue $e^{-\gamma_j}$. For example,

$$\begin{aligned}
(\tilde{\varphi}_{0,j} | \left(\frac{1}{z - U_{b0}} \delta U_b \right)^j \frac{1}{z - U_{b0}} | \varphi_{j,0}) &= \frac{1}{z - e^{-\gamma_j}} (\tilde{\varphi}_{0,j} | \delta U_b | \varphi_{1,j-1}) \frac{1}{z - e^{-\gamma_j}} (\tilde{\varphi}_{1,j-1} | \delta U_b | \varphi_{2,j-2}) \\
&\quad \cdots \frac{1}{z - e^{-\gamma_j}} (\tilde{\varphi}_{j-1,1} | \delta U_b | \varphi_{j,0}) \frac{1}{z - e^{-\gamma_j}} \\
&= \frac{(e^{-\gamma_{j-1}} b_1^2)^j}{(z - e^{-\gamma_j})^{j+1}},
\end{aligned} \tag{5.12}$$

where we used that $(\tilde{\varphi}_{n,m} | \delta U_b | \varphi_{n+1,m-1}) = e^{-\gamma_{m-1}} b_1^2$.

Because of the multiple poles, we cannot completely diagonalize the Frobenius-Perron operator U_b but only reduce it to a Jordan block form. Each degenerate eigenvalue belongs to an invariant subspace of dimension $k+1$. The form of the decomposition will thus be

$$U_b = \sum_{k=0}^{\infty} (|\psi_{k,0}\rangle \cdots |\psi_{k,k}\rangle) \begin{pmatrix} e^{-\gamma_k} & 1 & 0 & \cdots & 0 \\ 0 & e^{-\gamma_k} & 1 & \cdots & 0 \\ 0 & 0 & e^{-\gamma_k} & \cdots & 0 \\ \vdots & \vdots & \vdots & \ddots & \vdots \\ 0 & 0 & 0 & \cdots & e^{-\gamma_k} \end{pmatrix} \begin{pmatrix} \langle \tilde{\psi}_{k,0}| \\ \vdots \\ \langle \tilde{\psi}_{k,k}| \end{pmatrix}. \quad (5.13)$$

The right states satisfy

$$\begin{aligned} U_b |\psi_{k,0}\rangle &= e^{-\gamma_k} |\psi_{k,0}\rangle, \\ U_b |\psi_{k,l}\rangle &= e^{-\gamma_k} |\psi_{k,l}\rangle + |\psi_{k,l-1}\rangle, \quad l = 1, 2, \dots, k. \end{aligned} \quad (5.14)$$

These states evolve under successive applications of U_b as

$$U_b^t |\psi_{k,l}\rangle = \sum_{n=0}^{\min\{t,l\}} \frac{t!}{(t-n)!n!} e^{-\gamma_k(t-n)} |\psi_{k,l-n}\rangle. \quad (5.15)$$

This is a generalization of the result (4.67) given for the time evolution of the Jordan states of 2×2 blocks. Here the exponential decay is modified by polynomial factors in t up to t^l for $t > l$. The left states satisfy

$$\begin{aligned} \langle \tilde{\psi}_{k,k}| U_b &= e^{-\gamma_k} \langle \tilde{\psi}_{k,k}|, \\ \langle \tilde{\psi}_{k,l}| U_b &= e^{-\gamma_k} \langle \tilde{\psi}_{k,l}| + \langle \tilde{\psi}_{k,l+1}|, \quad l = 0, 1, \dots, k-1. \end{aligned} \quad (5.16)$$

These states evolve as

$$\langle \tilde{\psi}_{k,l}| U_b^t = \sum_{n=0}^{\min\{t,k\}} \frac{t!}{(t-n)!n!} e^{-\gamma_k(t-n)} \langle \tilde{\psi}_{k,l+n}|. \quad (5.17)$$

In each subspace there is one right eigenstate and one left eigenstate. These are easy to directly determine. Consider U_b acting on a density that is uniform in x , i.e., $\rho(x, y) = \rho(y)$. Then from (5.4) we have

$$\begin{aligned} U_b \rho(y) &= \left\{ U_y^\dagger + \frac{1}{2} \left[r\left(\frac{x}{2}\right) + r\left(\frac{1+x}{2}\right) \right] r(y) U_y^\dagger \right\} \rho(y) \\ &= U_y^\dagger \rho(y), \end{aligned} \quad (5.18)$$

where we used that $r(x/2) + r((1+x)/2) = 1 - 1 = 0$ for $x \in [0, 1]$. Thus, we immediately see that right eigenstates of U_b with eigenvalue $1/2^n$ are $\tilde{B}_n(y)$. Likewise, the left eigenstates of U_b with these eigenvalues are $\tilde{B}_n(x)$. Thus for U_b both the right and left eigenstates are distributions (generalized functions). This property will hold for the Jordan states as well. This means that the generalized spectral decomposition of U_b is not to be used like the one-dimensional maps to decompose a density itself. Here the decomposition corresponds to writing U_b in terms of bi-distributions that map a density and observable or the correlation of two observables to a real number.

Note that the Bernoulli map is not recovered by considering U_b acting on a density that is uniform in y . Such a density, if it is not uniform in x as well, will eventually become non-uniform in y . The Bernoulli map is recovered¹ by integrating over the y coordinate, i.e., essentially doing a reduction of the density or a projection as

$$\begin{aligned} \int_0^1 dy U_b \rho(x, y) &= \int_0^1 dy U_x [1 + r(x)r(y)] U_y^\dagger \rho(x, y) \\ &= U_x \rho_R(x), \end{aligned} \quad (5.19)$$

where $\rho_R(x) \equiv \int_0^1 dy \rho(x, y)$ and we used (by considering U_y^\dagger acting to the left in the first line) that $U_y 1 = 1$ and $U_y r(y) = 0$. Of course, this projection does not commute with U_b , since integrating over the y coordinate leads to a noninvertible evolution rule. Thus, irreversibility after this projection is trivial. The surprising fact is that it is possible to construct an exact irreversible representation, with corresponding decay modes, of the full operator U_b .

The first right Jordan states in each block may be expected to be linear in x , but still distributions in y . Thus, we take as an ansatz for such states

$$\psi_{k,1}(x, y) = \tilde{C}_k(y) + x \tilde{D}_k(y). \quad (5.20)$$

To determine $\tilde{C}_k(y)$ and $\tilde{D}_k(y)$ we use that $\psi_{k,1}(x, y)$ must satisfy

$$U_b \psi_{k,1}(x, y) = \frac{1}{2^k} \psi_{k,1}(x, y) + \psi_{k,0}(x, y), \quad (5.21)$$

where $\psi_{k,0}(x, y) = \tilde{B}_k(y)$ is the right eigenstate of order k as determined above. Now,

$$U_b \psi_{k,1}(x, y) = [U_x U_y^\dagger + U_x r(x)r(y) U_y^\dagger] [\tilde{C}_k(y) + x \tilde{D}_k(y)]$$

¹The baker transformation is a so-called K-automorphism (K after Kolmogorov), which has the property of being factored into a product of transformations, one of which is an exact transformation. The exact factor of the baker map is the Bernoulli map.

$$= U_y^\dagger \tilde{C}_k(y) + \frac{1}{4}[1 - r(y)]U_y^\dagger \tilde{D}_k(y) + \frac{x}{2}U_y^\dagger \tilde{D}_k(y). \quad (5.22)$$

Then, imposing (5.21) and identifying the coefficients of the terms in x^0 and x^1 gives the two equations

$$U_y^\dagger \tilde{C}_k(y) + \frac{1}{4}[1 - r(y)]U_y^\dagger \tilde{D}_k(y) = \frac{1}{2^k} \tilde{C}_k(y) + \tilde{B}_k(y) \quad (5.23a)$$

$$U_y^\dagger \tilde{D}_k(y) = \frac{1}{2^{k-1}} \tilde{D}_k(y) \quad (5.23b)$$

Equation (5.23b) is immediately solved by inspection as

$$\tilde{D}_k(y) = d\tilde{B}_{k-1}(y), \quad (5.24)$$

where d is a constant to be fixed in the solution of (5.23a). To solve (5.23a) for $\tilde{C}_k(y)$ we use the solution for $\tilde{D}_k(y)$ and then rewrite it by acting on an arbitrary function $f(y)$ and integrating over y as

$$\begin{aligned} \int_0^1 dy [U_y^\dagger \tilde{C}_k(y)]f(y) + \frac{d}{4} \int_0^1 dy [1 - r(y)][U_y^\dagger \tilde{B}_{k-1}(y)]f(y) \\ = \frac{1}{2^k} \int_0^1 dy \tilde{C}_k(y)f(y) + \int_0^1 dy \tilde{B}_k(y)f(y). \end{aligned} \quad (5.25)$$

We then expand $\tilde{C}_k(y)$ in terms of $\tilde{B}_k(y)$ as

$$\tilde{C}_k(y) = \sum_{m=k-1}^{\infty} c_m \tilde{B}_m(y), \quad (5.26)$$

where it is clear from (5.25) that the expansion begins at $m = k - 1$. In order to use (5.26) in (5.25) we have to rewrite the second term on the left hand side of (5.25) in terms of $\tilde{B}_m(y)$ itself. This term is

$$\begin{aligned} \int_0^1 dy [1 - r(y)][U_y^\dagger \tilde{B}_{k-1}(y)]f(y) &= 2 \int_{1/2}^1 dy [U_y^\dagger \tilde{B}_{k-1}(y)]f(y) \\ &= \int_0^1 dy \tilde{B}_{k-1}(y)f(\frac{1+y}{2}). \end{aligned} \quad (5.27)$$

Now we use an Euler–Maclaurin expansion of $f((1+y)/2)$ as

$$\begin{aligned} \int_0^1 dy \tilde{B}_{k-1}(y)f(\frac{1+y}{2}) &= \int_0^1 dy \tilde{B}_{k-1}(y) \sum_{m=0}^{\infty} B_m(\frac{1+y}{2}) \langle \tilde{B}_m | f \rangle \\ &= \sum_{m=0}^{\infty} \int_0^1 dy \tilde{B}_{k-1}(y) B_m(\frac{1+y}{2}) \langle \tilde{B}_m | f \rangle. \end{aligned} \quad (5.28)$$

The integration evaluates to

$$\begin{aligned} a_{n,m} &\equiv \int_0^1 dy \tilde{B}_n(y) B_m\left(\frac{1+y}{2}\right) \\ &= \frac{1}{2^{n-1}} \frac{m!}{n!(m-n+1)!} [B_{m-n+1}(1) - B_{m-n+1}\left(\frac{1}{2}\right)], \end{aligned} \quad (5.29)$$

for $m \geq k$ and equals zero otherwise. Thus,

$$\int_0^1 dy \tilde{B}_{k-1}(y) f\left(\frac{1+y}{2}\right) = \sum_{m=k-1}^{\infty} a_{k-1,m} \int_0^1 dy \tilde{B}_m(y) f(y). \quad (5.30)$$

Then using (5.26) in (5.25) with (5.30) we may rewrite (5.25) as

$$\sum_{m=k-1}^{\infty} c_m \frac{\tilde{B}_m(y)}{2^m} + \frac{d}{4} \sum_{m=k-1}^{\infty} a_{k-1,m} \tilde{B}_m(y) = \frac{1}{2^k} \sum_{m=k-1}^{\infty} c_m \tilde{B}_m(y) + \tilde{B}_k \quad (5.31)$$

and get a series of equations for c_m with m starting at $k-1$.

First for $m = k-1$

$$\frac{c_{k-1}}{2^{k-1}} + \frac{d}{4} a_{k-1,k-1} = \frac{1}{2^k} c_{k-1}, \quad (5.32)$$

so that

$$c_{k-1} = \frac{(d/4)a_{k-1,k-1}}{2^{-k} - 2^{-k+1}}. \quad (5.33)$$

For $m = k$ we have

$$\frac{c_k}{2^k} + \frac{d}{4} a_{k-1,k} = \frac{1}{2^k} c_k + 1, \quad (5.34)$$

so that

$$d = \frac{4}{a_{k-1,k}} = \frac{2^{k+3}}{k}, \quad (5.35)$$

and c_k is arbitrary. The arbitrariness of c_k is used to fix the orthogonality of $\psi_{k,1}(x, y)$ with the left states. For $m \geq k+1$ we have

$$\frac{c_m}{2^m} + \frac{d}{4} a_{k-1,m} = \frac{1}{2^k} c_m, \quad (5.36)$$

so that

$$c_m = \frac{(d/4)a_{k-1,m}}{2^{-k} - 2^{-m}}, \quad (5.37)$$

completing the construction of $\psi_{k,1}(x, y)$.

The higher order Jordan states may be obtained in a similar manner. The left states may be obtained from the right states simply by interchanging x and y .

5.3 Irreversibility and Test Spaces

As noted, the spectrum of U_b in Hilbert space is on the unit circle. This means that the resolvent of U_b will have a cut on the unit circle. Eigenvalues of U_b inside the unit circle correspond to an analytic continuation of the resolvent from outside the unit circle where it is analytic, to inside where it has poles. To illustrate this assertion consider the matrix element of the resolvent

$$R_1(z) \equiv (\tilde{B}_1, B_1 | (z - U_b)^{-1} | B_1, \tilde{B}_1). \quad (5.38)$$

Since $(\tilde{B}_1, B_1 | U_b | B_1, \tilde{B}_1) = 1/4$ we have that for $|z| > 1$

$$\begin{aligned} R_1^+(z) &= \frac{1}{z} (\tilde{B}_1, B_1 | \frac{1}{1 - \frac{U_b}{z}} | B_1, \tilde{B}_1) \\ &= \frac{1}{z} \sum_{n=0}^{\infty} \frac{1}{z^n} [(\tilde{B}_1, B_1 | U_b | B_1, \tilde{B}_1)]^n \\ &= \frac{1}{z} \sum_{n=0}^{\infty} \left(\frac{1}{4z} \right)^n = \frac{1}{z} \frac{1}{1 - \frac{1}{4z}} = \frac{1}{z - \frac{1}{4}}, \end{aligned} \quad (5.39)$$

showing that $R_1^+(z)$ is regular for $|z| > 1$ but that it has a pole inside the unit circle at $z = 1/4$. For $|z| < 1$ we have that

$$\begin{aligned} R_1^-(z) &= (\tilde{B}_1, B_1 | \frac{1}{U_b} \frac{1}{\frac{z}{U_b} - 1} | B_1, \tilde{B}_1) \\ &= -(\tilde{B}_1, B_1 | U_b^{-1} \sum_{n=0}^{\infty} (z U_b^{-1})^n | B_1, \tilde{B}_1) \\ &= -\sum_{n=0}^{\infty} \frac{1}{4} \left(\frac{z}{4} \right)^n = -\frac{1}{4} \frac{1}{1 - \frac{z}{4}} = \frac{1}{z - 4}, \end{aligned} \quad (5.40)$$

so that this branch of $R_1(z)$ is regular inside the unit circle but it has a pole at $z = 4$. The location of this pole outside of the unit circle corresponds to an eigenvalue in the spectral decomposition of U_b^{-1} , i.e., the semi-group corresponding to an approach to equilibrium in the past.

The decomposition given in the previous section of the baker map in terms of decaying contributions gives an approach to equilibrium for $t > 0$. As we mentioned, a spectral decomposition of the baker map may be performed in the Hilbert space $L_x^2 \otimes L_y^2$ (i.e., direct product of the functional spaces of square-integrable functions in x and y on $[0, 1]$) but then we would only obtain eigenvalues of modulus 1. The decaying contributions we have obtained, with eigenvalues $e^{-\gamma_n} = 2^{-n}$, do not appear in the Hilbert space

decomposition. This result is more striking than what we have seen for the one-dimensional maps, such as the Bernoulli map, where the generalized decomposition selects eigenstates with eigenvalues already included in the continuous spectrum.

The right and left eigenvectors and Jordan vectors of the generalized spectral decomposition are linear functionals over the spaces $L_x^2 \otimes \mathcal{P}_y$ and $\mathcal{P}_x \otimes L_y^2$ respectively (\mathcal{P}_x denotes the test space of functions expandable in terms of polynomials in x).² Thus U_b acts on functions in $\mathcal{P}_x \otimes L_y^2$ and gives another function in that space, i.e., it preserves smoothness in x (but not in y). On the contrary, if $U_b^\dagger (= U_b^{-1})$ acts on functions in this space it will eventually take them out of the space. The generalized spectral decomposition of U_b for a correlation $(f|(U_b)^t|g)$ is valid (with explicit decay modes for $t > 0$) for $f \in L_x^2 \otimes \mathcal{P}_y$ and $g \in \mathcal{P}_x \otimes L_y^2$. The generalized spectral decomposition of U_b^{-1} for a correlation $(f|(U_b^{-1})^t|g)$ is valid for $f \in \mathcal{P}_x \otimes L_y^2$ and $g \in L_x^2 \otimes \mathcal{P}_y$.

Thus the decomposition of U_b^t in terms of decay modes for densities in $L_x^2 \otimes \mathcal{P}_y$ has meaning only for $t > 0$. There is a distinct space of densities for which there is a decomposition of U_b^{-1} in terms of decay modes for $t < 0$ only. Thus, the group evolution of the Hilbert space decomposition splits into two distinct semi-groups in the generalized decomposition; the forward semi-group and the backward semi-group.

The baker map doesn't mix the x and y coordinates because the unstable and stable manifolds are just along these directions. In a more general setting, the distributions of the generalized spectral decomposition will involve the coordinate system defined by the unstable and stable manifolds and may in practice be a quite complicated function of the primary phase space coordinates of the system. In any event, the basic features we have found here can be applied to more general situations. The main result is that time symmetry breaking is manifest in the generalized spectral representation for densities and observables satisfying the appropriate physical conditions of smoothness.

Bibliographic Notes

The straightforward construction of the Jordan states given in Section 5.2 follows the *Chaos* paper of Gaspard cited in Chapter 2. The generalized spectral decomposition of the baker map, using subdynamics, is given in the *Physical Review* paper of

²Of course, more precise descriptions of the test spaces may be determined as was discussed in Section 3.6 for the Bernoulli map.

Hasegawa and Saphir cited in Chapter 3. The discussion of the analytic continuation of the resolvent in Section 5.3 is adapted from this paper. A decomposition in terms of Jordan states using subdynamics is given in

- I. Antoniou and S. Tasaki, “Generalized spectral decompostion of the β -adic baker’s transformation and intrinsic irreversibility,” *Physica A*, **190**, 303 (1992).

Fox has reproduced the the generalized spectral decomposition of the baker map using matrix manipulation in

- R. F. Fox, “Construction of the Jordan basis for the baker map,” *Chaos*, **7**, 254 (1997).

Another popular model of chaotic invertible dynamics is the Arnold cat map. It too has a generalized spectral decomposition that splits into two semi-groups. It is given in

- I. Antoniou, B. Qiao and Z. Suchanecki, “Generalized spectral decompositi-
tion and intrinsic irreversibility of the Arnold cat map,” *Chaos, Solitons &
Fractals*, **8**, 77 (1997).

Chapter 6

Deterministic Diffusion

In this chapter a simple model of deterministic diffusion is discussed. This system has more interesting physical features than the maps discussed so far in this book. The transport property of diffusion is seen explicitly as an element of the exact time evolution. The eigendistributions for this system also have interesting fractal features.

6.1 Dynamics of Diffusion

Diffusion is a simple transport property present in many nonequilibrium systems. Diffusive processes in nature are usually associated with systems consisting of a very large number of particles. Such is the case in the classic example of Brownian motion where a tagged particle is immersed in a medium of particles (a fluid) and the tagged particle is kicked by the random thermal motion of the particles of the medium. The tagged particle thus traverses an erratic zigzag path. The characteristic feature of diffusive motion is that the average of the square of the distance traversed is directly proportional to time. The proportionality factor defines the diffusion coefficient.

A first-principles theoretical approach to diffusion in a fluid or gas system starts with the Liouville equation. Then several steps are performed. First, reduction to the Boltzmann equation governing the one-particle distribution function. Then assuming the system is close to equilibrium a linearization of the Boltzmann equation is made. Finally, a limiting procedure (the so-called hydrodynamic limit) to select large-space scale inhomogeneities and long time-scale processes is performed. Even though one then obtains the diffusion equation, with a diffusion coefficient as a function of the microscopic

parameters, it is not entirely clear how to understand the diffusion process if the above steps are not carried out. In other words, is the irreversible process of diffusion dependent on the macroscopic character of the observation of it or is it an intrinsic element of the underlying dynamics? Is the diffusion coefficient contained explicitly in the spectrum of the full time evolution operator? In fluid systems these questions involve many-body dynamics and the thermodynamic limit. Here we are interested in the basic mechanism of the underlying instability of motion, i.e., the chaotic dynamics driving the diffusive process.

In order to investigate diffusion as a dynamical property, Gaspard introduced the two-dimensional multibaker map, a conservative system with unitary time evolution, which couples a chain of baker transformations to induce diffusion. We will discuss the full multibaker transformation later in this chapter. First we study the one-dimensional projection that governs the stretching dynamics of the multibaker map. It is in this dimension that the diffusion occurs so we will obtain most of the relevant features of the dynamics of the full multibaker map through a study of this one-dimensional map, which is called the multi-Bernoulli map.

Before turning to a detailed investigation of the model, consider the phenomenological diffusion equation

$$\frac{\partial n(x, t)}{\partial t} = D \frac{\partial^2 n(x, t)}{\partial x^2}, \quad (6.1)$$

on the interval $[0, L]$ with periodic boundary conditions. Then, introducing Fourier modes, $n_k(t)$, as

$$n(x, t) = \sum_{k=-\infty}^{\infty} e^{i \frac{2\pi}{L} kx} n_k(t), \quad (6.2)$$

the diffusion equation in wavenumber space becomes

$$\frac{\partial n_k(t)}{\partial t} = -D \left(\frac{2\pi k}{L} \right)^2 n_k(t), \quad (6.3)$$

which is immediately solved by

$$n_k(t) = e^{-D(\frac{2\pi k}{L})^2 t} n_k(0). \quad (6.4)$$

Thus, diffusion implies exponential decay modes in wavenumber space. These modes, as well as other more quick decay modes, will be determined directly from the generalized spectral decomposition of the model system we will consider.

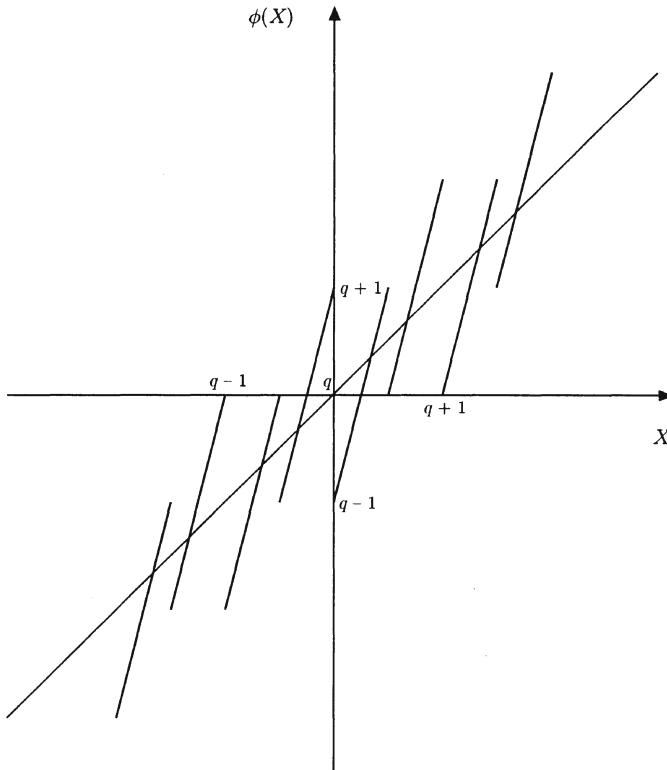


Figure 6.1: The multi-Bernoulli map. A line representing the identity map is also drawn for guidance.

6.2 The Multi-Bernoulli Map

The multi-Bernoulli map is given by the rule, $X_{t+1} = \phi(X_t)$, where

$$\phi(X) = \begin{cases} 4X - 3q - 1, & q \leq X < q + \frac{1}{2} \\ 4X - 3q - 2, & q + \frac{1}{2} \leq X < q + 1. \end{cases} \quad (6.5)$$

The coordinate X takes values along the real line and q is an integer, i.e., this map doesn't operate just in the unit interval, like the one-dimensional maps we have already considered, but on many intervals. The map is illustrated in Figure 6.1. We may consider the map on the whole real axis but for convenience we will later consider it on the interval $[0, L)$, where L is an integer, with periodic boundary conditions.

To get a feeling for how iterates behave in this map it is useful to decompose X into its integer, q , and fractional, x , parts as $X = q + x$, where $q = [X]$ and $x = X - [X]$ ($[\cdot]$ here and where it is clear from the context denotes the integer part of \cdot). The rule for the map is then

$$\phi(q+x) = \begin{cases} 4(q+x) - 3q - 1, & 0 \leq x < \frac{1}{2} \\ 4(q+x) - 3q - 2, & \frac{1}{2} \leq x < 1, \end{cases} \quad (6.6)$$

or

$$q_{t+1} + x_{t+1} = \begin{cases} 4x_t + q_t - 1, & 0 \leq x_t < \frac{1}{2} \\ 4x_t + q_t - 2, & \frac{1}{2} \leq x_t < 1. \end{cases} \quad (6.7)$$

Thus, the integer part of the iterate evolves as

$$q_{t+1} = [q_{t+1} + x_{t+1}] = \begin{cases} q_t - 1, & 0 \leq x_t < \frac{1}{4} \\ q_t, & \frac{1}{4} \leq x_t < \frac{3}{4} \\ q_t + 1, & \frac{3}{4} \leq x_t < 1. \end{cases} \quad (6.8)$$

Hence, the difference of the integer part of the iterate at two successive time steps is governed by a simple rule depending on the fractional part at the first time as

$$q_{t+1} - q_t \equiv \Delta(x_t) = \begin{cases} -1, & 0 \leq x_t < \frac{1}{4} \\ 0, & \frac{1}{4} \leq x_t < \frac{3}{4} \\ 1, & \frac{3}{4} \leq x_t < 1. \end{cases} \quad (6.9)$$

The fractional part obeys the rule

$$x_{t+1} = q_{t+1} + x_{t+1} - [q_{t+1} + x_{t+1}] = 4x_t \bmod 1 \equiv g(x_t). \quad (6.10)$$

So we see that the multi-Bernoulli map may be considered as two coupled dynamical laws. A 4-adic map governing x_t and the law, $\Delta(x_t)$, for q_t , which just produces jumps based on the input x_t . These two rules are depicted in Figure 6.2.

The x_t dynamics we know will produce over long times an essentially random input uniformly distributed over $[0, 1]$ to the jump map for q_t so it is reasonable to expect q_t to behave diffusively since from this point of view it is governed by a rule like a random walk (with probability $\frac{1}{2}$ to stay at a site and probability $\frac{1}{4}$ to jump to the right and $\frac{1}{4}$ to jump to the left). It is shown in many textbooks that such a process yields in a hydrodynamic limit of long times and large spatial extent the diffusion equation with diffusion coefficient of $1/4$. (In Appendix A.19 this diffusion coefficient is determined for the multi-Bernoulli map using a Green–Kubo formalism.)

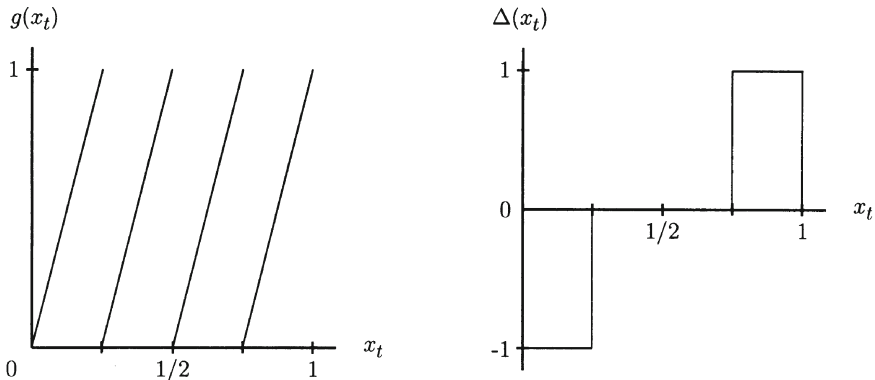


Figure 6.2: The two coupled maps, (6.9) and (6.10), equivalent to the multi-Bernoulli map.

We will show now from construction of the generalized spectral representation for this map that the diffusion coefficient, as well as all higher-order decay rates, are explicitly incorporated in the exact spectrum of the full time evolution operator of the system. We will also determine the modes (eigenstates) associated with the decay components.

6.3 The Generalized Spectral Decomposition

The Frobenius-Perron operator for the multi-Bernoulli map acts on a probability density as

$$\begin{aligned} U_{\text{mB}}\rho(q+x, t) = & \frac{1}{4} \left[\rho(q+1+\frac{x}{4}, t) + \rho(q+\frac{x}{4}+\frac{1}{4}, t) \right. \\ & + \rho(q+\frac{x}{4}+\frac{1}{2}, t) + \rho(q-1+\frac{x}{4}+\frac{3}{4}, t) \left. \right]. \end{aligned} \quad (6.11)$$

The determination of this operator from the rule (6.5) is given in Appendix A.20. The evolution of an initial probability density supported mainly in one cell is shown in Figure 6.3. Diffusion of the iterates, discussed qualitatively in the previous section, manifests itself as a spreading of the density. Besides the global approach to equilibrium by the spreading there is also a quick approach to local equilibrium (uniformity) in each cell.

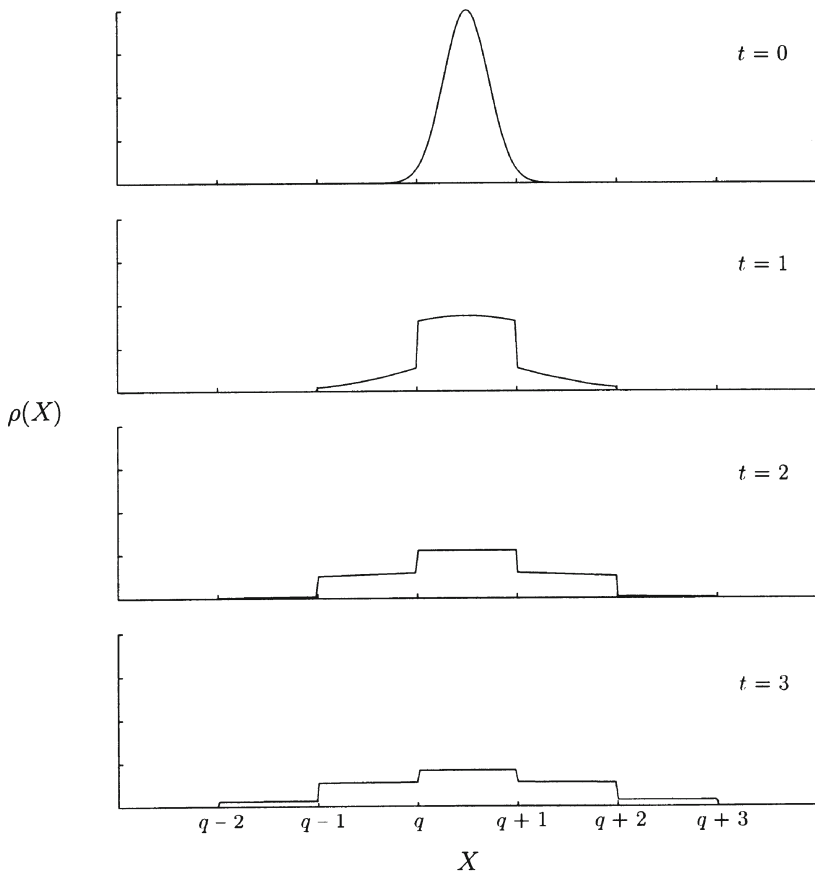


Figure 6.3: The evolution under the multi-Bernoulli map of a density, supported mainly in one cell at $t = 0$. Besides the spreading of the density note the rapid approach to uniformity in each cell.

Considering the system on the interval $(0, L]$ with periodic boundary conditions, we may separate the dynamics among unit intervals (i.e., in the variable q) from the internal motion (in x) through the discrete Fourier transform with respect to q as

$$\rho(q + x, t) = \frac{1}{\sqrt{L}} \sum_{s=0}^{L-1} e^{i \frac{2\pi}{L} qs} \rho_s(x, t), \quad (6.12a)$$

where the inverse transform is

$$\rho_s(x, t) = \frac{1}{\sqrt{L}} \sum_{q=0}^{L-1} e^{-i\frac{2\pi}{L}qs} \rho(q+x, t). \quad (6.12b)$$

This is a discrete transform because both q and the conjugate variable s are discrete. Introducing this transformation is natural because the map is translationally invariant, i.e., $U_{\text{mB}}T = TU_{\text{mB}}$ where $T\rho(X) \equiv \rho(X+1)$. The transformation (6.12b) projects onto the eigenspaces of T .

Taking the transform of (6.11) the modes ρ_s are seen to evolve independently as

$$\begin{aligned} \rho_s(x, t+1) &= \frac{1}{4} \left[e^{i\frac{2\pi}{L}s} \rho_s \left(\frac{x}{4}, t \right) + \rho_s \left(\frac{1+x}{4}, t \right) \right. \\ &\quad \left. + \rho_s \left(\frac{2+x}{4}, t \right) + e^{-i\frac{2\pi}{L}s} \rho_s \left(\frac{3+x}{4}, t \right) \right] \equiv U_s^2 \rho_s(x, t). \end{aligned} \quad (6.13)$$

The operator defining this transformation has been written as U_s^2 since it is equivalent to two successive applications of the operator U_s , where

$$U_s \rho_s(x, t) = \frac{1}{2} \left[e^{i\frac{\pi}{L}s} \rho_s \left(\frac{x}{2}, t \right) + e^{-i\frac{\pi}{L}s} \rho_s \left(\frac{1+x}{2}, t \right) \right]. \quad (6.14)$$

We will work with U_s because it is simpler and its eigenvectors will be the same as those of the operator that advances ρ_s by a full time step. (To see this suppose an operator V has eigenstates ϕ_λ as $V\phi_\lambda = \lambda\phi_\lambda$. Then $V^2\phi_\lambda = \lambda V\phi_\lambda = \lambda^2\phi_\lambda$.)

By introducing the discrete transform we have thus decomposed the evolution of the density under the multi-Bernoulli map as

$$\rho(q+x, t) = U_{\text{mB}}^t \rho(q+x, 0) = \frac{1}{\sqrt{L}} \sum_{s=0}^{L-1} e^{i\frac{2\pi}{L}qs} U_s^{2t} \rho_s(x, 0). \quad (6.15)$$

The fact that the ρ_s modes are independently evolving means that we have block diagonalized U_{mB} already. We will now diagonalize the blocks, coming from the matrix representation of U_s for each value of s , by constructing the generalized spectral representation of U_s .

The action of U_s differs from the Frobenius–Perron operator of the Bernoulli map only by the s -dependent phase factors, and is identical to it for $s = 0$.

This motivates us to write U_s in terms of U_B . From (6.14)

$$\begin{aligned} U_s \rho_s(x) &= \cos\left(\frac{\pi s}{L}\right) \left\{ \frac{1}{2} \left[\rho_s\left(\frac{x}{2}\right) + \rho_s\left(\frac{1+x}{2}\right) \right] \right. \\ &\quad \left. + i \tan\left(\frac{\pi s}{L}\right) \frac{1}{2} \left[\rho_s\left(\frac{x}{2}\right) - \rho_s\left(\frac{1+x}{2}\right) \right] \right\} \\ &= \cos\left(\frac{\pi s}{L}\right) U_B \left[1 + i \tan\left(\frac{\pi s}{L}\right) r(x) \right] \rho_s(x), \end{aligned} \quad (6.16)$$

where $r(x)$ is the Rademacher function defined in (5.5). In this way U_s is written in terms of its diagonal and off-diagonal parts with respect to the Bernoulli basis, i.e., $U_s = U_{s0} + \delta U_s$, where

$$\begin{aligned} U_{s0} &= \cos\left(\frac{\pi s}{L}\right) U_B, \\ \delta U_s &= i \sin\left(\frac{\pi s}{L}\right) U_B r(x). \end{aligned} \quad (6.17)$$

Their matrix elements in the Bernoulli basis are

$$\begin{aligned} \langle \tilde{B}_m | U_{s0} | B_n \rangle &= \frac{\cos\left(\frac{\pi s}{L}\right)}{2^m} \delta_{m,n}, \\ \langle \tilde{B}_m | \delta U_s | B_n \rangle &= i \sin\left(\frac{\pi s}{L}\right) b_{n-m}, \end{aligned} \quad (6.18)$$

where $b_{n-m} = 0$ if $m \geq n$ and for $m < n$ it is given by (5.11). We again have upper-triangularity and non-degenerate eigenvalues so the analysis of the resolvent proceeds as we have seen before to yield simple poles at the eigenvalues

$$e^{-\gamma_s^{(n)}} \equiv \frac{\cos\left(\frac{\pi s}{L}\right)}{2^n}. \quad (6.19)$$

Formal expressions for the right and left eigenstates of U_s in terms of the Bernoulli basis are

$$|\gamma_s^{(m)}\rangle = \left(1 + \frac{1}{e^{-\gamma_s^{(m)}} - U_s} \delta U_s \right) |B_m\rangle, \quad (6.20)$$

and

$$\langle \tilde{\gamma}_s^{(m)} | = \langle \tilde{B}_m | \left(1 + \delta U_s \frac{1}{e^{-\gamma_s^{(m)}} - U_s} \right). \quad (6.21)$$

Explicit evaluation of the right eigenstates of U_s yields for the first four,

$$\begin{aligned}\gamma_s^{(0)}(x) &= 1 \\ \gamma_s^{(1)}(x) &= x - \frac{1}{2} + \frac{1}{2}i \tan\left(\frac{\pi s}{L}\right) \\ \gamma_s^{(2)}(x) &= x^2 - x + \frac{1}{6} + (x - \frac{1}{2})i \tan\left(\frac{\pi s}{L}\right) + \frac{1}{3}i^2 \tan^2\left(\frac{\pi s}{L}\right) \\ \gamma_s^{(3)}(x) &= x^3 - \frac{3}{2}x^2 + \frac{1}{2}x + \frac{3}{2}(x^2 - x - \frac{1}{7})i \tan\left(\frac{\pi s}{L}\right) \\ &\quad + (x - \frac{1}{2})i^2 \tan^2\left(\frac{\pi s}{L}\right) + \frac{2}{7}i^3 \tan^3\left(\frac{\pi s}{L}\right)\end{aligned}\quad (6.22)$$

Note that for $s = 0$ we recover the Bernoulli polynomials (3.39). The explicit left eigenstates will be considered later in Section 6.5. We have diagonalized U_s and thus obtained a spectral decomposition of U_{mB} as

$$U_{\text{mB}}\rho(q+x) = \frac{1}{\sqrt{L}} \sum_{s=0}^{L-1} \sum_{m=0}^{\infty} e^{i\frac{2\pi}{L}qs} e^{-2\gamma_s^{(m)}} \gamma_s^{(m)}(x) \langle \tilde{\gamma}_s^{(m)} | \rho_s \rangle. \quad (6.23)$$

The eigenstates, $\Gamma^{(s,m)}(q+x)$, of the Frobenius-Perron operator U_{mB} of the full multi-Bernoulli map are obtained from the eigenstates, $\gamma_s^{(m)}$, of U_s as (see Appendix A.21 for the proof)

$$\Gamma^{(s,m)}(q+x) = \frac{1}{\sqrt{L}} e^{i\frac{2\pi}{L}qs} \gamma_s^{(m)}(x), \quad (6.24)$$

with the same relation holding for the left eigenstates (the sign of i *does not change*). This relation may seem a bit mysterious as s and q are conjugate variables but are appearing together. In fact, the s appearing in the above expression is a label for the eigenstate, and the eigenstates of the full multi-Bernoulli map require two labels, s and m , due to the periodicity of the system. We may thus, for an infinitely differentiable $\rho_s(x,0)$, write the spectral decomposition of U_{mB} as

$$U_{\text{mB}}^t \rho(q+x) = \sum_{s=0}^{L-1} \sum_{m=0}^{\infty} e^{-\Gamma^{(s,m)} t} \Gamma^{(s,m)}(q+x) \langle \tilde{\Gamma}^{(s,m)} | \rho \rangle, \quad (6.25)$$

where the left eigenfunctional is here defined on the full map as

$$\langle \tilde{\Gamma}^{(s,m)} | \rho \rangle = \sum_{q=0}^{L-1} \int_0^1 dx \tilde{\Gamma}^{*(s,m)}(q+x) \rho(q+x). \quad (6.26)$$

The eigenvalues, $e^{-\Gamma^{(s,m)}}$, of the Frobenius–Perron operator of the full multi-Bernoulli map, U_{mB} , are the squares of those of the operator U_s , i.e.,

$$e^{-\Gamma^{(s,m)}} = e^{-2\gamma_s^{(m)}} = \frac{\cos^2(\frac{\pi s}{L})}{4^m}. \quad (6.27)$$

Since s and $L - s$ have the same eigenvalue real eigenstates of the Frobenius–Perron operator of the full multi-Bernoulli map may be obtained as

$$\hat{\Gamma}^{(s,m)}(q + x) \equiv \frac{1}{2}[\Gamma^{(s,m)}(q + x) + \Gamma^{(L-s,m)}(q + x)], \quad (6.28a)$$

and

$$\check{\Gamma}^{(s,m)}(q + x) \equiv \frac{1}{2i}[\Gamma^{(s,m)}(q + x) - \Gamma^{(L-s,m)}(q + x)]. \quad (6.28b)$$

The first three $\hat{\Gamma}^{(s,m)}(q + x)$ are

$$\begin{aligned} \hat{\Gamma}^{(s,0)}(q + x) &= \frac{1}{\sqrt{L}} \cos\left(\frac{2\pi}{L}qs\right) \\ \hat{\Gamma}^{(s,1)}(q + x) &= \frac{1}{\sqrt{L}} \left[\left(x + \frac{1}{2}\right) \cos\left(\frac{2\pi}{L}qs\right) - \frac{1}{2} \tan\left(\frac{\pi s}{L}\right) \sin\left(\frac{2\pi}{L}qs\right) \right] \\ \hat{\Gamma}^{(s,2)}(q + x) &= \frac{1}{\sqrt{L}} \left\{ \left[\left(x^2 - x + \frac{1}{6}\right) - \frac{1}{3} \tan^2\left(\frac{\pi s}{L}\right) \right] \cos\left(\frac{2\pi}{L}qs\right) \right. \\ &\quad \left. - \left(x - \frac{1}{2}\right) \tan\left(\frac{\pi s}{L}\right) \sin\left(\frac{2\pi}{L}qs\right) \right\}. \end{aligned} \quad (6.29)$$

The other eigenstates, $\check{\Gamma}^{(s,m)}(q + x)$, may be obtained from the above expressions by replacing $\frac{2\pi}{L}qs$ by $\frac{2\pi}{L}qs - \frac{\pi}{2}$. A few of the right eigenstates for a system of size $L = 20$ are shown in Figure 6.4.

6.4 Transport as an Exact Dynamical Property

From (6.27) the decay rates for the full map are

$$\Gamma^{(s,m)} = m \ln 4 - 2 \ln \left| \cos\left(\frac{\pi s}{L}\right) \right|. \quad (6.30)$$

The $m \ln 4$ term comes from the dynamics inside the cells governed by the 4-adic map. It gives a quick approach (for $m > 0$) to local equilibrium. The other term comes from the intra-cell dynamics and gives a slow approach to global equilibrium through diffusion. The eigenvalues of the $m = 0, 1$ and 2 branches are plotted in Figure 6.5 for a system of size $L = 20$.

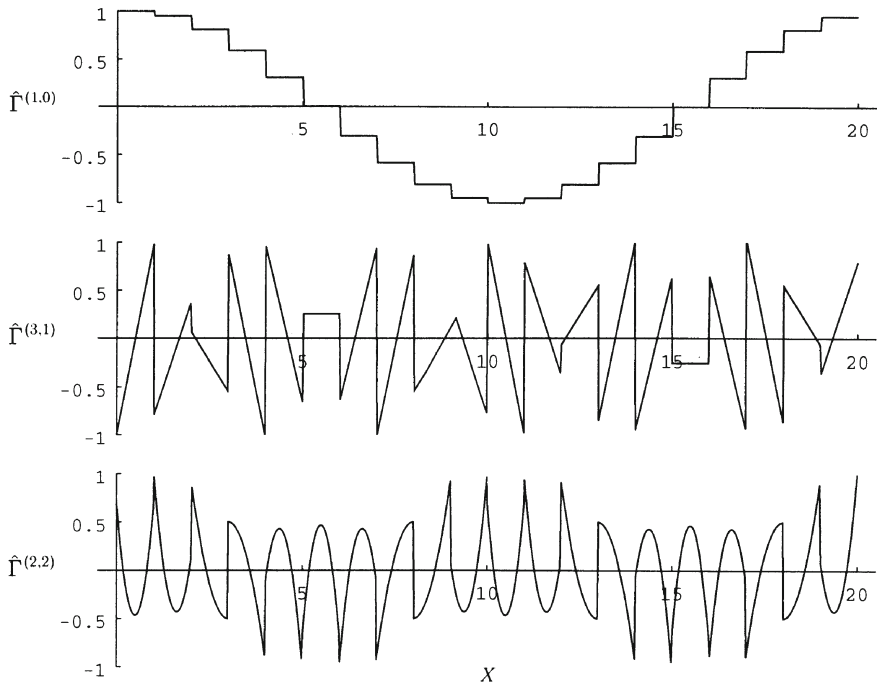


Figure 6.4: Three selected eigenstates of the multi-Bernoulli map for a system of size $L = 20$. The states have been scaled to fall between $[-1, 1]$ for illustration.

The $m = 0$ mode is the slowest decay mode and the decay rate, which for small s may be expanded as

$$\begin{aligned}\Gamma^{(s,0)} &= -2 \ln \left| \cos \left(\frac{\pi s}{L} \right) \right| \\ &= \frac{1}{4} \left(\frac{2\pi s}{L} \right)^2 + \frac{1}{96} \left(\frac{2\pi s}{L} \right)^4 + \dots,\end{aligned}\quad (6.31)$$

gives the diffusion coefficient as $1/4$ and the Burnett coefficient $1/96$. Higher order diffusion coefficients may be obtained by carrying the expansion further.

Using the spectral decomposition (6.25) we can sum over s to obtain independent modes just depending on m . First we define

$$\rho_s^{(m)}(x) \equiv \gamma_s^{(m)}(x) \langle \tilde{\gamma}_s^{(m)} | \rho_s \rangle. \quad (6.32)$$

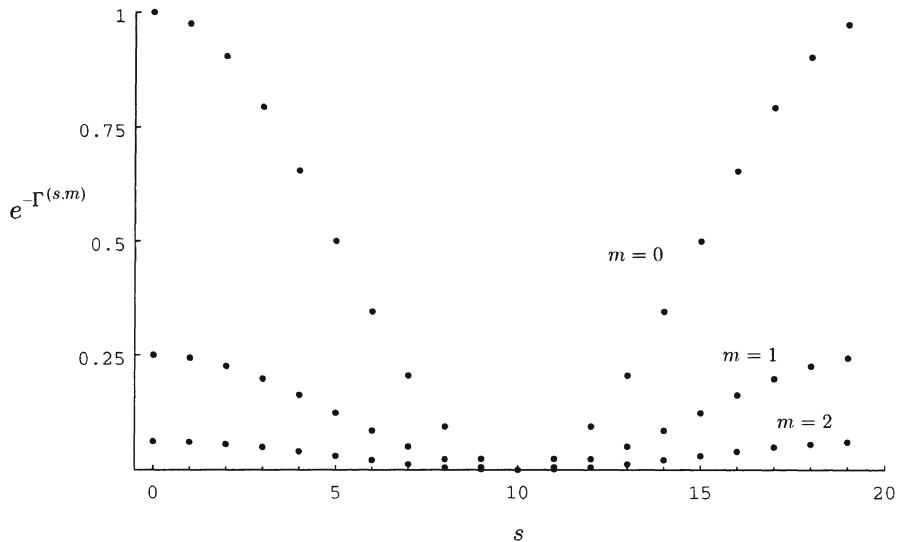


Figure 6.5: The first three branches of eigenvalues of the multi-Bernoulli map for a system of size $L = 20$.

Then by rewriting the eigenvalue as

$$e^{-\Gamma(s,m)} = \frac{1}{4^m} \left[\frac{1}{4} \left(e^{-i \frac{2\pi s}{L}} + e^{i \frac{2\pi s}{L}} \right) + \frac{1}{2} \right], \quad (6.33)$$

we use (6.23) to write the time evolution in terms of $\rho_s^{(m)}(x)$ as

$$\rho(q+x, t) = \sum_{m=0}^{\infty} \frac{1}{\sqrt{L}} \sum_{s=0}^{L-1} e^{i \frac{2\pi}{L} qs} \frac{1}{4^m} \left[\frac{1}{4} \left(e^{-i \frac{2\pi s}{L}} + e^{i \frac{2\pi s}{L}} \right) + \frac{1}{2} \right] \rho_s^{(m)}(x, t-1). \quad (6.34)$$

The summation over s is easy using (6.12a) giving the independent evolution equations

$$\begin{aligned} \rho^{(m)}(q+x, t) &= \frac{1}{4^m} \left[\frac{1}{4} \rho^{(m)}(q-1+x, t-1) + \frac{1}{2} \rho^{(m)}(q+x, t-1) \right. \\ &\quad \left. + \frac{1}{4} \rho^{(m)}(q+1+x, t-1) \right], \end{aligned} \quad (6.35)$$

where $\rho^{(m)}(q+x)$ is the transform of $\rho_s^{(m)}(x)$.

This infinite set of equations (one for each m) is a way of rewriting the full time evolution of the density given by (6.11) as independent “kinetic

equations". For $m = 0$ we obtain the well-known equation for the probability density of a random walk process with symmetric probability $1/4$ to jump right or left and $1/2$ to stay at a site. This equation governs the component of the full density that is constant inside each cell, but in general varying from cell to cell. The higher m modes govern the components of the density that are nonconstant in each cell and so decay. It is interesting to calculate expectation values with respect to the $\rho^{(m)}$ modes using (6.35). To neglect boundary effects we consider the system here on the whole real axis so that q takes all integer values.

First, the expectation of $X = q + x$ with respect to the m -th mode is

$$\begin{aligned} \langle q + x \rangle_t^{(m)} &= \sum_q \int_0^1 dx (q + x) \rho^{(m)}(q + x, t) \\ &= \frac{1}{4^m} \sum_q \int_0^1 dx \left[\frac{1}{4}(q + 1 + x) + \frac{1}{2}(q + x) + \frac{1}{4}(q - 1 + x) \right] \\ &\quad \times \rho^{(m)}(q + x, t - 1) \\ &= \frac{1}{4^m} \langle q + x \rangle_{t-1}^{(m)}, \end{aligned} \tag{6.36}$$

where for the second line we substituted in the right hand side of (6.35) and changed the summation variable of the first and third terms. Iterating this result down to the initial expectation gives

$$\langle q + x \rangle_t^{(m)} = \frac{1}{4^{mt}} \langle q + x \rangle_0^{(m)}. \tag{6.37}$$

So for $m = 0$ there is no change in the average position (as in a symmetric random walk) and for $m > 0$ this quantity decays due to the decay of the mode $\rho^{(m)}(q + x, t)$.

More interesting is the mean-squared position as a function of time. A similar calculation, using that $\int_0^1 dx \rho^{(m)}(q + x) = \delta_{m,0}$, gives for $m = 0$ the familiar diffusive behavior of

$$\langle (q + x)^2 \rangle_t^{(0)} = \langle (q + x)^2 \rangle_0^{(0)} + 2Dt. \tag{6.38}$$

For $m > 0$ the term linear in t is absent and a result similar to (6.37) is obtained as

$$\langle (q + x)^2 \rangle_t^{(m)} = \frac{1}{4^{mt}} \langle (q + x)^2 \rangle_0^{(m)}. \tag{6.39}$$

6.5 Eigenfunctionals of Diffusion

For $s = 0$ the first eigenvalue of U_s is $e^{-\gamma_0^{(0)}} = 1$. But for $s > 0$ the first eigenvalue $e^{-\gamma_s^{(0)}} = \cos(\pi s/L) < 1$. This means that U_s , like the Cantor map studied in Section 4.3, does not preserve Lebesgue measure for $s > 0$. We may expect though that there exists a singular invariant measure of U_s and that the left eigenfunctions will involve an integration over this measure.

The adjoint of U_s is determined as the operator that satisfies $\langle f|U_s g\rangle = \langle U_s^\dagger f|g\rangle$. This gives

$$U_s^\dagger f(x) = \begin{cases} e^{-i\frac{\pi s}{L}} f(2x) & 0 \leq x < \frac{1}{2} \\ e^{i\frac{\pi s}{L}} f(2x - 1) & \frac{1}{2} \leq x < 1, \end{cases} \quad (6.40)$$

or in terms of U_B^\dagger :

$$U_s^\dagger = e^{-i(\frac{\pi s}{L})r(x)} U_B^\dagger. \quad (6.41)$$

Recall that $(U_B^\dagger)^t$ generates 2^t copies of whatever it acts on. Here $(U_s^\dagger)^t$ also generates 2^t copies but multiplied by x -dependent complex phase factors.

To determine an explicit form for the eigenstates of U_s^\dagger we follow the construction that was done for U_C^\dagger in Section 4.3. It is sufficient to consider in detail only the 0th-order eigenstate since

$$\langle \tilde{\gamma}_s^{(m)} | \rho_s \rangle = \langle \tilde{\gamma}_s^{(0)} | \frac{1}{m!} \frac{d^m}{dx^m} \rho_s \rangle. \quad (6.42)$$

This may be seen by inserting a complete set of states to the right of δU_s in (6.21) and using the intertwining relation between U_s and the m -th derivative operator of

$$\frac{d^m}{dx^m} U_s = \frac{1}{2^m} U_s \frac{d^m}{dx^m}. \quad (6.43)$$

From the general expression for the left state in terms of the Bernoulli basis, (6.21), we have that

$$\langle \tilde{\gamma}_s^{(0)} | \rho_s \rangle = \langle \tilde{B}_0 | \rho_s \rangle + \langle \tilde{B}_0 | \delta U_s \frac{1}{e^{-\gamma_s^{(0)}} - U_s} | \rho_s \rangle. \quad (6.44)$$

Inserting the completeness relation (4.98) of the Bernoulli basis (with $M = 1$) to the right of δU_s in the second term here and then using the intertwining relation (6.43) gives

$$\langle \tilde{B}_0 | \delta U_s [|B_1\rangle\langle\tilde{B}_1| - |\mathcal{B}_1\rangle\langle\mathbf{e}\tilde{B}_1|] \frac{1}{e^{-\gamma_s^{(0)}} - U_s} | \rho_s \rangle$$

$$\begin{aligned}
&= \langle \tilde{B}_0 | \delta U_s [|B_1\rangle\langle\tilde{B}_0| - |\mathcal{B}_1\rangle\langle e\tilde{B}_0|] \frac{1}{e^{-\gamma_s^{(0)}} - \frac{U_s}{2}} | \rho_s \rangle \\
&= i \tan(\frac{\pi s}{L}) \int_0^1 dx dx' r(x) [B_1(x) - B_1(x-x')] \frac{1}{1 - \frac{e^{-\gamma_s^{(0)}} U_s}{2}} \frac{d}{dx'} \rho_s(x') \\
\end{aligned} \tag{6.45}$$

The integration over x evaluates to

$$-\int_0^1 dx r(x) [B_1(x) - B_1(x-x')] = \lambda_1(x) \equiv \begin{cases} x' & 0 \leq x' < \frac{1}{2} \\ 1-x' & \frac{1}{2} \leq x' < 1. \end{cases} \tag{6.46}$$

So the 0-th-order eigenfunctional is

$$\langle \tilde{\gamma}_s^{(0)} | \rho_s \rangle = \langle 1 | \rho_s \rangle - i \tan(\frac{\pi s}{L}) \langle w_{s,\lambda_1} | \rho_s^{(1)} \rangle, \tag{6.47}$$

where

$$w_{s,\lambda_1}(x) \equiv \frac{1}{1 - \frac{e^{-\gamma_s^{(0)}} U_s^\dagger}{2}} \lambda_1(x). \tag{6.48}$$

This expression is restricted to values of s such that $|e^{\gamma_s^{(0)}}/2| < 1$ or $s < L/3$. To get an expression valid for higher values of s we should use the completeness relation in (6.44) with the remainder term at $M > 1$. We'll analyze here just the case we have already begun to consider.

From (6.48) and using (6.41) we see that $w_{s,\lambda_1}(x)$ satisfies the functional equation

$$U_B^\dagger w_{s,\lambda_1}(x) = 2e^{-\gamma_s^{(0)} - i(\frac{\pi s}{L})r(x)} [w_{s,\lambda_1}(x) - \lambda_1(x)]. \tag{6.49}$$

As was done for the eigenfunctionals of the Cantor map, we may integrate (6.47) by parts to rewrite it as a Riemann–Stieltjes integral. This gives

$$\langle \tilde{\gamma}_s^{(0)} | \rho_s \rangle = \int_0^1 dG_s(x) \rho_s(x), \tag{6.50}$$

where

$$G_s(x) = x + i \tan(\frac{\pi s}{L}) w_{s,\lambda_1}^*(x). \tag{6.51}$$

Using (6.49) it can be shown that $G_s(x)$ satisfies the functional equation

$$G_s(x) = \begin{cases} \alpha_s G_s(2x) & 0 \leq x < \frac{1}{2} \\ (1-\alpha_s) G_s(2x-1) + \alpha_s & \frac{1}{2} \leq x < 1, \end{cases} \tag{6.52}$$

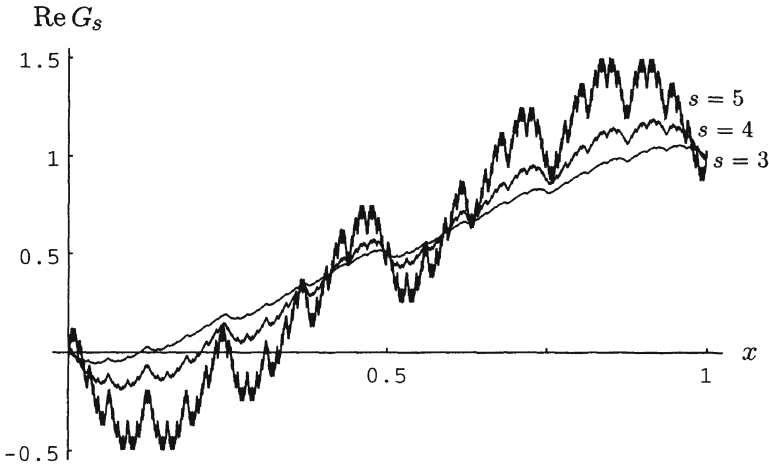


Figure 6.6: The real part of the cumulative singular measure G_s of a system of size $L = 20$ for $s = 3, 4$ and 5 .

where

$$\alpha_s \equiv \frac{1}{2} [1 + i \tan(\frac{\pi s}{L})]. \quad (6.53)$$

The functions $G_s(x)$ define a family of singular (except for $s = 0$) invariant measures, μ_s of the multi-Bernoulli map as

$$\mu_s[a, b] = \{G_s(b - [b]) + [b]\} - \{G_s(a - [a]) + [a]\}, \quad (6.54)$$

where the square brackets here denote integer parts. The real and imaginary parts of $G_s(x)$ for several values of s are shown in Figures 6.6 and 6.7. The figures are obtained by iterating (6.52) starting with an initial trial function such as $G_s^{(0)}(x) = x$. The iteration is a contractive mapping and the procedure converges after a finite number of steps to a function that looks stable and is then plotted.

In the complex plane, if we plot $\text{Im}[G_s(x)]$ vs. $\text{Re}[G_s(x)]$ we obtain a fractal set with dimension

$$\dim [G_s(x)] = \frac{-\ln 2}{\ln |\alpha_s|} > 1. \quad (6.55)$$

This is shown in Figure 6.8 for $s = 4$ and $L = 20$. The fractal dimension (6.55) is obtained from the iterative procedure used to make the plot. At each step the length and number of sides of the curve is counted and then the limit of infinite iterations is taken.

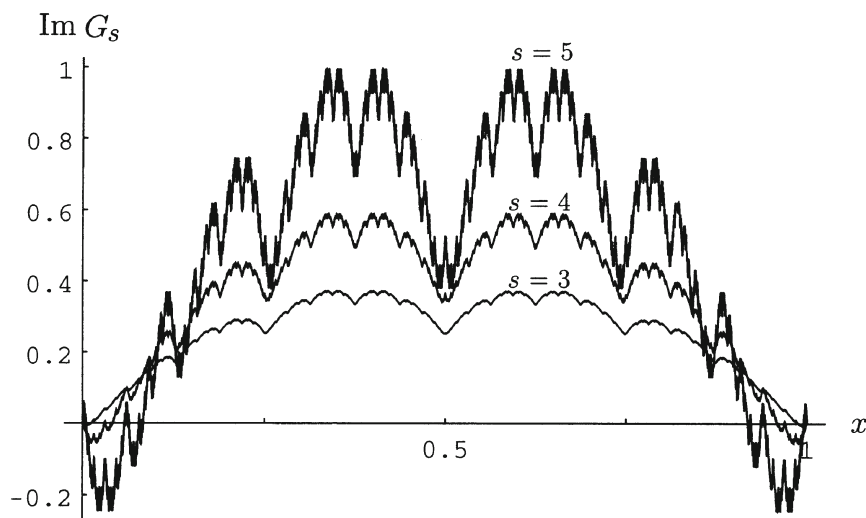


Figure 6.7: The imaginary part of the cumulative singular measure G_s of a system of size $L = 20$ for $s = 3, 4$ and 5 .

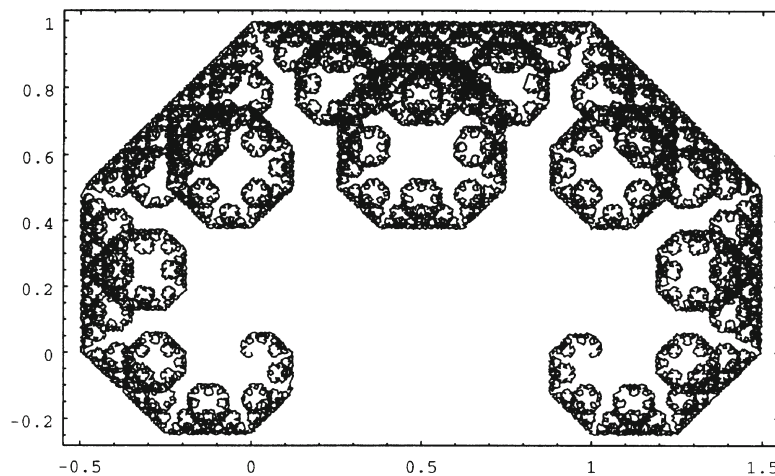


Figure 6.8: Parametric plot of $\text{Im}[G_s(x)]$ vs. $\text{Re}[G_s(x)]$ for $s = 4$ and $L = 20$.

6.6 The Multi-baker Map

The multi-baker transformation models deterministic diffusion in a system with invertible trajectory evolution. The map is constructed on a chain of squares along the X -axis. It may be considered as the successive action of two baker transformations. The first map acts on the unit squares centered at integer locations as

$$\Phi_1(X, y) = \begin{cases} (2X - q + \frac{1}{2}, \frac{y}{2}) & q - \frac{1}{2} \leq X < q, 0 \leq y < 1 \\ (2X - q - \frac{1}{2}, \frac{y}{2} + \frac{1}{2}) & q \leq X < q + \frac{1}{2}, 0 \leq y < 1. \end{cases} \quad (6.56)$$

The second map acts on the unit squares centered at half integers as

$$\Phi_2(X, y) = \begin{cases} (2X - q, \frac{y}{2}) & q \leq X < q + \frac{1}{2}, 0 \leq y < 1 \\ (2X - q - 1, \frac{y}{2} + \frac{1}{2}) & q + \frac{1}{2} \leq X < q + 1, 0 \leq y < 1. \end{cases} \quad (6.57)$$

The multi-baker transformation is given by the composition of these two maps, $\Phi(X, y) = \Phi_2(X, y) \circ \Phi_1(X, y)$, which then maps regions of each cell to the adjoining cells as

$$\Phi(X, y) = \begin{cases} (4X - 3q - 1, \frac{y}{4} + \frac{3}{4}) & q \leq X < q + \frac{1}{4}, 0 \leq y < 1 \\ (4X - 3q - 1, \frac{y}{4} + \frac{1}{4}) & q + \frac{1}{4} \leq X < q + \frac{1}{2}, 0 \leq y < 1 \\ (4X - 3q - 2, \frac{y}{4} + \frac{1}{2}) & q + \frac{1}{2} \leq X < q + \frac{3}{4}, 0 \leq y < 1 \\ (4X - 3q - 2, \frac{y}{4}) & q + \frac{3}{4} \leq X < q + 1, 0 \leq y < 1. \end{cases} \quad (6.58)$$

The map is shown in Figure 6.9. The map has the Lyapunov exponent $\log 4$ associated with stretching in the X direction and $-\log 4$ associated with contraction in the y direction. It is invertible and preserves two-dimensional Lebesgue measure. Note that the projection of the multi-baker map onto the X -axis is the multi-Bernoulli map. Figure 6.10 shows the trajectory evolution of 100 initial points randomly distributed in a small region of the phase space. Diffusion of the iterates in the x direction is evident.

Since Φ is invertible we may immediately write down the action of the Frobenius–Perron operator as

$$\begin{aligned} \rho(X, y; t+1) &= U_{\text{mb}}\rho(X, y; t) = \rho(\Phi^{-1}(X, y); t) \\ &= \begin{cases} \rho(\frac{X}{4} + \frac{3q}{4} - \frac{1}{4}, 4y; t) & q \leq X < q + 1, 0 \leq y < \frac{1}{4} \\ \rho(\frac{X}{4} + \frac{3q}{4} + \frac{1}{4}, 4y - 1; t) & q \leq X < q + 1, \frac{1}{4} \leq y < \frac{1}{2} \\ \rho(\frac{X}{4} + \frac{3q}{4} + \frac{1}{2}, 4y - 2; t) & q \leq X < q + 1, \frac{1}{2} \leq y < \frac{3}{4} \\ \rho(\frac{X}{4} + \frac{3q}{4} + 1, 4y - 3; t) & q \leq X < q + 1, \frac{3}{4} \leq y < 1. \end{cases} \end{aligned} \quad (6.59)$$

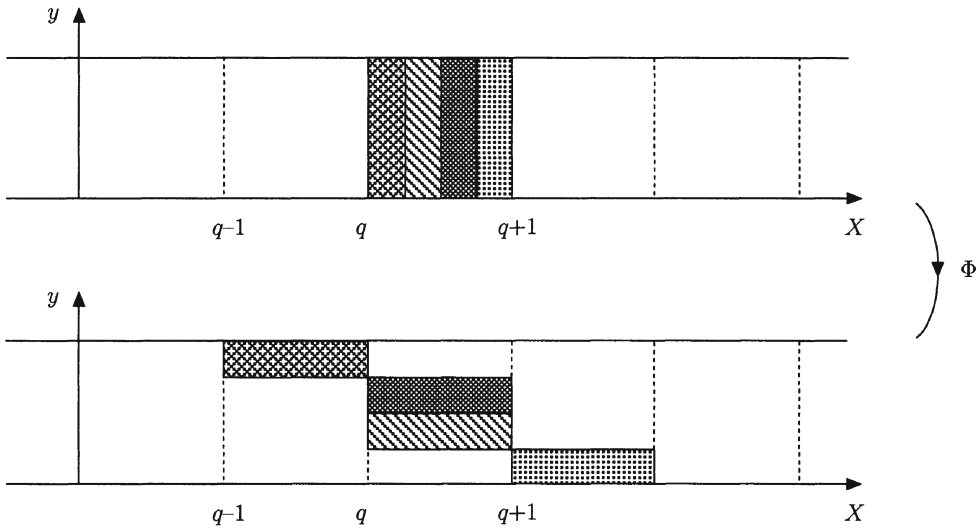


Figure 6.9: The multibaker map.

Like the baker map, U_{mb} is unitary in Hilbert space and a decomposition of it may be constructed there with eigenvalues on the unit circle. We want to obtain explicit decay modes and especially diffusion modes like we have for the multi-Bernoulli map.

Decomposing X into its integer, q , and fractional part, x , we separate the motion among cells from the internal motion in the cells through the discrete Fourier transform (6.12b) with respect to q as we did for the multi-Bernoulli map. The modes ρ_s evolve under the map then as

$$\rho_s(x, y; t + 1) = \begin{cases} e^{-i\frac{2\pi}{L}s} \rho_s(\frac{x}{4} + \frac{3}{4}, 4y; t) & 0 \leq y < \frac{1}{4} \\ \rho_s(\frac{x}{4} + \frac{1}{4}, 4y - 1; t) & \frac{1}{4} \leq y < \frac{1}{2} \\ \rho_s(\frac{x}{4} + \frac{1}{2}, 4y - 2; t) & \frac{1}{2} \leq y < \frac{3}{4} \\ e^{i\frac{2\pi}{L}s} \rho_s(\frac{x}{4}, 4y - 3; t) & \frac{3}{4} \leq y < 1. \end{cases} \quad (6.60)$$

This transformation corresponds to the square of the transformation

$$U_{bs}\rho_s(x, y; t) = \begin{cases} e^{-i\frac{\pi}{L}s} \rho_s(\frac{x}{2} + \frac{1}{2}, 2y; t) & 0 \leq y < \frac{1}{2} \\ e^{i\frac{\pi}{L}s} \rho_s(\frac{x}{2}, 2y - 1; t) & \frac{1}{2} \leq y < 1. \end{cases} \quad (6.61)$$

As we did for the baker transformation, it is useful to rewrite U_{bs} in terms of the Frobenius–Perron and Koopman operators of the Bernoulli map. This

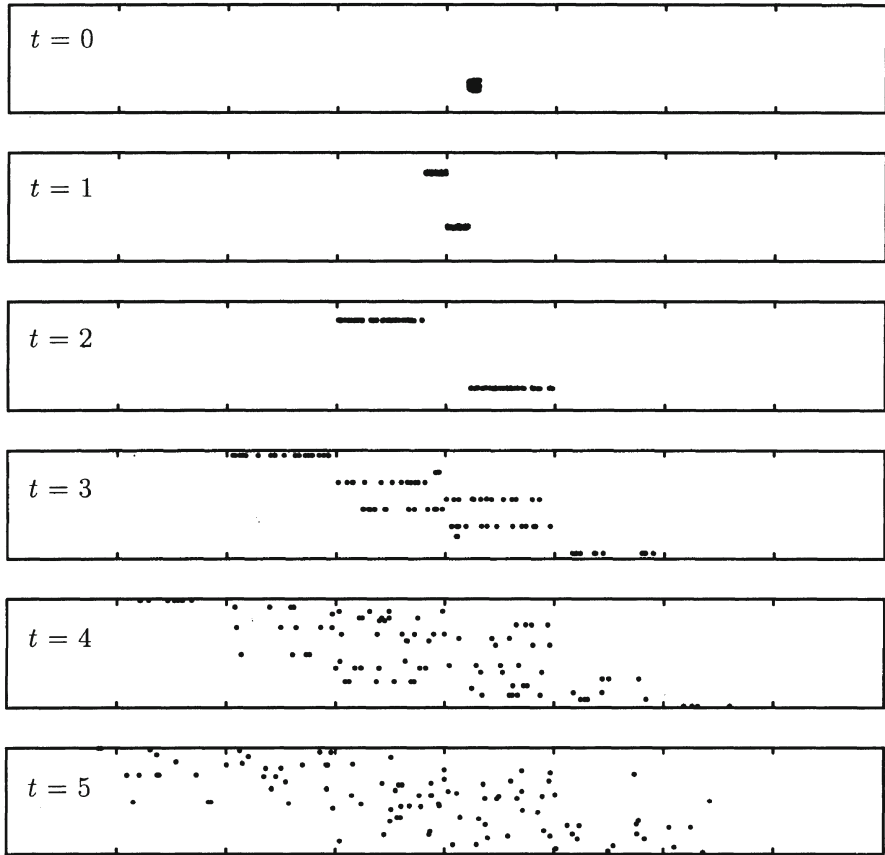


Figure 6.10: The multibaker map acting on 100 initial points randomly distributed in a small region of the phase space.

gives

$$\begin{aligned}
 U_{\text{bs}}\rho_s(x, y; t) &= \cos\left(\frac{\pi s}{L}\right)U_x \left\{ 1 - r(x)r(y) \right. \\
 &\quad \left. - i \tan\left(\frac{\pi s}{L}\right)[r(y) - r(x)] \right\} U_y^\dagger \rho_s(x, y; t).
 \end{aligned} \tag{6.62}$$

It is then convenient to consider U_{bs} in the same two-dimensional Bernoulli basis, (5.6), as we did for the baker map. The diagonal part in this basis is the same, apart from the factor of $\cos(\pi s/L)$, as for the baker map but the

off-diagonal part allows for more transitions. Note that taking $s = 0$ does not recover the baker map discussed in Chapter 5, but a variation of it where the left half of the unit square is stretched and squeezed and then cut and put on top of the right half, which has also been stretched and squeezed.

The eigenvalues of U_{bs} are the same as the multi-Bernoulli map but with degeneracies as

$$e^{-\gamma_s^{(n+m)}} \equiv \frac{\cos(\pi s/L)}{2^{m+n}} = \frac{\cos(\pi s/L)}{2^j} \quad \text{in } j+1 \text{ ways.} \quad (6.63)$$

An analysis of the resolvent of U_{bs} shows that each eigenvalue of multiplicity $j+1$ is associated with poles up to order $j+1$ so that the decomposition of U_{bs} is of Jordan block form.

As for the baker map we may easily determine the eigenstates associated with each block. Considering a density independent of x we have from (6.62) that

$$\begin{aligned} U_{bs}\rho_s(y) &= \cos\left(\frac{\pi s}{L}\right) \left[1 - i \tan\left(\frac{\pi s}{L}\right) r(y) \right] U_y^\dagger \rho_s(y) \\ &= e^{-i(\frac{\pi s}{L})r(y)} U_y^\dagger \rho_s(y). \end{aligned} \quad (6.64)$$

Comparing with (6.41) we see then that the right eigenstates of U_{bs} are the same as the left eigenstates, with respect to the variable y , of the transformed multi-Bernoulli map. The left eigenstates of U_{bs} are the complex conjugate of the left eigenstates of U_s , with respect to the variable x . The Jordan states may be obtained in a direct fashion as was done for the baker map. The reader is referred to the papers cited in the bibliographic notes for the explicit results.

In summary, we see that the common thermodynamic property of diffusion is completely compatible with time-reversible trajectory dynamics. No projection or coarse-graining is necessary to understand how the irreversible diffusion phenomena appears.

Bibliographic Notes

The first papers to construct the generalized decomposition for the multi-Bernoulli map were published concurrently. They are

- P. Gaspard, “Diffusion in Uniformly Hyperbolic One-dimensional Maps and Appell Polynomials,” *Physics Letters A*, **168**, 13 (1992).
- H.H. Hasegawa and D.J. Driebe, “Transport as a dynamical property of a simple map,” *Physics Letters A*, **168**, 18 (1992).

More complete presentations, including the decomposition of the multi-baker map, are in the paper by Gaspard in *Chaos* cited in Chapter 2 and the *Physical Review E* paper of Hasegawa and Driebe cited in Chapter 3.

An analysis of the fractality of the left eigenstates of the multi-Bernoulli map, including the DeRham equation for the measure is in

- S. Tasaki, I. Antoniou and Z. Suchanecki, “Deterministic Diffusion, DeRham Equation and Fractal Eigenvectors,” *Physics Letters A*, **179**, 97 (1993).

The paper of Gaspard that introduced the multi-baker transformation and showed that Ruelle’s resonances for this system gave the phenomenological diffusion coefficient and other decay rates is

- P. Gaspard, “Diffusion, Effusion and Chaotic Scattering: An Exactly Solvable Liouvillian Dynamics,” *Journal of Statistical Physics*, **68**, 673 (1992).

A discussion of nonequilibrium stationary states in the multi-baker map is in

- S. Tasaki and P. Gaspard, “Fick’s law and fractality of nonequilibrium stationary states in a reversible multibaker map,” *Journal of Statistical Physics*, **81**, 935 (1995).

Chapter 7

Afterword

Chaotic dynamics presents a kind of complementarity in that there are co-existing aspects of both disorder and coherence. Disorder is manifest on the level of trajectories where there is sensitivity to initial conditions and erratic trajectory motion. On the statistical level, characterized by evolving probability densities, there is a remarkable coherence with an approach to equilibrium and identifiable decay modes. Interestingly, these decay modes are elements of generalized functional spaces.

The real beauty of the approach described in this book is its application to the understanding of irreversibility in measure-preserving, invertible transformations. This was illustrated with the baker and multi-baker transformations. But the approach is also important for one-dimensional systems, especially since the decay modes of the isometric Koopman operator already lead us outside regular functional spaces. The generalized spectral decomposition of the Frobenius–Perron operator directly gives the physical decay characteristics of the system. This is in contrast to decompositions in regular functional spaces with continuous spectra that yield specific decay contributions only when considered in conjunction with specific observables.

Diverging trajectory motion and stretching in phase space are associated with the derivative operator, which determines the validity of the generalized spectral representations. These natural physical conditions of smoothness that the densities and observables must satisfy are determined by the dynamics of the system. In this way irreversibility is seen as an intrinsic property of fully chaotic systems. In more realistic thermodynamic systems, such as fluids, many degrees of freedom play a crucial role in the elucidation of irreversibility. In such systems, for the existence of intensive variables, probability densities must be restricted to the class of densities that exclude

trajectories. Thus the existence of thermodynamics in such systems leads right away to the representation of the time evolution in generalized function spaces and the breaking of time symmetry.

For the systems we have considered the basic dynamical laws that include irreversibility are on the level of irreducible probability densities. Irreducible because trajectories, corresponding to non-differentiable point densities, are outside the domain of the generalized spectral representation. Thus, by going to a representation that breaks time symmetry, and is in accordance with our experience of nature, we find that trajectories are not the primary kinematical object to consider in chaotic systems but that smooth densities are. From this point of view trajectories are seen as stochastic realizations of more fundamental probability densities. In this way classical mechanics appears similar to quantum mechanics and a new perspective for understanding quantum chaos is provided.

Much of the art of doing physics involves finding an appropriate mathematical framework for a description of the aspect of nature in which one is interested. The work described in this book utilizes generalized functional analysis to express the deep connection between time and dynamical instability. This connection is obscured by consideration of these systems in regular functional spaces but expresses itself naturally in the framework discussed in this book.

Appendices

A.1 Complex Microstructure of Phase Space

To illustrate the complex microstructure of phase space in fully chaotic systems we consider the dyadic Bernoulli map: $x_{t+1} = 2x_t \bmod 1$, where $x_t \in [0, 1)$. This is a fully chaotic system so there are no regular regions surrounded by chaotic regions or any “island” structure in the phase space. Nevertheless, there is a microstructure in this simple phase space of the unit interval with different points yielding either periodic or “chaotic” trajectories. The imbedding of periodic trajectories densely in chaotic trajectories can best be seen by considering the evolution of a trajectory written in binary notation. (Note that the idea of a chaotic trajectory is not so well defined since chaos, meaning sensitivity to initial conditions, is measured by a positive Lyapunov exponent obtained by considering two closely spaced initial points. Awareness of this simple point makes it clear that an ensemble description is natural for chaotic systems and that the Lyapunov time, being the inverse of the Lyapunov exponent, should play a role in the time evolution of smooth densities.)

Let us write an initial point, x_0 , in binary notation

$$x_0 = \sum_{n=1}^{\infty} \alpha_n 2^{-n} = 0.\alpha_1\alpha_2\alpha_3\dots, \quad (\text{A.1})$$

where $\alpha_n = 0$ or 1 . Applying the Bernoulli map gives

$$x_1 = 2x_0 \bmod 1 = 0.\alpha_2\alpha_3\alpha_4\dots, \quad (\text{A.2})$$

so in binary notation time evolution by one step means shifting the binary expansion of the trajectory one place to the right and chopping off the first digit.

From the shift picture we see immediately that trajectories arising from initial conditions of rational numbers, which have periodic or eventually

terminating binary expansions, lead to periodic or eventually fixed point behavior. Irrational initial conditions may be classified into so-called normal or non-normal irrational numbers. Normal irrational numbers have every possible finite sequence of digits occurring somewhere in their expansion. Such initial conditions lead to trajectories forever wandering throughout the unit interval and over time coming arbitrarily close to any point in the interval. Non-normal irrational numbers (such as $0.10100100010000\dots$) will lead to non-periodic trajectories but they will not visit everywhere in the unit interval.

As is well known, rational numbers are densely distributed among irrational numbers. But because the rationals are denumerable they are of measure zero with respect to the irrational numbers. Furthermore, within the set of irrational numbers it is the normal ones that are overwhelmingly prevalent. This means that qualitatively different behavior, in the sense of trajectory dynamics, arises from initial conditions that are infinitesimally close. This kind of complicated microstructure of phase space for chaotic systems is in contrast to systems with regular dynamics where initial conditions throughout finite regions of phase space lead to similar behavior.

A nice discussion of normal and non-normal numbers and their relation to chaotic dynamics is in

- M. Schroeder, *Fractals, Chaos, Power Laws*, (Freeman, San Francisco, 1992).

A.2 More on Mixing

The classic way to motivate the definition (2.10) is to consider the mixing of one fluid in another, such as gin in tonic water. After mixing the drink we expect that the percentage of gin in a sip is the same as the percentage of gin in the total drink. Let D denote the region of the drink occupied by the gin just after it is poured in and take E as the sip that is sampled after the drink is mixed. Taking the measure of a set here as the volume it occupies the above statement is expressed mathematically as

$$\lim_{t \rightarrow \infty} \frac{\mu(S_t(D) \cap E)}{\mu(E)} = \frac{\mu(D)}{\mu(M)}, \quad (\text{A.3})$$

where S_t is the act of stirring and M is the volume of the whole drink. Normalizing the measure so that $\mu(M) = 1$ and writing $S_{-t}(D)$ so that the definition is also valid for non-invertible transformations gives the mixing condition

$$\lim_{t \rightarrow \infty} \mu(S_{-t}(D) \cap E) = \mu(D)\mu(E), \quad (\text{A.4})$$

which is (2.10).

In order to show that this definition of mixing implies the approach to equilibrium of observables expressed by (1.11) and the decay of correlations, (2.9), we begin by rewriting the left hand side of (A.4) as

$$\begin{aligned} \lim_{t \rightarrow \infty} \mu(S_{-t}(D) \cap E) &= \lim_{t \rightarrow \infty} \int_{S_{-t}(D) \cap E} dx \rho^{\text{eq}}(x) \\ &= \lim_{t \rightarrow \infty} \int_M dx \chi_{S_{-t}(D) \cap E}(x) \rho^{\text{eq}}(x) \\ &= \lim_{t \rightarrow \infty} \int_M dx \chi_{S_{-t}(D)}(x) \chi_E(x) \rho^{\text{eq}}(x) \\ &= \lim_{t \rightarrow \infty} \int_M dx \chi_D(S_t(x)) \chi_E(x) \rho^{\text{eq}}(x) \\ &= \lim_{t \rightarrow \infty} \langle K^t \chi_D | \chi_E \rho^{\text{eq}}(x) \rangle \\ &= \lim_{t \rightarrow \infty} \langle \chi_D | U^t (\chi_E \rho^{\text{eq}}(x)) \rangle, \end{aligned} \quad (\text{A.5})$$

where χ_A is the indicator function on the set A . For the right hand side of (A.4) we have

$$\begin{aligned} \mu(D)\mu(E) &= \int_M dx \chi_D(x) \rho^{\text{eq}}(x) \int_M dx \chi_E(x) \rho^{\text{eq}}(x) \\ &= \langle \chi_D | \rho^{\text{eq}}(x) \rangle \langle 1 | \chi_E \rho^{\text{eq}} \rangle. \end{aligned} \quad (\text{A.6})$$

Letting $f = \chi_D$ and $g = \chi_E \rho^{\text{eq}}$ we see that we may thus rewrite the mixing definition (A.4) as

$$\lim_{t \rightarrow \infty} \langle f | U^t g \rangle = \langle f | \rho^{\text{eq}} \rangle \langle 1 | g \rangle. \quad (\text{A.7})$$

We have shown this relation for f and g chosen as the above indicator functions but since so-called simple functions are just linear superpositions of indicator functions and more general functions in L^p spaces are limits of simple functions the result holds for quite general f 's and g 's. Taking f as $B(x)$ and g as ρ^{eq} yields (1.11) (where we use that $\langle 1 | \rho^{\text{eq}} \rangle = 1$). The expression (2.9) is obtained by choosing $f = \sigma$ and $g = \eta \rho^{\text{eq}}$.

The above results are standard. I have adapted the proofs from the book of Mackey cited in Chapter 1.

A.3 Isometry of U_B^\dagger

The fact that U_B^\dagger is the adjoint of U_B is straightforward as

$$\begin{aligned}
 \langle f | U_B g \rangle &= \int_0^1 dx f^*(x) \left\{ \frac{1}{2} [g(\frac{x}{2}) + g(\frac{x+1}{2})] \right\} \\
 &= \frac{1}{2} \int_0^1 dx f^*(x) g(\frac{x}{2}) + \frac{1}{2} \int_0^1 dx f^*(x) g(\frac{x+1}{2}) \\
 &= \int_0^{1/2} dx' f^*(2x') g(x') + \int_{1/2}^1 dx'' f^*(2x'' - 1) g(x'') \\
 &= \langle U_B^\dagger f | g \rangle.
 \end{aligned} \tag{A.8}$$

It is also easy to prove that U_B^\dagger is isometric in L^p spaces as

$$\begin{aligned}
 \|U_B^\dagger f\|_p &= \left(\int_0^1 dx |U_B^\dagger f(x)|^p \right)^{\frac{1}{p}} \\
 &= \left(\int_0^{1/2} dx |f(2x)|^p + \int_{1/2}^1 dx |f(2x-1)|^p \right)^{\frac{1}{p}} \\
 &= \left(\frac{1}{2} \int_0^1 dx' |f(x')|^p + \frac{1}{2} \int_0^1 dx'' |f(x'')|^p \right)^{\frac{1}{p}} \\
 &= \|f\|_p.
 \end{aligned} \tag{A.9}$$

If U_B is taken to act on functions in L^1 , then the dual space on which U_B^\dagger acts is L^∞ . The L^∞ norm is just the maximum of the absolute value of the function (here on $[0, 1]$). The isometry of U_B^\dagger in this space is also easy to see as

$$\begin{aligned}
 \|U_B^\dagger f\|_\infty &= \begin{cases} \|f(2x)\|_\infty & 0 \leq x < \frac{1}{2} \\ \|f(2x-1)\|_\infty & \frac{1}{2} \leq x < 1. \end{cases} \\
 &= \|f\|_\infty.
 \end{aligned} \tag{A.10}$$

A.4 Dual States

We use the right eigenstates, say $|\phi_n\rangle$, of U to write a function in terms of them as

$$|f\rangle = \sum_n c_n |\phi_n\rangle, \quad (\text{A.11})$$

where we employ a Dirac bra-ket notation for the states. As is well known, the expansion coefficients, c_n , are obtained from the dual states, $\langle\tilde{\phi}_n|$, that satisfy $\langle\tilde{\phi}_n|\phi_m\rangle = \delta_{nm}$. The coefficients are given by

$$c_n = \langle\tilde{\phi}_n|f\rangle. \quad (\text{A.12})$$

To show that the dual states are left eigenstates of U we act on $|f\rangle$ with U and use that $U|\phi_n\rangle = \lambda_n|\phi_n\rangle$ to obtain

$$U|f\rangle = \sum_n \lambda_n c_n |\phi_n\rangle. \quad (\text{A.13})$$

Then we act with $\langle\tilde{\phi}_n|$ and use (A.12) for c_n to give

$$\langle\tilde{\phi}_n|U|f\rangle = \lambda_n c_n = \lambda_n \langle\tilde{\phi}_n|f\rangle. \quad (\text{A.14})$$

Since $|f\rangle$ is arbitrary here it follows that

$$\langle\tilde{\phi}_n|U = \lambda_n \langle\tilde{\phi}_n|, \quad (\text{A.15})$$

or,

$$U^\dagger \langle\tilde{\phi}_n| = \lambda_n^* \langle\tilde{\phi}_n|. \quad (\text{A.16})$$

A.5 The Resolvent Formalism

We introduce the following z transform of $\rho(t)$ defined by

$$\bar{\rho}(z) = \sum_{t=0}^{\infty} z^{-(t+1)} \rho(t). \quad (\text{A.17})$$

(For convenience we don't indicate the x dependence of ρ here.) Since $\|\rho(t)\| \leq \|\rho(0)\|$ (this comes from the contractive property (2.5) of the Frobenius–Perron operator) $\bar{\rho}(z)$ is convergent for all $|z| > 1$. The inverse transform is given by

$$\rho(t) = \frac{1}{2\pi i} \oint_{|z|=1} dz z^t \bar{\rho}(z), \quad (\text{A.18})$$

where the contour is indicated as being taken outside the unit circle.

The Frobenius–Perron operator acts on $\rho(t)$ as

$$U\rho(t) = \rho(t+1). \quad (\text{A.19})$$

Taking the z transform of this equation gives

$$U\bar{\rho}(z) = z\bar{\rho}(z) - \rho(0), \quad (\text{A.20})$$

so that

$$\bar{\rho}(z) = \frac{1}{z-U} \rho(0). \quad (\text{A.21})$$

The operator appearing on the right hand side here, $R(z) \equiv 1/(z-U)$, is known as the resolvent corresponding to U . Using the expression for the inverse transform we may then write the time evolution, $\rho(t) = U^t \rho(0)$, in terms of the resolvent of U as

$$\rho(t) = \frac{1}{2\pi i} \oint_{|z|=1} dz \frac{z^t}{z-U} \rho(0). \quad (\text{A.22})$$

This way of expressing U^t is quite useful because it allows us to employ the tools of calculus in the complex plane to investigate the operator U . Note that U acting on ρ corresponds to z inside the integral in (A.22).

The simplest spectrum U may have consists of discrete eigenvalues, say λ_n , each of unit multiplicity. The projectors, $\Pi^{(n)}$, onto the one-dimensional subspaces defined by these eigenvalues satisfy $U\Pi^{(n)} = \lambda_n \Pi^{(n)}$. Using the

assumed completeness of the projectors, $\sum_n \Pi^{(n)} = \mathbf{1}$, the resolvent may be expressed as

$$R(z) = \sum_n R(z)\Pi^{(n)} = \sum_n \frac{\Pi^{(n)}}{z - \lambda_n}. \quad (\text{A.23})$$

Thus, for this case, the eigenvalues correspond to the location of simple poles of the resolvent and the residues of the poles are formally the projection operators $\Pi^{(n)}$. By Cauchy's theorem the projectors are thus given as

$$\Pi^{(n)} = \frac{1}{2\pi i} \oint_{z=\lambda_n} R(z) dz, \quad (\text{A.24})$$

where the contour encircles (in the counterclockwise direction) only the pole at λ_n .

An extensive discussion of the resolvent formalism is in the book by Kato cited in Chapter 3.

A.6 Rescaled Legendre Polynomials

The standard Legendre polynomials are defined on the interval $[-1, 1]$. A concise way of defining them is through Rodrigues' formula

$$P_n(x) = \frac{1}{2^n n!} \frac{d^n}{dx^n} (x^2 - 1)^n. \quad (\text{A.25})$$

These polynomials are orthogonal on $[-1, 1]$ with the weight factor of 1, and normalization such that

$$\int_{-1}^1 dx P_m(x) P_n(x) = \frac{2}{2n+1} \delta_{mn}. \quad (\text{A.26})$$

To rescale the polynomials to the unit interval we replace x by $2x - 1$. We thus define the Legendre polynomials on $[0, 1]$ by

$$\hat{P}_n(x) \equiv \sqrt{2n+1} P_n(2x - 1). \quad (\text{A.27})$$

The factor, $\sqrt{2n+1}$, is put so that the polynomials form an orthonormal set as

$$\int_0^1 dx \hat{P}_m(x) \hat{P}_n(x) = \delta_{mn}. \quad (\text{A.28})$$

The first six rescaled polynomials are shown in Figure A.1. Rodrigues' for-

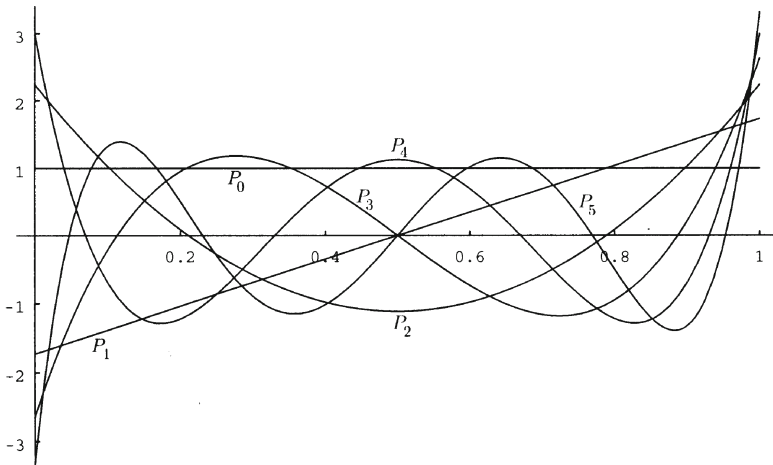


Figure A.1: The first six rescaled Legendre polynomials.

mula for the rescaled polynomials is

$$\hat{P}_n(x) = \frac{\sqrt{2n+1}}{n!} \frac{d^n}{dx^n} [x(x-1)]^n. \quad (\text{A.29})$$

These polynomials are symmetric (or anti-symmetric) with respect to the midpoint of the unit interval, as can be see from Figure A.1 or (A.29) as

$$\hat{P}_n(1-x) = (-1)^n \hat{P}_n(x). \quad (\text{A.30})$$

The result (3.20) for the matrix elements of U_B in the rescaled Legendre polynomial basis is obtained by first using (A.29) as

$$\begin{aligned} I_{m,n} &= \int_0^1 dx \hat{P}_m(x) \hat{P}_n\left(\frac{x}{2}\right) \\ &= \frac{\sqrt{(2m+1)(2n+1)}}{m!n!} \int_0^1 dx \left[\frac{d^m}{dx^m} x^m (x-1)^m \right] \\ &\quad \times \left[\frac{d^n}{d(x/2)^n} (x/2)^n [(x/2)-1]^n \right] \\ &= \frac{\sqrt{(2m+1)(2n+1)}}{2^n m! n!} \int_0^1 dx x^m (x-1)^m \left[\frac{d^{n+m}}{dx^{n+m}} x^n (x-2)^n \right], \end{aligned} \quad (\text{A.31})$$

where integration by parts m times was performed to get the last line. If $m > n$ the integral vanishes. For $m \leq n$ the integral may be evaluated as

$$\begin{aligned} &\int_0^1 dx x^m (x-1)^m \left[\frac{d^{n+m}}{dx^{n+m}} x^n (x-2)^n \right] \\ &= \int_0^1 dx x^m (x-1)^m \frac{d^{n+m}}{dx^{n+m}} x^n \sum_{j=0}^n \frac{n!}{j!(n-j)!} (-2)^{n-j} x^j \\ &= \sum_{j=m}^n (-1)^{n-j} \frac{n!(n+j)! 2^{n-j}}{(n-j)!(j-m)! j!} \int_0^1 dx x^j (x-1)^m. \end{aligned} \quad (\text{A.32})$$

Using then that

$$\int_0^1 dx x^j (x-1)^m = \frac{(-1)^m j! m!}{(j+m+1)!},$$

and changing the summation variable to $l = j - m$ gives finally

$$I_{m,n} = \frac{(-1)^{n+m} \sqrt{(2m+1)(2n+1)}}{2^m} \sum_{l=0}^{n-m} \frac{(-\frac{1}{2})^l (n+m+l)!}{(n-m-l)!(2m+l+1)! l!}. \quad (\text{A.33})$$

For $m = n$ this becomes $I_{n,n} = 1/2^n$.

In the calculation of the left eigenstates of U_B we use the fact that \hat{P}_n is orthogonal to any monomial, say x^p , of degree less than n . This follows from simply expanding x^p in Legendre polynomials (each necessarily of degree p and lesser) and then using the orthogonality of \hat{P}_n with every Legendre polynomial in the expansion.

A.7 Formal Expression for the Eigenstates

We may verify the formal expressions obtained for the eigenstates by applying U_B . For the right eigenstate, (3.33), we have

$$\begin{aligned}
 U_B|\gamma_j\rangle &= U_B \left[1 + \frac{1}{e^{-\gamma_j} - U_B} \delta U_B \right] |j\rangle \\
 &= \left[U_B + \frac{U_B}{e^{-\gamma_j} - U_B} \delta U_B \right] |j\rangle \\
 &= \left[U_B + \frac{U_B - e^{-\gamma_j} + e^{-\gamma_j}}{e^{-\gamma_j} - U_B} \delta U_B \right] |j\rangle \\
 &= \left[U_B - \delta U_B + \frac{e^{-\gamma_j}}{e^{-\gamma_j} - U_B} \delta U_B \right] |j\rangle \\
 &= \left[U_0 + \frac{e^{-\gamma_j}}{e^{-\gamma_j} - U_B} \delta U_B \right] |j\rangle \\
 &= e^{-\gamma_j} \left[1 + \frac{1}{e^{-\gamma_j} - U_B} \delta U_B \right] |j\rangle = e^{-\gamma_j} |\gamma_j\rangle. \quad (\text{A.34})
 \end{aligned}$$

The verification for the left eigenstates is similar.

To show that the eigenstates form an orthonormal set we use first that

$$\langle \tilde{\gamma}_j | U_B | \gamma_k \rangle = e^{-\gamma_k} \langle \tilde{\gamma}_j | \gamma_k \rangle, \quad (\text{A.35})$$

when U_B is considered acting to the right. If we act with U_B to the left we obtain

$$\langle \tilde{\gamma}_j | U_B | \gamma_k \rangle = e^{-\gamma_j} \langle \tilde{\gamma}_j | \gamma_k \rangle. \quad (\text{A.36})$$

Thus,

$$[e^{-\gamma_j} - e^{-\gamma_k}] \langle \tilde{\gamma}_j | \gamma_k \rangle = 0, \quad (\text{A.37})$$

showing that $\langle \tilde{\gamma}_j | \gamma_k \rangle = 0$ for $j \neq k$ since in this case $e^{-\gamma_j} - e^{-\gamma_k} \neq 0$. If $j = k$ then we have from the formal expressions for the right and left eigenstates

$$\begin{aligned}
 \langle \tilde{\gamma}_j | \gamma_j \rangle &= \langle j | \left(1 + \delta U \frac{1}{e^{-\gamma_j} - U_B} \right) \left(1 + \frac{1}{e^{-\gamma_j} - U_B} \delta U \right) |j\rangle \\
 &= \langle j | j \rangle = 1, \quad (\text{A.38})
 \end{aligned}$$

where the terms involving δU vanish due to the non-recurrence property of δU .

A.8 Explicit Evaluation of Eigenpolynomials

Here we show how to evaluate (3.38) in order to express $|\gamma_j\rangle$ entirely in terms of the “unperturbed” basis states $|j\rangle$. We won’t utilize the fact that the matrix elements $\langle m|\delta U|n\rangle$ are vanishing for $m + n$ odd (and also for $m = 0$) because we want to show how (3.38) is evaluated for a general case.

For $j = 0$ it is best to use (3.33) directly to see (because $\delta U|0\rangle = 0$) that

$$|\gamma_0\rangle = |0\rangle. \quad (\text{A.39})$$

For $j = 1$ (3.38) gives

$$|\gamma_1\rangle = |1\rangle + \left[\frac{1}{e^{-\gamma_1} - e^{-\gamma_0}} \langle 0|\delta U|1\rangle \langle 1|\gamma_1\rangle \right] |0\rangle. \quad (\text{A.40})$$

But $\langle 1|\gamma_1\rangle = 1$, which follows from the general result $\langle j|\gamma_j\rangle = \langle j|j\rangle = 1$ obtained from (3.33), the strict upper-triangularity of δU , and orthonormality of the basis states. So

$$|\gamma_1\rangle = |1\rangle + |0\rangle \frac{1}{e^{-\gamma_1} - e^{-\gamma_0}} \langle 0|\delta U|1\rangle. \quad (\text{A.41})$$

For $j = 2$ we have

$$\begin{aligned} |\gamma_2\rangle &= |2\rangle + \left[\frac{1}{e^{-\gamma_2} - e^{-\gamma_1}} \langle 1|\delta U|2\rangle \langle 2|\gamma_2\rangle \right] |1\rangle \\ &\quad + \frac{1}{e^{-\gamma_2} - e^{-\gamma_0}} [\langle 0|\delta U|1\rangle \langle 1|\gamma_2\rangle + \langle 0|\delta U|2\rangle \langle 2|\gamma_2\rangle] |0\rangle. \end{aligned} \quad (\text{A.42})$$

We use again that $\langle j|\gamma_j\rangle = 1$ and then $\langle 1|\gamma_2\rangle$ needed in the second line of (A.42) is obtained from the coefficient of $|1\rangle$ given in the first line. The result is

$$\begin{aligned} |\gamma_2\rangle &= |2\rangle + |1\rangle \frac{1}{e^{-\gamma_2} - e^{-\gamma_1}} \langle 1|\delta U|2\rangle + |0\rangle \frac{1}{e^{-\gamma_2} - e^{-\gamma_0}} \langle 0|\delta U|2\rangle \\ &\quad + |0\rangle \frac{1}{e^{-\gamma_2} - e^{-\gamma_0}} \langle 0|\delta U|1\rangle \frac{1}{e^{-\gamma_2} - e^{-\gamma_1}} \langle 1|\delta U|2\rangle. \end{aligned} \quad (\text{A.43})$$

The pattern is now clear. The coefficient of each basis state in the expansion consists of all possible transitions from the basis state corresponding to the eigenstate to that basis state. After each transition appears the “propagator”, which is the reciprocal of the difference of the eigenvalues of the

eigenstate and the intermediate transition state. For $j = 3$ then we may follow this procedure to write down the result

$$\begin{aligned}
|\gamma_3\rangle &= |3\rangle + |2\rangle \frac{1}{e^{-\gamma_3} - e^{-\gamma_2}} \langle 2|\delta U|3\rangle + |1\rangle \frac{1}{e^{-\gamma_3} - e^{-\gamma_1}} \langle 1|\delta U|3\rangle \\
&\quad + |1\rangle \frac{1}{e^{-\gamma_3} - e^{-\gamma_1}} \langle 1|\delta U|2\rangle \frac{1}{e^{-\gamma_3} - e^{-\gamma_2}} \langle 2|\delta U|3\rangle \\
&\quad + |0\rangle \frac{1}{e^{-\gamma_3} - e^{-\gamma_0}} \langle 0|\delta U|3\rangle \\
&\quad + |0\rangle \frac{1}{e^{-\gamma_3} - e^{-\gamma_0}} \langle 0|\delta U|2\rangle \frac{1}{e^{-\gamma_3} - e^{-\gamma_2}} \langle 2|\delta U|3\rangle \\
&\quad + |0\rangle \frac{1}{e^{-\gamma_3} - e^{-\gamma_0}} \langle 0|\delta U|1\rangle \frac{1}{e^{-\gamma_3} - e^{-\gamma_1}} \langle 1|\delta U|3\rangle \\
&\quad + |0\rangle \frac{1}{e^{-\gamma_3} - e^{-\gamma_0}} \langle 0|\delta U|1\rangle \frac{1}{e^{-\gamma_3} - e^{-\gamma_1}} \langle 1|\delta U|2\rangle \frac{1}{e^{-\gamma_3} - e^{-\gamma_2}} \langle 2|\delta U|3\rangle.
\end{aligned} \tag{A.44}$$

Substitution of the explicit matrix elements for U_B and the rescaled Legendre polynomial basis states will yield (multiples of) the Bernoulli polynomials as eigenstates of U_B .

A.9 Bernoulli Polynomials

The Bernoulli polynomials, $B_m(x)$, may be defined from their generating function as

$$\frac{pe^{xp}}{e^p - 1} = \sum_{m=0}^{\infty} \frac{B_m(x)}{m!} p^m. \quad (\text{A.45})$$

The explicit form of the first few Bernoulli polynomials is given by (3.39). Taking the derivative with respect to x of the generating function gives

$$\frac{p^2 e^{xp}}{e^p - 1} = \sum_{m=0}^{\infty} \frac{\frac{d}{dx} B_m(x)}{m!} p^m. \quad (\text{A.46})$$

Comparing with (A.45) gives that

$$\frac{d}{dx} B_m(x) = m B_{m-1}(x), \quad (\text{A.47})$$

for $m \geq 1$ and $(d/dx)B_0(x) = 0$. Also from (A.45) we see that

$$\sum_{m=0}^{\infty} \frac{B_m(1) - B_m(0)}{m!} p^m = \frac{p(e^p - 1)}{e^p - 1} = p, \quad (\text{A.48})$$

so

$$B_m(1) - B_m(0) = \delta_{m,1}. \quad (\text{A.49})$$

Using this in conjunction with (A.47) gives

$$\int_0^1 dx B_m(x) = \delta_{m,0}. \quad (\text{A.50})$$

In Section 3.6 and elsewhere we use the Fourier expansion of $B_m(x)$ given by

$$B_m(x) = \sum_{k=-\infty}^{\infty} B_m^k e^{2\pi i k x}, \quad (\text{A.51})$$

where the Fourier coefficients are given by

$$B_m^k = \int_0^1 B_m(x) e^{-2\pi i k x}. \quad (\text{A.52})$$

For $k = 0$, using (A.50) we see that $B_m^0 = \delta_{m,0}$. By recursive use of (A.47) and repeated integration by parts of (A.52), we find

$$B_m^k = \frac{-m!}{(2\pi i k)^m}, \quad (\text{A.53})$$

for $k \neq 0$. Thus for $m \neq 0$, we have

$$B_m(x) = - \sum_{k \neq 0} \frac{m!}{(2\pi i k)^m} e^{2\pi i k x}. \quad (\text{A.54})$$

Using the Fourier expansion of the Bernoulli polynomials and the shift property, (3.12), of the Fourier basis states it is very easy to prove that the Bernoulli polynomials are eigenstates of U_B . Writing $k = 2^n(2l+1)$, as is used in (3.10) we have

$$\begin{aligned} U_B B_m(x) &= \sum_{l=-\infty}^{\infty} \sum_{n=1}^{\infty} \frac{-m!}{[2\pi i 2^n(2l+1)]^m} e^{2\pi i 2^{n-1}(2l+1)x} \\ &= \frac{1}{2^m} \sum_{l=-\infty}^{\infty} \sum_{n=0}^{\infty} \frac{-m!}{[2\pi i 2^n(2l+1)]^m} e^{2\pi i 2^n(2l+1)x} \\ &= \frac{1}{2^m} B_m(x). \end{aligned} \quad (\text{A.55})$$

A.10 Generating Function Technique

A generating function, $G(x, p)$, will define a polynomial set, $\{\phi_n(x)\}$, as

$$G(x, p) = \sum_{n=0}^{\infty} \phi_n(x) p^n. \quad (\text{A.56})$$

To determine the generating function for the eigenpolynomials of the Bernoulli map it is useful to determine the class of polynomials they belong to so that an ansatz for the generating function can be made. To this end, differentiation of an eigenpolynomial is considered.

Consider U_B and (d/dx) acting successively on a function in either order. If the derivative acts first then

$$U_B \frac{d}{dx} f(x) = \frac{1}{2} \left[f'\left(\frac{x}{2}\right) + f'\left(\frac{1+x}{2}\right) \right]. \quad (\text{A.57})$$

If U_B acts first then

$$\begin{aligned} \frac{d}{dx} U_B f(x) &= \frac{d}{dx} \left\{ \frac{1}{2} \left[f\left(\frac{x}{2}\right) + f\left(\frac{1+x}{2}\right) \right] \right\} \\ &= \frac{1}{2} \left[\frac{1}{2} f'\left(\frac{x}{2}\right) + \frac{1}{2} f'\left(\frac{1+x}{2}\right) \right] \\ &= \frac{1}{4} \left[f'\left(\frac{x}{2}\right) + f'\left(\frac{1+x}{2}\right) \right]. \end{aligned} \quad (\text{A.58})$$

So we see that U_B intertwines with the derivative operator as

$$\frac{d}{dx} U_B = \frac{1}{2} U_B \frac{d}{dx} \quad (\text{A.59})$$

Thus, if we act on an eigenstate, $\gamma_n(x)$, with eigenvalue 2^{-n} we have that

$$\frac{d}{dx} U_B \gamma_n(x) = 2^{-n} \frac{d}{dx} \gamma_n(x) = \frac{1}{2} U_B \frac{d}{dx} \gamma_n(x) \quad (\text{A.60})$$

So, $(d/dx)\gamma_n(x)$ is an eigenstate of U_B with eigenvalue $2^{-(n-1)}$, i.e., it is proportional to $\gamma_{n-1}(x)$:

$$\frac{d}{dx} \gamma_n(x) = c_{n-1} \gamma_{n-1}(x). \quad (\text{A.61})$$

This means that the eigenpolynomials belong to the class of Appell polynomials. Appell (also known as Scheffer A-type zero) polynomials, $A_n(x)$, are such that

$$\frac{d}{dx} A_n(x) = A_{n-1}(x). \quad (\text{A.62})$$

If we know the constant c_n then we can make the $\gamma_n(x)$ Appell polynomials as

$$A_n(x) = \frac{\gamma_n(x)}{\prod_{i=1}^n c_i}. \quad (\text{A.63})$$

Choosing the coefficient of x^n in $\gamma_n(x)$ as 1 we will have that $c_n = n$, for $n > 0$, so that $\gamma_n(x)/n!$ will be Appell polynomials.

The generating functions of Appell polynomials have the form

$$G(x, p) = \frac{e^{xp}}{C(p)} \quad (\text{A.64})$$

To determine the generating function, $G_B(x, p)$, of the polynomials which are the right eigenstates of the Frobenius–Perron operator of the Bernoulli map we use first that the action of U_B gives

$$U_B G_B(x, p) = \frac{1}{2} \left[G_B\left(\frac{x}{2}, p\right) + G_B\left(\frac{x+1}{2}, p\right) \right]. \quad (\text{A.65})$$

Since the polynomials are eigenstates we also have

$$U_B G_B(x, p) = \sum_{n=0}^{\infty} U_B \frac{\gamma_n(x)}{n!} p^n = \sum_{n=0}^{\infty} \frac{\gamma_n(x)}{2^n n!} p^n = G_B\left(x, \frac{p}{2}\right). \quad (\text{A.66})$$

Thus, using the form (A.64) of $G_B(x, p)$ in terms of $C_B(p)$, equating the above two expressions gives

$$\frac{1}{2} \left[\frac{e^{\frac{x}{2}p}}{C_B(p)} + \frac{e^{\frac{x+1}{2}p}}{C_B(p)} \right] = \frac{e^{x\frac{p}{2}}}{C_B(\frac{p}{2})},$$

or

$$\frac{C_B(p)}{C_B(\frac{p}{2})} = \frac{1}{2} \left[1 + e^{\frac{p}{2}} \right]. \quad (\text{A.67})$$

This functional equation may be solved by several methods. A straightforward way is to write a Taylor expansion for $C_B(p)$ and then use the functional equation to determine the coefficients.

Writing,

$$C_B(p) = \sum_{m=0}^{\infty} a_m p^m, \quad (\text{A.68})$$

the relation (A.67) between $C_B(p)$ and $C_B(\frac{p}{2})$ becomes

$$\begin{aligned} \sum_{m=0}^{\infty} a_m p^m &= \frac{1}{2} \left[1 + \sum_{k=0}^{\infty} \frac{1}{k!} \left(\frac{p}{2} \right)^k \right] \sum_{m=0}^{\infty} a_m \left(\frac{p}{2} \right)^m \\ &= \frac{1}{2} \sum_{m=0}^{\infty} \frac{a_m}{2^m} p^m + \frac{1}{2} \sum_{m=0}^{\infty} \sum_{k=0}^{\infty} \frac{a_m}{k! 2^{m+k}} p^{m+k}. \end{aligned} \quad (\text{A.69})$$

By equating powers of p on both sides of this expansion we obtain a recursion relation for the expansion coefficients as

$$a_n = \frac{1}{2} \frac{a_n}{2^n} + \frac{1}{2} \sum_{k=0}^n \frac{a_{n-k}}{k! 2^n},$$

or,

$$a_n = \frac{1}{2(2^n - 1)} \sum_{k=0}^{n-1} \frac{a_{n-k}}{k!}. \quad (\text{A.70})$$

Fixing $\gamma_0(x) = 1$ requires that $a_0 = 1$ so we obtain that $a_n = 1/(n+1)!$. This means that

$$C_B(p) = \sum_{m=0}^{\infty} \frac{p^m}{(m+1)!} = \frac{e^p - 1}{p}, \quad (\text{A.71})$$

so

$$G_B(x, p) = \frac{pe^{xp}}{e^p - 1}, \quad (\text{A.72})$$

which is recognized as the generating function for the Bernoulli polynomials.

To determine the duals of the eigenpolynomials we utilize a theorem of Boas and Buck (referred to below). For one-dimensional maps whose right eigenstates belong to the class of Appell polynomials, a function $f(x)$, which is entire and of exponential type¹ $\tau < r$, may be expanded in terms of the Appell polynomials as

$$f(x) = \sum_{n=0}^{\infty} \varphi_n(x) \mathcal{L}_n[f], \quad (\text{A.73})$$

where $\mathcal{L}_n[f]$ is the functional

$$\mathcal{L}_n[f] = \frac{1}{2\pi i} \oint_{\Omega} dp p^n C(p) F(p). \quad (\text{A.74})$$

The contour Ω is the circle $|p| = \omega$ with $\tau < \omega < r$ and $F(p)$ the Laplace transform of $f(x)$ as

$$F(p) = \int_0^{\infty} dx e^{-px} f(x), \quad (\text{A.75})$$

so that

$$f(x) = \frac{1}{2\pi i} \oint_{\Omega} dp e^{xp} F(p). \quad (\text{A.76})$$

¹A complex function $f(z)$ is of exponential type τ if for all $\epsilon > 0$, there exists a constant $A_\epsilon(f) > 0$, such that $|f(z)| \leq A_\epsilon \exp[(\tau + \epsilon)|z|]$; for all complex numbers z .

Using (A.71) in (A.74) the left eigenfunctionals of U_B are thus given by

$$\mathcal{L}_n[f] = \frac{1}{2\pi i} \oint_{\Omega} dp p^{n-1} (e^p - 1) F(p). \quad (\text{A.77})$$

But from (A.76), for $m \geq 0$

$$\frac{1}{2\pi i} \oint_{\Omega} dp p^m e^p F(p) = \left. \frac{d^m f}{dx^m} \right|_{x=1}, \quad (\text{A.78})$$

and

$$\frac{1}{2\pi i} \oint_{\Omega} dp p^m F(p) = \left. \frac{d^m f}{dx^m} \right|_{x=0}, \quad (\text{A.79})$$

so that for $n \geq 1$ (A.77) yields

$$\mathcal{L}_n[f] = f^{(n-1)}(1) - f^{(n-1)}(0). \quad (\text{A.80a})$$

Note that the factor of $1/n!$ that appears in the left state (3.55a) has appeared in this derivation on the right state (see (A.63)) so that the eigenpolynomials, $B_n(x)/n!$, were Appell polynomials. For $n = 0$ we have that

$$\mathcal{L}_0[f] = \int_0^1 dx f(x). \quad (\text{A.80b})$$

Thus, for all n the left eigenfunctional is

$$\mathcal{L}_n[f] = \int_0^1 dx f^{(n)}(x). \quad (\text{A.81})$$

The results on polynomial expansions of analytic functions employed by the generating function technique are from

- R.P. Boas, Jr. and R.C. Buck, *Polynomial Expansions of Analytic Functions* (Springer-Verlag, Berlin 1964).

This approach has been used mainly by Gaspard, first in his paper cited in Chapter 3; his *Chaos* paper cited in Chapter 2; and his *Physics Letters A* paper cited in Chapter 6.

A.11 Jordan States

First we show that the expression (4.57) for the Jordan state $|\lambda_{2n}\rangle$ corresponding to the double pole at $z = \lambda_{2n}$ satisfies the Jordan state equation (4.58a), where the eigenstate is given by (4.56). From (4.58a) we need to check that

$$(U_J - \lambda_{2n})|\lambda_{2n}\rangle = |\lambda_{2n-1}\rangle. \quad (\text{A.82})$$

Using (4.57) we have

$$(U_J - \lambda_{2n})|\lambda_{2n}\rangle = \frac{1}{\langle \tilde{B}_{2n-1} | \delta U | B_{2n} \rangle} \frac{1}{2\pi i} \oint_{z=\lambda_{2n}} dz \frac{z - \lambda_{2n}}{z - U_J} |B_{2n}\rangle. \quad (\text{A.83})$$

First we expand the resolvent of U_J acting on $|B_{2n}\rangle$ and insert a complete set of states as

$$\begin{aligned} \frac{1}{z - U_J} |B_{2n}\rangle &= \sum_{m=0}^{\infty} \left(\frac{1}{z - U_0} \delta U \right)^m \frac{1}{z - U_0} |B_{2n}\rangle \\ &= \frac{1}{z - \lambda_{2n}} |B_{2n}\rangle \\ &\quad + \sum_{m=1}^{\infty} \sum_{k=0}^{2n-1} \left(\frac{1}{z - U_0} \delta U \right)^{m-1} \frac{1}{z - U_0} |B_k\rangle \langle \tilde{B}_k | \delta U | B_{2n} \rangle \frac{1}{z - \lambda_{2n}} \\ &= \frac{1}{z - \lambda_{2n}} |B_{2n}\rangle \\ &\quad + \sum_{m=0}^{\infty} \left(\frac{1}{z - U_0} \delta U \right)^m |B_{2n-1}\rangle \langle \tilde{B}_{2n-1} | \delta U | B_{2n} \rangle \frac{1}{(z - \lambda_{2n})^2} \\ &\quad + \sum_{m=0}^{\infty} \sum_{k=0}^{2n-2} \left(\frac{1}{z - U_0} \delta U \right)^m \frac{1}{z - U_0} |B_k\rangle \langle \tilde{B}_k | \delta U | B_{2n} \rangle \frac{1}{z - \lambda_{2n}}, \end{aligned} \quad (\text{A.84})$$

where all of the singularities at λ_{2n} have been made explicit. Using this in (A.83) only the middle term contributes since the other two terms multiplied by $z - \lambda_{2n}$ are regular at $z = \lambda_{2n}$. We then rewrite $(z - \lambda_{2n})^{-1}|B_{2n-1}\rangle$ as $(z - U_0)^{-1}|B_{2n-1}\rangle$ giving

$$\begin{aligned} (U_J - \lambda_{2n})|\lambda_{2n}\rangle &= \frac{1}{2\pi i} \oint_{z=\lambda_{2n}} dz \sum_{m=0}^{\infty} \left(\frac{1}{z - U_0} \delta U \right)^m \frac{1}{z - U_0} |B_{2n-1}\rangle \\ &= \frac{1}{2\pi i} \oint_{z=\lambda_{2n}} dz \frac{1}{z - U_J} |B_{2n-1}\rangle = |\lambda_{2n-1}\rangle, \end{aligned} \quad (\text{A.85})$$

demonstrating (A.82) and thus (4.58a).

To obtain the formal expression (4.59) for the Jordan states we use (A.84) in the resolvent expression (4.57) giving

$$\begin{aligned} |\lambda_{2n}\rangle &= \frac{1}{\langle \tilde{B}_{2n-1} | \delta U | B_{2n} \rangle} \frac{1}{2\pi i} \oint_{z=\lambda_{2n}} dz \left\{ \frac{1}{z - \lambda_{2n}} |B_{2n}\rangle \right. \\ &\quad + \left(1 + \frac{1}{z - U_J} \delta U \right) |B_{2n-1}\rangle \langle \tilde{B}_{2n-1}| \frac{1}{(z - \lambda_{2n})^2} \delta U |B_{2n}\rangle \\ &\quad \left. + \sum_{k=0}^{2n-2} \frac{1}{z - U_J} |B_k\rangle \langle \tilde{B}_k| \frac{1}{z - \lambda_{2n}} \delta U |B_{2n}\rangle \right\}. \end{aligned} \quad (\text{A.86})$$

Evaluating the residues gives

$$\begin{aligned} |\lambda_{2n}\rangle &= \frac{1}{\langle \tilde{B}_{2n-1} | \delta U | B_{2n} \rangle} \left\{ |B_{2n}\rangle + \sum_{k=0}^{2n-2} \frac{1}{\lambda_{2n} - U_J} |B_k\rangle \langle \tilde{B}_k| \delta U |B_{2n}\rangle \right. \\ &\quad \left. - \frac{\langle \tilde{B}_{2n-1} | \delta U | B_{2n} \rangle}{(\lambda_{2n} - U_J)^2} \delta U |B_{2n-1}\rangle \right\}. \end{aligned} \quad (\text{A.87})$$

We then use the completeness of the Bernoulli basis states to replace the sum over k as

$$\sum_{k=0}^{2n-2} |B_k\rangle \langle \tilde{B}_k| = 1 - |B_{2n-1}\rangle \langle \tilde{B}_{2n-1}|, \quad (\text{A.88})$$

to yield

$$\begin{aligned} |\lambda_{2n}\rangle &= \frac{1}{\langle \tilde{B}_{2n-1} | \delta U | B_{2n} \rangle} \left\{ |B_{2n}\rangle - \frac{\langle \tilde{B}_{2n-1} | \delta U | B_{2n} \rangle}{\lambda_{2n} - U_J} \frac{1}{\lambda_{2n} - U_J} \delta U |B_{2n-1}\rangle \right. \\ &\quad \left. + \frac{1}{\lambda_{2n} - U_J} [1 - |B_{2n-1}\rangle \langle \tilde{B}_{2n-1}|] \delta U |B_{2n}\rangle \right\}. \end{aligned} \quad (\text{A.89})$$

Rearranging gives the expression (4.59). Introduction of (A.88) leads to ill-defined terms in (A.89) involving $(\lambda_{2n} - U_J)^{-1} |B_{2n-1}\rangle$. These terms cancel so that (A.89) makes sense as a whole.

The self-consistent equation (4.60) satisfied by the Jordan states may be derived from the formal expression (4.59). We insert complete sets of states and separate out irregular terms as

$$|\lambda_{2n}\rangle = c_{2n}^{-1} |B_{2n}\rangle + c_{2n}^{-1} \sum_{k=0}^{2n-2} |B_k\rangle \langle \tilde{B}_k| \frac{1}{\lambda_{2n} - U_J} \delta U |B_{2n}\rangle$$

$$\begin{aligned}
& + c_{2n}^{-1} |B_{2n-1}\rangle \langle \tilde{B}_{2n-1}| \frac{1}{\lambda_{2n} - U_J} \delta U |B_{2n}\rangle \\
& - \sum_{k=0}^{2n-2} |B_k\rangle \langle \tilde{B}_k| \frac{1}{\lambda_{2n} - U_J} \left(1 + \frac{1}{\lambda_{2n} - U_J} \delta U \right) |B_{2n-1}\rangle \\
& - |B_{2n-1}\rangle \langle \tilde{B}_{2n-1}| \frac{1}{\lambda_{2n} - U_J} \left(1 + \frac{1}{\lambda_{2n} - U_J} \delta U \right) |B_{2n-1}\rangle,
\end{aligned} \tag{A.90}$$

where $c_{2n} = \langle \tilde{B}_{2n-1} | \delta U | B_{2n} \rangle$. Similar to (3.36) we have that

$$\begin{aligned}
\langle \tilde{B}_k | \frac{1}{\lambda_{2n} - U_J} \delta U | B_{2n} \rangle & = \langle \tilde{B}_k | \frac{1}{\lambda_{2n} - U_0} (\lambda_{2n} - U_0) \frac{1}{\lambda_{2n} - U_J} \delta U | B_{2n} \rangle \\
& = \frac{1}{\lambda_{2n} - \lambda_k} \langle \tilde{B}_k | (\lambda_{2n} - U_J + \delta U) \frac{1}{\lambda_{2n} - U_J} \delta U | B_{2n} \rangle \\
& = \frac{1}{\lambda_{2n} - \lambda_k} \langle \tilde{B}_k | \delta U \left(1 + \frac{1}{\lambda_{2n} - U_J} \delta U \right) | B_{2n} \rangle,
\end{aligned} \tag{A.91}$$

and also that

$$\begin{aligned}
& \langle \tilde{B}_k | \frac{1}{\lambda_{2n} - U_J} \left(1 + \frac{1}{\lambda_{2n} - U_J} \delta U \right) | B_{2n-1} \rangle \\
& = \langle \tilde{B}_k | \frac{1}{\lambda_{2n} - U_0} (\lambda_{2n} - U_0) \frac{1}{\lambda_{2n} - U_J} \left(1 + \frac{1}{\lambda_{2n} - U_J} \delta U \right) | B_{2n-1} \rangle \\
& = \frac{1}{\lambda_{2n} - \lambda_k} \langle \tilde{B}_k | (\lambda_{2n} - U_J + \delta U) \frac{1}{\lambda_{2n} - U_J} \left(1 + \frac{1}{\lambda_{2n} - U_J} \delta U \right) | B_{2n-1} \rangle \\
& = \frac{1}{\lambda_{2n} - \lambda_k} \langle \tilde{B}_k | \left(1 + \delta U \frac{1}{\lambda_{2n} - U_J} \right) \left(1 + \frac{1}{\lambda_{2n} - U_J} \delta U \right) | B_{2n-1} \rangle.
\end{aligned} \tag{A.92}$$

Using both of these in (4.59) and a few manipulations yields the relation (4.60).

A.12 Dual States of Jordan States

Here we extend the discussion in Appendix A.4 to the case of Jordan blocks. We start with a function expanded in terms of the Jordan canonical states (which includes eigenstates) of U as

$$|f\rangle = \sum_n c_n |\phi_n\rangle. \quad (\text{A.93})$$

Assuming that the dual states form a bi-orthonormal set with the right states as $\langle \tilde{\phi}_m | \phi_n \rangle = \delta_{mn}$ gives the usual expression for the expansion coefficients of

$$c_n = \langle \tilde{\phi}_n | f \rangle. \quad (\text{A.94})$$

Without loss of generality we assume that there is one Jordan block of size $l + 1$ from $n = k$ to $n = k + l$ and that the rest of U is diagonal. Then

$$U|f\rangle = \sum_{n=0}^k c_n \lambda_n |\phi_n\rangle + \sum_{n=k+1}^{k+l} c_n (\lambda_n |\phi_n\rangle + |\phi_{n-1}\rangle) + \sum_{n=k+l+1}^{\infty} c_n \lambda_n |\phi_n\rangle. \quad (\text{A.95})$$

Acting on this with $\langle \tilde{\phi}_m |$ and then using (A.94) gives

$$\begin{aligned} \langle \tilde{\phi}_m | U | f \rangle &= \begin{cases} \lambda_m c_m, & m < k \\ \lambda_m c_m + c_{m+1}, & m = k, \dots, k+l-1 \\ \lambda_m c_m, & m \geq k+l \end{cases} \\ &= \begin{cases} \lambda_m \langle \tilde{\phi}_m | f \rangle, & m < k \text{ or } m \geq k+l \\ \lambda_m \langle \tilde{\phi}_m | f \rangle + \langle \tilde{\phi}_{m+1} | f \rangle, & m = k, \dots, k+l-1. \end{cases} \quad (\text{A.96}) \end{aligned}$$

Since $|f\rangle$ is arbitrary we have then that

$$\begin{aligned} \langle \tilde{\phi}_m | U &= \lambda_m \langle \tilde{\phi}_m |, & m < k \text{ or } m \geq k+l \\ \langle \tilde{\phi}_m | U &= \lambda_m \langle \tilde{\phi}_m | + \langle \tilde{\phi}_{m+1} |, & m = k, \dots, k+l-1, \end{aligned} \quad (\text{A.97})$$

showing that the left states of U (or the right states of U^\dagger) also are Jordan states (within the block) but with the location of the eigenstate being here at the opposite end of the block than the right states.

A.13 Shift Polynomial Duals

As noted, we just need to determine the dual of the vacuum state since we can apply U_A^\dagger successively on it to get the higher-order duals. We suppose that a generic shift polynomial is expanded in terms of the Bernoulli polynomials as

$$\phi_{2n-1}(x) = \sum_{j=1}^n b_{2j-1}^{(2n-1)} B_{2j-1}(x). \quad (\text{A.98})$$

The vacuum dual state, $\tilde{\phi}_1(x)$ satisfies

$$\langle \tilde{\phi}_1 | \phi_{2n-1} \rangle = \delta_{1,n}. \quad (\text{A.99})$$

In order to determine it we expand $\tilde{\phi}_1(x)$ in terms of the duals of the Bernoulli polynomials as

$$\tilde{\phi}_1(x) = \sum_{k=1}^{\infty} a_{2k-1} \tilde{B}_{2k-1}(x) \quad (\text{A.100})$$

and then impose the orthogonality condition (A.99) to determine the expansion coefficients.

First, we must have that $\langle \tilde{\phi}_1 | \phi_1 \rangle = 1$, but

$$\langle \tilde{\phi}_1 | \phi_1 \rangle = a_1 b_1^{(1)}, \quad (\text{A.101})$$

so that

$$a_1 = \frac{1}{b_1^{(1)}}. \quad (\text{A.102})$$

Next we impose that $\langle \tilde{\phi}_1 | \phi_3 \rangle = 0$, but

$$\langle \tilde{\phi}_1 | \phi_3 \rangle = a_1 b_1^{(3)} + a_3 b_3^{(3)}. \quad (\text{A.103})$$

Using the result (A.102) for a_1 and solving for a_3 here then gives

$$a_3 = -\frac{1}{b_1^{(1)}} \frac{b_1^{(3)}}{b_3^{(3)}}. \quad (\text{A.104})$$

Carrying on this procedure gives the result (4.88).

A.14 Symmetries in a Class of One-Dimensional Maps

Here we employ symmetry and the algebraic technique to obtain explicit results for a class of piecewise-linear one-dimensional maps on the unit interval. The class consists of maps with linear branches where each branch maps onto the unit interval and the absolute value of the slope of every branch is the same. Most of the one-dimensional maps studied in this book belong to this class. Within this class of uniformly chaotic maps (i.e., the stretching factor is the same everywhere) there is rich variety of spectra in the generalized decomposition. This is easy to determine by just looking at the action of the Frobenius–Perron operator on monomials.

For a general map with r branches belonging to the class we denote the Frobenius–Perron operator as $U_{[r]}$. Assuming there are p branches with positive slope $+r^{-1}$ and q branches with negative slope $-r^{-1}$ we have that

$$\begin{aligned} U_{[r]} x^n &= \frac{1}{r} \left[p \left(\frac{x}{r} \right)^n + q(-1)^n \left(\frac{x}{r} \right)^n + \dots \right] \\ &= \begin{cases} \frac{1}{r^n} x^n + \dots, & n \text{ even} \\ \frac{p-q}{r} \frac{1}{r^n} x^n + \dots, & n \text{ odd}, \end{cases} \end{aligned} \quad (\text{A.105})$$

where the remaining terms consist of lower-order monomials and we used that $p + q = r$. Thus the eigenvalues associated with polynomial eigenstates are

$$\left\{ 1, \frac{p-q}{r^2}, \frac{1}{r^2}, \frac{p-q}{r^4}, \frac{1}{r^4}, \dots \right\}. \quad (\text{A.106})$$

There are only two ways to get degenerate eigenvalues. First if $p - q = 1$, so that there is one more positive branch than negative branch, the eigenvalues are two-fold degenerate as

$$\left\{ 1, \frac{1}{r^2}, \frac{1}{r^2}, \frac{1}{r^4}, \frac{1}{r^4}, \dots \right\}. \quad (\text{A.107})$$

The N map and 3-branch map with Jordan blocks studied in Section 4.2.2 are examples of this case. As was seen there the degeneracy may or may not be associated with a Jordan block. The other case of degeneracy is when $p - q = 0$ so that 0 is an eigenvalue of infinite degeneracy (associated with odd-order polynomial states) as

$$\left\{ 1, 0, \frac{1}{r^2}, 0, \frac{1}{r^4}, \dots \right\}. \quad (\text{A.108})$$

Examples of this case are the tent and V map and the map with polynomial shift states studied in Section 4.2.3. (It can be shown that for the class under consideration there are no finite size Jordan blocks associated with the degenerate zero eigenvalue.)

In order to determine something about the eigenstates we notice that the projector, P_+ , onto the space of even functions (with respect to the midpoint of the unit interval) given in (4.2) intertwines any $U_{[r]}$ with the Frobenius–Perron operator, U_r , of the r -adic map (3.59) (where all the r branches have slope $+r$) as

$$U_r P_+ = P_+ U_{[r]}. \quad (\text{A.109})$$

First we use this relation to tell us something about the odd-order polynomial states of $U_{[r]}$. Unless $p - q = 0$, and the infinitely degenerate zero eigenvalue is associated with an infinite size Jordan block, the odd-order states are eigenstates. Then

$$U_{[r]} \varphi_{2n-1}(x) = \frac{p - q}{r^{2n}} \varphi_{2n-1}(x). \quad (\text{A.110})$$

Acting with (A.109) on $\varphi_{2n-1}(x)$ and using (A.110) gives

$$U_r [P_+ \varphi_{2n-1}(x)] = \frac{p - q}{r^{2n}} [P_+ \varphi_{2n-1}(x)]. \quad (\text{A.111})$$

Since we know that U_r only has polynomial eigenstates of degree m with associated eigenvalues r^{-m} the only solution to (A.111) is

$$P_+ \varphi_{2n-1}(x) = 0, \quad (\text{A.112})$$

showing that the odd-order eigenstates of $U_{[r]}$ are entirely in the P_- subspace. If $\varphi_{2n-1}(x)$ is a shift polynomial then (A.112) also holds since then the intertwining relation (A.109) leads to $U_r[P_+ \varphi_{2n-1}(x)] = P_+ \varphi_{2n-3}(x)$ for $n \geq 2$ and $U_r[P_+ \varphi_1(x)] = 0$, which implies $P_+ \varphi_1(x) = 0$ and by induction (A.112).

Unless $p - q = 1$ and there are 2×2 Jordan blocks the even-order polynomial states of $U_{[r]}$ are eigenstates. Then (A.109) gives

$$U_r [P_+ \varphi_{2n}(x)] = r^{-2n} [P_+ \varphi_{2n}(x)], \quad (\text{A.113})$$

so that $P_+ \varphi_{2n}(x)$ is an eigenpolynomial of U_r with eigenvalue r^{-2n} , which we know to be the Bernoulli polynomial of degree $2n$, so

$$P_+ \varphi_{2n}(x) = B_{2n}(x). \quad (\text{A.114})$$

If $\varphi_{2n}(x)$ is a Jordan state then (A.109) gives

$$U_r[P_+ \varphi_{2n}(x)] = r^{-2n}[P_+ \varphi_{2n}(x)] + P_+ \varphi_{2n-1}(x), \quad (\text{A.115})$$

but we know from above that $P_+ \varphi_{2n-1}(x) = 0$ so we again obtain (A.114).

That's all we can determine about the right states unless more about the particular $U_{[r]}$ is given. The even-order duals though may be completely determined. The adjoint of the relation (A.109) is

$$U_{[r]}^\dagger P_+ = P_+ U_r^\dagger. \quad (\text{A.116})$$

Acting with this on $\tilde{B}_{2n}(x)$ and using that it is an eigenstate of U_r^\dagger and is entirely in P_+ gives

$$U_{[r]}^\dagger \tilde{B}_{2n}(x) = r^{-2n} \tilde{B}_{2n}(x), \quad (\text{A.117})$$

which shows that the even-order left eigenstates of any map in the class $U_{[r]}$ are the Bernoulli polynomial duals.

If the map from the class we are considering is symmetric so that the map on $[\frac{1}{2}, 1]$ is the mirror image of the map on $[0, \frac{1}{2}]$ then it must have an even number of branches and its Frobenius–Perron operator satisfies

$$U_{[r]} = U_{[r]} R, \quad (\text{A.118})$$

where R is the reflection operator (4.1). Then we may determine all the elements of its generalized spectral decomposition.

Denoting the Frobenius–Perron operator of a map from this symmetric subclass as U_S , we have from (A.118) that

$$U_S P_- = 0, \quad (\text{A.119})$$

so the odd-order eigenpolynomials of U_S (belonging to the null space) may be taken as any set of odd-symmetric polynomials complete in the P_- subspace. Let us denote an even-order eigenpolynomial of U_S as $\phi_{2n}(x)$. From above we know that the P_+ projection of $\phi_{2n}(x)$ is $B_{2n}(x)$ so we have

$$\phi_{2n}(x) = B_{2n}(x) + P_- \phi_{2n}(x). \quad (\text{A.120})$$

Since $U_S P_- = 0$, acting on $\phi_{2n}(x)$ with U_S is thus equivalent to acting on just $B_{2n}(x)$, i.e.,

$$U_S \phi_{2n}(x) = U_S B_{2n}(x). \quad (\text{A.121})$$

But $\phi_{2n}(x)$ is an eigenpolynomial, with eigenvalue λ_{2n} , so

$$U_S \phi_{2n}(x) = \lambda_{2n} \phi_{2n}(x). \quad (\text{A.122})$$

Note that even though U_S annihilates the P_- component of whatever it acts on, it creates a P_- component out of its action so that an eigenstate should have a P_- component. Comparing (A.121) and (A.122) gives the eigenpolynomial as

$$\phi_{2n}(x) = \lambda_{2n}^{-1} U_S B_{2n}(x). \quad (\text{A.123})$$

As we showed above for the general class, the even-order duals are just the Bernoulli duals. The odd-order duals may then be determined from the completeness relation as was done in Section 4.1.1 for the tent map. Note that the tent and V maps are the simplest examples of maps from the symmetric subclass.

A.15 Invariant Measure of the Cantor Map

Here we show that the measure given by $\mu_C([a, b]) = \int_a^b dF_C(x)$, where $F_C(x)$ satisfies (4.93), is an invariant measure for the Cantor map, $S_C(x)$, given by (4.92). The inverse image, under the Cantor map, of the interval $[a, b]$ is

$$S_C^{-1}[a, b] = \left[\frac{a}{3}, \frac{b}{3} \right) \cup \left[\frac{2}{3} + \frac{a}{3}, \frac{2}{3} + \frac{b}{3} \right). \quad (\text{A.124})$$

We thus have that

$$\begin{aligned} \mu_C(S_C^{-1}[a, b]) &= \int_{S_C^{-1}[a, b]} dF_C(x) \\ &= \int_{a/3}^{b/3} dF_C(x) + \int_{(2+a)/3}^{(2+b)/3} dF_C(x) \\ &= \frac{1}{2} \int_{a/3}^{b/3} dF_C(3x) + \frac{1}{2} \int_{(2+a)/3}^{(2+b)/3} dF_C(3x - 2), \end{aligned} \quad (\text{A.125})$$

where we used (4.93) in the last line. Making the substitution $y = 3x$ in the first term on the last line and $y = 3x - 2$ in the second term gives

$$\mu_C(S_C^{-1}[a, b]) = \frac{1}{2} \int_a^b dF_C(y) + \frac{1}{2} \int_a^b dF_C(y) = \int_a^b dF_C(y) = \mu_C[a, b], \quad (\text{A.126})$$

completing the demonstration.

A.16 Explicit Form of $\eta_n(x)$

The function $\eta_n(x)$ used in the calculation of the left states of U_C is given by

$$\begin{aligned}\eta_n(x) &= \langle 1 | U_C | B_1 \rangle - \langle 1 | U_C | \mathcal{B}_1 \rangle \mathbf{e}(x) \\ &= \langle U_C^\dagger 1 | B_1 \rangle - \langle U_C^\dagger 1 | \mathcal{B}_1 \rangle \mathbf{e}(x) \\ &= \int_0^1 dx' (U_C^\dagger 1)[B_1(x') - B_1(x' - x)].\end{aligned}\quad (\text{A.127})$$

The effect of U_C^\dagger removes the integration from $1/3$ to $2/3$. Now, because the argument of B_1 must be taken modulo 1 we have

$$B_1(x' - x) = \begin{cases} x' - x + \frac{1}{2} & x' < x \\ x' - x - \frac{1}{2} & x' > x, \end{cases}\quad (\text{A.128})$$

so that

$$B_1(x') - B_1(x' - x) = \begin{cases} x - 1 & x' < x \\ x & x' > x. \end{cases}\quad (\text{A.129})$$

Thus, for $x < 1/3$

$$\begin{aligned}\eta_n(x) &= \int_0^x dx' (x - 1) + \int_x^{1/3} dx' x + \int_{2/3}^1 dx' x \\ &= -\frac{1}{3}x.\end{aligned}\quad (\text{A.130})$$

For $1/3 < x < 2/3$

$$\begin{aligned}\eta_n(x) &= \int_0^{1/3} dx' (x - 1) + \int_{2/3}^1 dx' x \\ &= -\frac{1}{3}(1 - 2x).\end{aligned}\quad (\text{A.131})$$

For $2/3 < x < 1$

$$\begin{aligned}\eta_n(x) &= \int_0^{1/3} dx' (x - 1) + \int_{2/3}^x dx' (x - 1) + \int_x^1 dx' x \\ &= -\frac{1}{3}(x - 1).\end{aligned}\quad (\text{A.132})$$

A.17 Decomposition with Asymptotic Periodicity

Here we consider a system that does not approach a unique equilibrium state but rather approaches a steady state with oscillating modes. This is known as asymptotic periodicity. A simple system with such behavior is the tent map with height $\sqrt{2}/2$ given by

$$S_F(x) = \begin{cases} \sqrt{2}x & 0 \leq x \leq \frac{1}{2} \\ \sqrt{2}(1-x) & \frac{1}{2} \leq x < 1. \end{cases} \quad (\text{A.133})$$

We will exploit the self-similarity of a part of this map to the tent map with unit height (and the V map) by using topological conjugacy.

Unlike the tent map with unit height studied in Section 4.1.1 the map (A.133) does not have images on the whole unit interval. The dynamics is

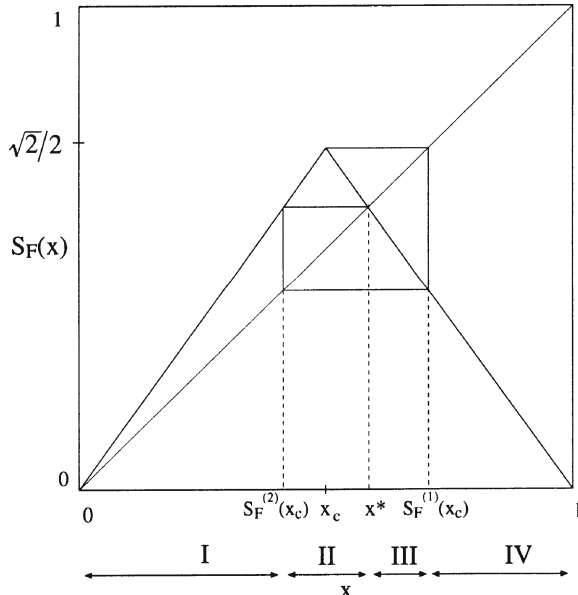


Figure A.2: The tent map with height $\sqrt{2}/2$ and iterates of the critical point of the map defining the four intervals around which the dynamics is organized.

organized around four intervals determined by the trajectory of the critical point, $x_c = 1/2$, of the map. At the third iteration the critical trajectory settles onto the fixed point, $x^* = 2 - \sqrt{2}$. The four intervals: $I = [0, S_F^{(2)}(x_c)]$,

$\text{II} = [S_F^{(2)}(x_c), S_F^{(3)}(x_c)]$, $\text{III} = [S_F^{(3)}(x_c), S_F^{(1)}(x_c)]$ and $\text{IV} = [S_F^{(1)}(x_c), 1]$, define a Markov partition² for the map. Any point in the interior of interval IV is mapped into interval I in one iteration. Under successive iterations all points in the interior of I are eventually mapped into II. Any point in interval II will fall into interval III in one iteration and any point in interval III will fall into II in one iteration. Thus the intervals II and III together form the attracting set Ω . The map and the intervals described above are shown in Figure A.2

The Frobenius–Perron operator for the map (A.133) acts on a density defined on the unit interval as

$$U_F \rho(x) = \frac{1}{\sqrt{2}} \left[\rho\left(\frac{x}{\sqrt{2}}\right) + \rho\left(\frac{\sqrt{2}-x}{\sqrt{2}}\right) \right] \Theta\left(\frac{\sqrt{2}}{2} - x\right), \quad (\text{A.134})$$

where

$$\Theta(a-x) = \begin{cases} 1 & x \leq a \\ 0 & x > a. \end{cases} \quad (\text{A.135})$$

The step function appears here because the map has no inverse images for $x > \sqrt{2}/2$, but U_F still preserves probability. Under time evolution a general initial density continuous over the unit interval develops discontinuities at the endpoints of the four intervals described above. We thus choose a function space to consider U_F in as the space of piecewise-polynomial functions where the pieces are the four intervals described above.

The invariant density has support only on the attractor, $\Omega \equiv \text{II} \cup \text{III}$, on which the dynamics is closed as iterates in Ω stay there. For the consideration of long-time averages, such as time correlation functions, it is sufficient to just consider the dynamics on the attractor. But in the general context of a nonequilibrium density the transients may not be neglected. We will first consider the map just on Ω and will then briefly consider decay modes associated with the transient dynamics from I and IV onto Ω . Ironically, the modes associated with the transients off the attractor are the slowest decay modes in this system.

To consider the map on Ω it is convenient to rescale the map there back to the full unit interval. The linear function that makes this stretch is

$$\phi(x) = (2/x^*)x - \sqrt{2}, \quad (\text{A.136})$$

²A finite partition $\mathcal{P} = \{P_1, \dots, P_n\}$ is Markov for a map S if $S(P_i)$ is the union of some P_j 's for all $i \in \{1, 2, \dots, n\}$.

where $S_F^{(2)}(x_c) \leq x < S_F^{(1)}(x_c)$. The part of the map S_F on Ω transforms to $S_L = \phi \circ S_F \circ \phi^{-1}$, and is given by

$$S_L(x) = \begin{cases} \sqrt{2}x + x^* & 0 \leq x < x^*/2 \\ \sqrt{2}(1-x) & x^*/2 \leq x < 1, \end{cases} \quad (\text{A.137})$$

where $x^* = 2 - \sqrt{2}$ is the fixed point of the map $S_L(x)$, which is the same as the fixed point of the map $S_F(x)$. Under the transformation (A.136) the intervals II and III are stretched to the intervals $A \equiv [0, x^*)$ and $B \equiv [x^*, 1)$ respectively. Like the flipping between II and III under S_F any point in A

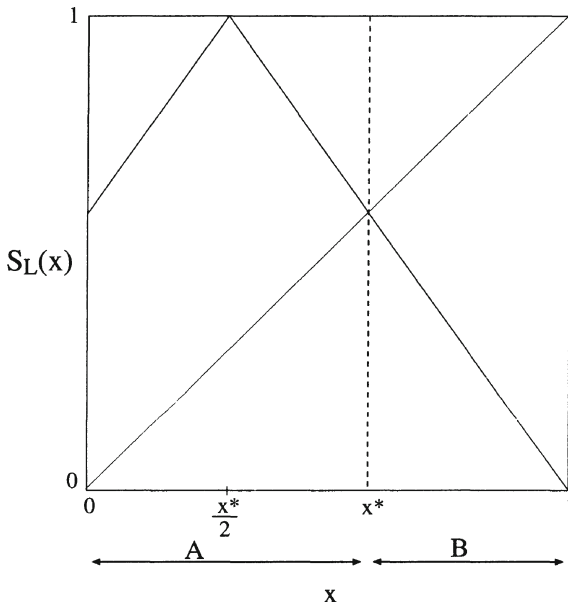


Figure A.3: The rescaled tent map, $S_L(x)$

goes into B under S_L and vice-versa. This is easily seen in Figure A.3.

The Frobenius–Perron operator corresponding to the rescaled map S_L acts on a density as

$$U_L \rho(x) = \frac{1}{\sqrt{2}} \left[\rho \left(\frac{\sqrt{2} - x}{\sqrt{2}} \right) + \rho \left(\frac{x - x^*}{\sqrt{2}} \right) \Theta(x - x^*) \right]. \quad (\text{A.138})$$

Just as trajectory iterates shuttle back and forth between A and B, elements of the density supported on these intervals oscillate between them as well.

This suggests that a simpler analysis may be obtained from considering the map corresponding to two iterations of S_L , thereby eliminating the oscillation. This map, $S_G \equiv S_L \circ S_L$, is given by

$$S_G(x) = \begin{cases} -2x + x^* & 0 \leq x < x^*/2 \\ 2x - x^* & x^*/2 \leq x < (1+x^*)/2 \\ -2x + (2+x^*) & (1+x^*)/2 \leq x < 1. \end{cases} \quad (\text{A.139})$$

As expected, S_G is metrically decomposable over $[0, 1]$ into the two intervals A and B.

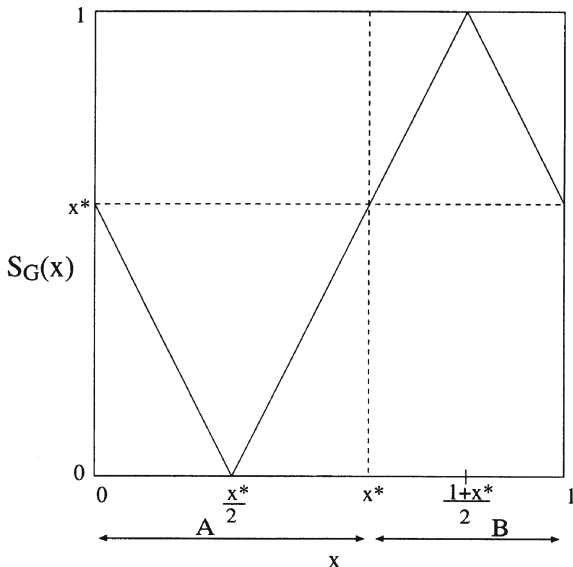


Figure A.4: The square of the rescaled tent map

As is clear from Figure A.4, S_G on A is just a rescaling of the V map considered in Section 4.1.2 and the map on B is a rescaling of the tent map with unit height considered in Section 4.1.1. The map S_A is topologically conjugate to the V map as

$$S_A(x) = \phi_A^{-1}(x) \circ S_V(x) \circ \phi_A(x), \quad (\text{A.140})$$

where the conjugating function $\phi_A(x)$ is

$$\phi_A(x) = x/x^*, \quad (\text{A.141})$$

for $x \in [0, x^*]$. Similarly, S_B is topologically conjugate to the tent map with unit height as

$$S_B(x) = \phi_B^{-1}(x) \circ S_T(x) \circ \phi_B(x), \quad (\text{A.142})$$

where the conjugating function $\phi_B(x)$ is

$$\phi_B(x) = \left(\sqrt{2}/x^* \right) x - \sqrt{2}, \quad (\text{A.143})$$

for $x \in [x^*, 1]$.

Following the discussion in Section 4.4 on how the right eigenvectors transform under a topological conjugacy, and using the right eigenvectors of the tent and V maps we find the right eigenvectors of the Frobenius–Perron operators corresponding to S_A and S_B to be

$$|2^{-2n}\rangle_A = \frac{1}{x^*} B_{2n} \left(\frac{x^* - x}{2x^*} \right) \chi_A \quad (\text{A.144a})$$

$$|0_{2n+1}\rangle_A = \frac{1}{x^*} E_{2n+1} \left(\frac{x}{x^*} \right) \chi_A \quad (\text{A.144b})$$

$$|2^{-2n}\rangle_B = \frac{\sqrt{2}}{x^*} B_{2n} \left(\frac{x - x^*}{\sqrt{2}x^*} \right) \chi_B \quad (\text{A.145a})$$

$$|0_{2n+1}\rangle_B = \frac{\sqrt{2}}{x^*} E_{2n+1} \left(\frac{\sqrt{2}}{x^*} (x - x^*) \right) \chi_B, \quad (\text{A.145b})$$

where the associated eigenvalue is the argument of the ket vector with $|0_{2n+1}\rangle$ meaning a null eigenpolynomial of degree $2n + 1$ and χ_A and χ_B are indicator functions on the intervals A and B respectively. Due to the metric decomposability of S_G these states are eigenstates of U_G as well.

Similarly, the generalized left eigenvectors of the Frobenius–Perron operators corresponding to S_A and S_B are

$$\langle 2^{-2n}|_A = \frac{(-1)^{2n-1} (2x^*)^{2n}}{(2n)!} \left[\delta_-^{(2n-1)}(x - x^*) - \delta_+^{(2n-1)}(x) \right] \quad (\text{A.146a})$$

$$\langle 0_{2n+1}|_A = -\frac{(x^*)^{2n+2}}{(2n+1)!} \delta_+^{(2n+1)}(x) \quad (\text{A.146b})$$

$$\begin{aligned} \langle 2^{-2n}|_B &= \frac{(-1)^{2n-1} (\sqrt{2}x^*)^{2n}}{(2n)!} \\ &\quad \times \left[\delta_-^{(2n-1)}(x - 1) - \delta_+^{(2n-1)}(x - x^*) \right] \end{aligned} \quad (\text{A.147a})$$

$$\langle 0_{2n+1}|_B = \frac{-1}{(2n+1)!} \left(\frac{x^*}{\sqrt{2}} \right)^{2n+2} \delta_-^{(2n+1)}(x - 1) \quad (\text{A.147b})$$

Now we return to the determination of the spectrum and eigenfunctions of U_L . Since $U_G = U_L^2$ the spectrum of U_L is a subset of $\{0, \pm 2^{-n}\}$. Consider the non-zero eigenvalue, 2^{-2n} , of U_G . There are two eigenvectors associated with this eigenvalue, each a polynomial of order n . Since the function space on which U_L acts has two basis elements for each degree n , i.e., a polynomial in A and a polynomial in B, there should be either two eigenvectors or one eigenvector and one Jordan vector that are polynomials of degree n , associated with either one or both the eigenvalues $\{+2^{-n}, -2^{-n}\}$. Since U_G does not have any Jordan vectors (with non-zero eigenvalues) it follows that U_L doesn't either. The eigenvalues of U_L cannot be twofold degenerate since that would imply that all the eigenvectors of U_G are also eigenvectors of U_L , which is impossible since S_G is metrically decomposable and S_L has the flip property. Therefore the non-zero eigenvalues of U_L are $+2^{-n}$ and -2^{-n} .

The eigenvectors of U_L with eigenvalue $\pm 2^{-n}$ are in the eigenspace spanned by the two eigenvectors of U_G corresponding to $+2^{-2n}$. Thus they will be linear combinations as

$$|+2^{-n}\rangle_L = \frac{1}{2} (|+2^{-2n}\rangle_A + c_n |+2^{-2n}\rangle_B) \quad (\text{A.148a})$$

and

$$|-2^{-n}\rangle_L = \frac{1}{2} (|+2^{-2n}\rangle_A + d_n |+2^{-2n}\rangle_B), \quad (\text{A.148b})$$

where the factor of $1/2$ is put for normalization. To determine c_n we use that $|+2^{-n}\rangle_L$ is an eigenvector of U_L as

$$U_L [|+2^{-2n}\rangle_A + c_n |+2^{-2n}\rangle_B] = 2^{-n} [|+2^{-2n}\rangle_A + c_n |+2^{-2n}\rangle_B]. \quad (\text{A.149})$$

Since the part of the function supported on B goes into A when acted on by U_L we know that

$$U_L [c_n |+2^{-2n}\rangle_B] = 2^{-n} |+2^{-2n}\rangle_A. \quad (\text{A.150})$$

Substituting the explicit form (A.144a) of $|+2^{-2n}\rangle_A$ and (A.145a) of $|+2^{-2n}\rangle_B$ in (A.150) and solving for c_n we find that $c_n = 2^{-n}$. A similar analysis shows that $d_n = -2^{-n}$; hence

$$|\pm 2^{-n}\rangle_L = \frac{1}{2x^*} \left(B_{2n} \left(\frac{x^* - x}{2x^*} \right) \chi_A \pm \frac{\sqrt{2}}{2^n} B_{2n} \left(\frac{x - x^*}{\sqrt{2}x^*} \right) \chi_B \right). \quad (\text{A.151})$$

We single out for mention the two $n = 0$ eigenstates, which are piecewise-constant. The state

$$|+1\rangle_L = \frac{1}{2x^*} (\chi_A + \sqrt{2} \chi_B) \quad (\text{A.152})$$

corresponds to the invariant density of U_L . The state

$$|-1\rangle_L = \frac{1}{2x^*}(\chi_A - \sqrt{2}\chi_B) \quad (\text{A.153})$$

is the persistent oscillating mode representing the asymptotic periodicity of the system. Note that this state, like decaying states, does not carry any probability.

Now we consider the null space of U_L . The operator U_G has two independent null vectors (one in A and one in B) for each odd degree. This implies that U_L can have either a corresponding 2×2 Jordan block or have 2 independent eigenvectors for each odd degree. The latter case is not possible since null vectors of U_L cannot have support in interval B because only one of the terms on the rhs of (A.138) acts on functions in B. Thus there is a 2×2 Jordan block for each odd degree associated with eigenvalue 0.

Consider the action of $U_G = U_L^2$ on a null state, $|0_{2n+1}\rangle_A$, of S_A as

$$U_L [U_L |0_{2n+1}\rangle_A] = 0. \quad (\text{A.154})$$

The function inside the square brackets has support only in B, and U_L acting on any non-zero function with support in B cannot vanish in one iteration. Thus $|0_{2n+1}\rangle_L = |0_{2n+1}\rangle_A$ is a null vector of U_L with explicit form given in (A.144b).

The Jordan vector associated with this eigenvector satisfies

$$U_L |0_{J_{2n+1}}\rangle_L = |0_{2n+1}\rangle_L, \quad (\text{A.155})$$

where $|0_{J_{2n+1}}\rangle_L$ denotes the Jordan state corresponding to the null eigenstate of degree $2n + 1$. We may choose the Jordan vector, $|0_{J_{2n+1}}\rangle_L$, as having support only in B so we have

$$|0_{J_{2n+1}}\rangle_L = \eta_{2n+1}|0_{2n+1}\rangle_B, \quad (\text{A.156})$$

where η_{2n+1} is a constant to be determined. To determine η_{2n+1} we apply U_L on (A.156) and use (A.155) and the explicit forms (A.144b) and (A.145b) (remembering that $|0_{2n+1}\rangle_L = |0_{2n+1}\rangle_A$) to obtain $\eta_{2n+1} = -1$ so that

$$|0_{J_{2n+1}}\rangle_L = -\frac{\sqrt{2}}{x^*} E_{2n+1} \left(\frac{\sqrt{2}}{x^*} (x - x^*) \right) \chi_B. \quad (\text{A.157})$$

The left states of U_L may be determined in a similar way as the right states. We just give the results here, which are:

$$\begin{aligned} \langle \pm 2^{-n} |_L &= \frac{(2x^*)^{2n}}{(2n)!} \left[\delta_+^{(2n-1)}(x) - \delta_-^{(2n-1)}(x - x^*) \right. \\ &\quad \left. \pm \delta_+^{(2n-1)}(x - x^*) \mp \delta_-^{(2n-1)}(x - 1) \right]. \end{aligned} \quad (\text{A.158})$$

$$\langle 0_{J_{2n+1}} |_L = -\frac{1}{(2n+1)!} \delta_+^{(2n+1)}(x) \quad (\text{A.159})$$

$$\langle 0_{2n+1} |_L = +\frac{1}{(2n+1)!} \left(\frac{x^*}{\sqrt{2}}\right)^{2n+2} \delta_-^{(2n+1)}(x-1). \quad (\text{A.160})$$

We have thus obtained all of the elements of the generalized spectral decomposition of the operator U_L , which corresponds to U_F on the attractor Ω rescaled to the unit interval. The right eigenstates (and Jordan states) can just be rescaled back to Ω to get the right eigenstates of U_F (the eigenvalues remain the same). The left states we have obtained when rescaled back to Ω will form an orthonormal set with the rescaled right eigenstates but will not be orthonormal to the eigenstates related to transient decay that are described below. After they are determined a procedure similar to that employed in Section 4.1.1 to determine the odd-order left eigenstates of the full height tent map (using the formal completeness relation) may be used to get the correct left states of U_F .

We briefly discuss just the right eigenstates associated with the transient decay out of the intervals I and IV onto Ω . Since the action of U_F gives a function with vanishing support on interval IV, there are only null eigenstates with support there. Due to the degeneracy there is a lot of freedom in the choice of these states. One choice is

$$|0_n\rangle_{IV} = (-1)^{n+1} x^n \chi_I + (x-1)^n (\chi_{III} + \chi_{IV}). \quad (\text{A.161})$$

The transient decay out of interval I onto Ω is governed by the stretching dynamics on I. Acting with U_F on a monomial in I gives

$$U_F[x^n \chi_I] = \frac{x^n}{(\sqrt{2})^{n+1}} (\chi_I + \chi_{II}). \quad (\text{A.162})$$

We can find eigenpolynomials of degree n with associated eigenvalues of $2^{-(n+1)/2}$. Note that the $n = 0$ mode here is the slowest decay mode in this system, even though it is associated with the transient dynamics. The explicit form of this eigenstate is

$$|2^{-1/2}\rangle_I = \chi_I + \frac{1}{2(1-\sqrt{2})}|1\rangle_\Omega + \frac{1}{2(1+\sqrt{2})}| -1\rangle_\Omega, \quad (\text{A.163})$$

where the states $|\pm 1\rangle_\Omega$ are the states $|\pm 1\rangle_L$ rescaled back to Ω .

The Frobenius–Perron operator of the tent map with varying height is extensively discussed in

- M. Dörfle, “Spectrum and eigenfunctions of the Frobenius–Perron operator of the tent map” *J. Stat. Phys.*, **40**, 93 (1985).

The results presented here are extracted from

- S. Subbiah and D.J. Driebe, “Spectral decomposition of the tent map with varying height” *to be published*.

Asymptotic periodicity is extensively discussed in the book of Lasota and Mackey cited in Chapter 1. Its appearance in the tent map with varying height is studied in

- N. Provatas and M.C. Mackey, “Asymptotic periodicity and banded chaos” *Physica D*, **53**, 295 (1991).

A.18 Frobenius–Perron Operator of the Baker Map

From (5.3) the action of the Frobenius–Perron operator of the baker map on a density may also be written as

$$U_b \rho(x, y) = \rho\left(\frac{x}{2}, 2y\right) \Theta\left(\frac{1}{2} - y\right) + \rho\left(\frac{1+x}{2}, 2y-1\right) \Theta\left(y - \frac{1}{2}\right), \quad (\text{A.164})$$

where $\Theta(x)$ is the step function (A.135). But $\Theta\left(\frac{1}{2} - y\right) = \frac{1}{2}[1 + r(y)]$ and $\Theta\left(y - \frac{1}{2}\right) = \frac{1}{2}[1 - r(y)]$, where $r(y)$ is the Rademacher function defined in (5.5), so (A.164) may be rewritten as

$$\begin{aligned} U_b \rho(x, y) &= \frac{1}{2} \left[\rho\left(\frac{x}{2}, 2y\right) + \rho\left(\frac{1+x}{2}, 2y-1\right) \right] \\ &\quad + \frac{1}{2} \left[\rho\left(\frac{x}{2}, 2y\right) r\left(\frac{x}{2}\right) r(y) + \rho\left(\frac{1+x}{2}, 2y-1\right) r\left(\frac{1+x}{2}\right) r(y) \right], \end{aligned} \quad (\text{A.165})$$

where we used that for $x \in [0, 1]$: $r(x/2) = 1$ and $r((1+x)/2) = -1$. Written this way the action of U_b appears close to a combination of U_x and U_y^\dagger . In order to isolate parts involving U_x and U_y^\dagger we add and subtract terms to obtain, first for $0 \leq y < \frac{1}{2}$:

$$\begin{aligned} U_b \rho(x, y) &= \frac{1}{2} \left[\rho\left(\frac{x}{2}, 2y\right) + \rho\left(\frac{1+x}{2}, 2y\right) \right] \\ &\quad + \frac{1}{2} \left[\rho\left(\frac{x}{2}, 2y\right) r\left(\frac{x}{2}\right) + \rho\left(\frac{1+x}{2}, 2y\right) r\left(\frac{1+x}{2}\right) \right] r(y), \end{aligned} \quad (\text{A.166})$$

and for $\frac{1}{2} \leq y < 1$:

$$\begin{aligned} U_b \rho(x, y) &= \frac{1}{2} \left[\rho\left(\frac{x}{2}, 2y-1\right) + \rho\left(\frac{1+x}{2}, 2y-1\right) \right] \\ &\quad + \frac{1}{2} \left[\rho\left(\frac{x}{2}, 2y-1\right) r\left(\frac{x}{2}\right) + \rho\left(\frac{1+x}{2}, 2y-1\right) r\left(\frac{1+x}{2}\right) \right] r(y). \end{aligned} \quad (\text{A.167})$$

Considering these two parts together, their first terms are just the action of $U_x U_y^\dagger$ and the second terms act as $U_x r(x) r(y) U_y^\dagger$, thus obtaining (5.4).

A.19 Green–Kubo Formalism for the Multi-Bernoulli map

First we derive the Green–Kubo formula for diffusion in a discrete-time process and then evaluate it for the multi-Bernoulli map. We start with the usual definition of the diffusion coefficient, D , in terms of the average of the mean-squared deviation from the initial condition as

$$2Dt = \lim_{t \rightarrow \infty} \langle (x_t - x_0)^2 \rangle. \quad (\text{A.168})$$

Introducing a velocity for the discrete-time process as

$$v_t \equiv x_{t+1} - x_t, \quad (\text{A.169})$$

enables us to rewrite $x_t - x_0$ in terms of a sum over the velocity as

$$x_t - x_0 = \sum_{\tau=0}^{t-1} (x_{\tau+1} - x_\tau) = \sum_{\tau=0}^{t-1} v_\tau. \quad (\text{A.170})$$

The mean-squared deviation is then

$$\langle (x_t - x_0)^2 \rangle = \left\langle \sum_{\tau=0}^{t-1} v_\tau \sum_{\sigma=0}^{t-1} v_\sigma \right\rangle = \sum_{\tau, \sigma} \langle v_\tau v_\sigma \rangle. \quad (\text{A.171})$$

We consider time-independent dynamical laws so the velocity auto-correlation will only depend on the absolute value of the time difference, i.e., $|\tau - \sigma|$; hence, $\langle v_\tau v_\sigma \rangle = \langle v_{|\tau-\sigma|} v_0 \rangle$. Using this we may carry out the summation in (A.171) to obtain

$$\sum_{\tau=0}^{t-1} \sum_{\sigma=0}^{t-1} \langle v_\tau v_\sigma \rangle = t \langle v_0 v_0 \rangle + 2 \sum_{\tau=1}^{t-1} [(t-1) - (\tau-1)] \langle v_\tau v_0 \rangle. \quad (\text{A.172})$$

From (A.168) then the diffusion coefficient is given by

$$D = \lim_{t \rightarrow \infty} \left[\frac{\langle v_0 v_0 \rangle}{2} + \frac{1}{t} \sum_{\tau=1}^{t-1} (t-\tau) \langle v_\tau v_0 \rangle \right]. \quad (\text{A.173})$$

Assuming that $\langle v_\tau v_0 \rangle$ decays sufficiently fast as $t \rightarrow \infty$ so that

$$\lim_{t \rightarrow \infty} \frac{1}{t} \sum_{\tau=1}^{t-1} \tau \langle v_\tau v_0 \rangle = 0, \quad (\text{A.174})$$

and $\sum_{\tau=1}^{\infty} \langle v_{\tau} v_0 \rangle$ converges gives then the Green-Kubo formula

$$D = \frac{\langle v_0 v_0 \rangle}{2} + \sum_{\tau=1}^{\infty} \langle v_{\tau} v_0 \rangle. \quad (\text{A.175})$$

For the multi-Bernoulli map the velocity can be expressed in terms of the two coupled dynamical laws (6.9) and (6.10) as

$$\begin{aligned} V_t &= X_{t+1} - X_t \\ &= q_{t+1} - q_t + x_{t+1} - x_t \\ &= \Delta(x_t) + g(x_t) - x_t. \end{aligned} \quad (\text{A.176})$$

The velocity autocorrelation is then

$$\begin{aligned} \langle V_t V_0 \rangle &= \langle \Delta(x_t) \Delta(x_0) \rangle + \langle \Delta(x_t) g(x_0) \rangle - \langle \Delta(x_t) x_0 \rangle \\ &\quad + \langle g(x_t) \Delta(x_0) \rangle + \langle g(x_t) g(x_0) \rangle - \langle g(x_t) x_0 \rangle \\ &\quad - \langle x_t \Delta(x_0) \rangle - \langle x_t g(x_0) \rangle + \langle x_t x_0 \rangle, \end{aligned} \quad (\text{A.177})$$

where the averaging on the right hand side is with respect to the invariant density of the 4-adic map, $g(x_t)$, governing the x_t dynamics. All of the correlation terms in (A.177) are of the form

$$\langle F(x_t) G(x_0) \rangle = \langle (U_g^\dagger)^t F(x_0) | G(x_0) \rangle = \langle F(x_0) | U_g^t G(x_0) \rangle. \quad (\text{A.178})$$

We can thus employ the generalized spectral decomposition of U_g (the same as for the dyadic Bernoulli map except for the eigenvalues here of 4^{-n}) giving

$$U_g^t \Delta(x) = \delta_{t,0} \Delta(x), \quad (\text{A.179a})$$

$$U_g^t g(x) = \frac{1}{2} + \frac{4}{4^t} (x - \frac{1}{2}), \quad (\text{A.179b})$$

$$U_g^t x = \frac{1}{2} + \frac{1}{4^t} (x - \frac{1}{2}). \quad (\text{A.179c})$$

Using these results all of the terms in (A.177) may be evaluated and when collected together yield

$$\langle V_t V_0 \rangle = \frac{3}{8} \frac{1}{4^t} - \frac{1}{8} \delta_{t,0}. \quad (\text{A.180})$$

Since the decay of the velocity auto-correlation is exponential we are assured that the Green-Kubo formalism is valid for this system. Using (A.180) in (A.175) then gives

$$D = \frac{1}{2} \left(\frac{3}{8} - \frac{1}{8} \right) + \sum_{\tau=1}^{\infty} \frac{3}{8} \frac{1}{4^{\tau}} = \frac{1}{4}. \quad (\text{A.181})$$

A.20 Frobenius–Perron Operator of the Multi-Bernoulli map

To determine the Frobenius–Perron operator of the multi-Bernoulli map we use the “primative” form (1.3) of the operator as

$$U_{\text{mB}}\rho(X) = \int_{[0,L)} dX' \delta(X - \phi(X'))\rho(X'). \quad (\text{A.182})$$

From the rule (6.6) for the map and using $X = q + x$

$$\begin{aligned} U_{\text{mB}}\rho(q+x) &= \sum_{q'=0}^{L-1} \left\{ \int_0^{1/2} dx' \delta(q+x-4x'-q'+1) \rho(q'+x') \right. \\ &\quad \left. + \int_{1/2}^1 dx' \delta(q+x-4x'-q'+2) \rho(q'+x') \right\}. \end{aligned} \quad (\text{A.183})$$

The integrals over x' will be non-vanishing only if the argument of the delta function in the integrand vanishes over the integration region. This imposes the conditions on q and q' of

$$q - q' = \begin{cases} -1, & 0 \leq x' < \frac{1}{4} \\ 0, & \frac{1}{4} \leq x' < \frac{3}{4} \\ +1, & \frac{3}{4} \leq x' < 1. \end{cases} \quad (\text{A.184})$$

Then (A.183) splits into the sum of four terms as

$$\begin{aligned} U_{\text{mB}}\rho(q+x) &= \sum_{q'} \left\{ \delta_{q',q+1} \int_0^{1/4} dx' \delta(x-4x') \rho(q'+x') \right. \\ &\quad + \delta_{q',q} \int_{1/4}^{1/2} dx' \delta(x-4x'+1) \rho(q'+x') \\ &\quad + \delta_{q',q} \int_{1/2}^{3/4} dx' \delta(x-4x'+2) \rho(q'+x') \\ &\quad \left. + \delta_{q',q-1} \int_{1/2}^{3/4} dx' \delta(x-4x'+3) \rho(q'+x') \right\}. \end{aligned} \quad (\text{A.185})$$

The result (6.11) then follows immediately.

A.21 Eigenstates of the Full Multi-Bernoulli Map

Using the fact that $\gamma_s^{(m)}(x)$ is an eigenstate of U_s we may demonstrate that $\Gamma^{(s,m)}(q + x)$ given by (6.24) is an eigenstate of U_{mB} . The action of U_{mB} decomposed in Fourier modes like (6.15) is

$$U_{\text{mB}}\Gamma^{(s,m)}(q + x) = \frac{1}{\sqrt{L}} \sum_{s'=0}^{L-1} e^{i\frac{2\pi}{L}qs'} U_{s'}^2 \Gamma_{s'}^{(s,m)}(x), \quad (\text{A.186})$$

where $\Gamma_{s'}^{(s,m)}(x)$ is the transform of $\Gamma^{(s,m)}(q + x)$ given as

$$\begin{aligned} \Gamma_{s'}^{(s,m)}(x) &= \frac{1}{\sqrt{L}} \sum_{q=0}^{L-1} e^{-i\frac{2\pi}{L}qs'} \Gamma^{(s,m)}(q + x) \\ &= \frac{1}{\sqrt{L}} \sum_{q=0}^{L-1} e^{-i\frac{2\pi}{L}qs'} \frac{1}{\sqrt{L}} e^{-i\frac{2\pi}{L}qs} \gamma_s^{(m)}(x) \\ &= \delta_{s,s'} \gamma_s^{(m)}(x). \end{aligned} \quad (\text{A.187})$$

Thus,

$$\begin{aligned} U_{\text{mB}}\Gamma^{(s,m)}(q + x) &= \frac{1}{\sqrt{L}} \sum_{s'=0}^{L-1} e^{-i\frac{2\pi}{L}qs'} U_{s'}^2 \delta_{s',s} \gamma_s^{(m)}(x) \\ &= \frac{1}{\sqrt{L}} e^{-i\frac{2\pi}{L}qs'} U_s^2 \gamma_s^{(m)}(x) \\ &= e^{-2\gamma_s^{(m)}} \frac{1}{\sqrt{L}} e^{-i\frac{2\pi}{L}qs'} \gamma_s^{(m)}(x) \\ &= e^{-\Gamma^{(s,m)}} \Gamma^{(s,m)}(q + x). \end{aligned} \quad (\text{A.188})$$

Index

- Appell polynomials, 133
asymptotic periodicity, 77, 148, 154
- baker map, 9, 81–91
Frobenius–Perron operator of, 82, 157
intrinsic irreversibility of, 90
inverse of, 81
Koopman operator of, 82
- Bernoulli basis, 58
completeness relation, 70
- Bernoulli map, 9, 19–42, 117
as binary shift, 117
as reduction of baker map, 87
coherent eigenstates, 24
densities in, 19
exactness of, 20
Frobenius–Perron operator of, 19
Koopman operator of, 21, 121
left eigenstates, 37
Lyapunov exponent of, 19
right eigenstates, 33
shift states, 23
spectral decomposition of, 38
 x auto-correlation function, 21, 39
- Bernoulli polynomials, 33, 131
Fourier expansion of, 131
multiplication theorem, 39
- Boltzmann equation, 93
- Brownian motion, 93
- Burnett coefficient, 103
- Cantor map, 67–72
singular invariant measure, 146
- correlation decay, 14–16
in Bernoulli map, 21
in mixing systems, 15
with initial growth, 61
- density, 3–5
diffusion, 93
and decay modes, 94
- diffusion coefficient, 93
Green–Kubo formula for, 159
of multi-Bernoulli map, 103, 159
- diffusion equation, 94
- discrete Fourier transform, 98
- dual states, 122
of Jordan states, 140
- equilibrium density, 7
- ergodic system, 6
- ergodicity, 8
- Euler polynomials, 49
dual states, 49
relation to Bernoulli polynomials, 56
- Euler–Maclaurin expansion, 42
- exact system, 9
as factor of K-automorphism, 87
- measure-theoretic definition, 12

- Frobenius–Perron operator, 4, 13
contractive property, 13
- generating function, 133
for Bernoulli polynomials, 131
for Euler polynomials, 49
technique for spectral decompositions, 133–136
- Green–Kubo formalism, 158
- hat map, *see* tent map
- induced operator, *see* Koopman operator
- intertwining relation
of Bernoulli map and derivative operator, 133
of Cantor map and derivative operator, 70
- of tent and Bernoulli maps, 48
- invariant density, 12
- invariant measure, 12
- irreversibility, 1
of baker transformation, 90
- isometric operator, 14
- Jordan blocks, 54, 86, 142
- Jordan state, 57, 59, 137
dual states, 140
of baker map, 87
- K-automorphism, 87
- Koopman operator, 14
isometry of, 14
- Lebesgue measure, 11
- Legendre polynomials, 26, 125
- Liouville equation, 93
- Liouvillian, 14
- logistic map, 74–77
invariant density of, 76
- Lyapunov exponent, 4, 117
- Lyapunov time, 26
- map, 3
- Markov partition, 149
- measure function, 11
- measure-preserving transformation, 12
- microstructure of phase space, 117
- mixing system, 8, 119
correlation decay in, 15
measure-theoretic definition, 15
- modified exponential decay, 57, 86
- multi-baker map, 110–113
- multi-Bernoulli map, 95–108
as two coupled dynamical laws, 96
- diffusion coefficient, 103, 159
- Frobenius–Perron operator of, 97, 160
- spectral decomposition of, 101
- translational invariance of, 99
- N map, 54–56, 142
- non-normal irrational numbers, 118
- observable, 12
expectation value, 13
- polynomial shift states, 64
creation operator for, 65
dual states of, 66
- probability density, 13
- projection operator
associated with pole of the re-solvent, 29, 123
for even and odd parts of a function, 46
- r -adic map, 38
- Rademacher function, 84

- reflected Bernoulli map, 53
- reflection operator, 46
- resolvent, 26, 123
 - analytic continuation of, 90
 - analytic structure of, 29
 - double pole of, 57
 - expansion of, 28
- resonance, 16

- σ -algebra, 11
- singular invariant measure, 12
 - of Cantor map, 68, 146
 - of multi-Bernoulli map, 108
- spectral decomposition
 - of baker map, 86
 - of Bernoulli map, 38
 - of multi-Bernoulli map, 101
 - of N map, 56
 - of the tent map, 50
 - of topologically conjugate maps, 74
- spectral function, 15, 22
 - analytic continuation of, 16
- spectrum, 24
- symmetric map, 144
- symmetry, 45
 - in a class of one-dimensional maps, 142
- of Bernoulli polynomials, 33
- of Legendre polynomials, 126

- tent map, 46–51
 - Frobenius–Perron operator of, 46
 - intertwining relation with Bernoulli map, 48
 - spectral decomposition of, 50
 - x auto-correlation function, 51
- time average, 6
- time correlation, 14

- topological conjugacy, 72
 - of tent and logistic maps, 75
- V map, 51–53

- z transform, 123

Nonlinear Phenomena and Complex Systems

1. E. Tirapegui and W. Zeller (eds.): *Instabilities and Nonequilibrium Structures* V. 1996 ISBN 0-7923-3992-4
2. E. Goles and S. Martínez (eds.): *Dynamics of Complex Interacting Systems.* 1996 ISBN 0-7923-4173-2
3. E. Goles and S. Martínez (eds.): *Cellular Automata and Complex Systems.* 1999 ISBN 0-7923-5512-1
4. D. J. Driebe: *Fully Chaotic Maps and Broken Time Symmetry.* 1999 ISBN 0-7923-5564-4